

GENE-BY-ENVIRONMENT INTERACTION OF HEPATIC XENOBIOTIC TRANSPORTER
POLYMORPHISMS AND NONALCOHOLIC STEATOHEPATITIS ON DRUG DISPOSITION
AND TOXICITY

by

Erica L. Toth

Copyright © Erica L. Toth 2019

A Dissertation Submitted to the Faculty of the

DEPARTMENT OF PHARMACOLOGY AND TOXICOLOGY

In Partial Fulfillment of the Requirements

For the Degree of

DOCTOR OF PHILOSOPHY

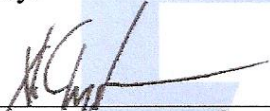
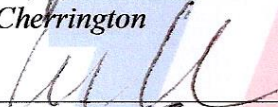



In the Graduate College

THE UNIVERSITY OF ARIZONA

2019


THE UNIVERSITY OF ARIZONA
GRADUATE COLLEGE

As members of the Dissertation Committee, we certify that we have read the dissertation prepared by Erica L. Toth titled Gene-by-Environment Interaction of Hepatic Xenobiotic Transporter Polymorphisms and Nonalcoholic Steatohepatitis on Drug Disposition and Toxicity and recommend that it be accepted as fulfilling the dissertation requirement for the Degree of Doctor of Philosophy.

 _____ <i>Nathan Cherrington</i>	Date: <u>8/16/19</u>
 _____ <i>Walt Klimecki</i>	Date: <u>8/16/19</u>
 _____ <i>Eli Chapman</i>	Date: <u>8/16/19</u>
 _____ <i>Patrick Ronalason</i>	Date: <u>8/16/19</u>
 _____ <i>Stephen Wright</i>	Date: <u>8/16/19</u>

Final approval and acceptance of this dissertation is contingent upon the candidate's submission of the final copies of the dissertation to the Graduate College.

I hereby certify that I have read this dissertation prepared under my direction and recommend that it be accepted as fulfilling the dissertation requirement.

 _____ <i>Nathan Cherrington</i> Dissertation Committee Chair Pharmacology and Toxicology	Date: <u>8/16/19</u>
--	----------------------

ACKNOWLEDGEMENTS

To say that I have many people to thank for helping me in various ways throughout the journey that has been my graduate school experience would be a vast understatement. First, though, and perhaps most obviously, I would like to thank Dr. Nathan Cherrington. Not just for his guidance, both in the areas of science and career-building and throughout the many ups and downs of research, but also for his good humor, compassion, and understanding; for being both a mentor and a friend. Graduate school would have been a very different beast had I been in any other lab, and I am continually glad to have been part of this one.

I would also like to thank the past members of the Cherrington lab; Dr. John Clarke, for being both an excellent teacher and an excellent conversationalist, in topics both scientific and otherwise, and, at times, like Obi Won Kenobi, for being my only hope; Dr. Anika Dzierlenga, both for her help in the lab and for board game nights outside of it; and to Dr. Hui Li and Dr. David Klein. I would also like to thank the newer members of the lab as well, Kayla Frost, Siannah Miller, Ray Hau, and Dr. Joe Jilek. Good company makes hard work lighter.

I also would like to thank my friends outside of the lab for the many ways that they've helped bolster me through graduate school; for the many Sunday nights spent with Dr. Mike Kerins and Karen Kerins, playing board games; my friends across the country who have given up their Saturday nights for the past year to play Dungeons and Dragons like the nerds we all are.

I would also like to thank my family, for having the patience to endure phone calls full of long-winded explanations of failed experiments and, despite that, still encouraging me. I want to thank my mom in particular for her daily good-night texts, and my dad for calling during his long commutes home, while I was in lab for the evening. I want to thank my sister Colleen, for

always having room for me up in Portland. Sometimes, there's nothing better than watching old TV with your sister and having a corgi to throw a ball for.

Thank you, everyone, for everything.

TABLE OF CONTENTS

LIST OF FIGURES	8
LIST OF TABLES	10
ABSTRACT.....	11
CHAPTER ONE: TRANSPORTER ALTERATIONS DURING NASH, GENE-BY- ENVIRONMENT INTERACTIONS, AND THEIR IMPACT ON ADVERSE DRUG REACTIONS	
Adverse Drug Reactions.....	13
Pharmacogenomics and Precision Medicine.....	14
Nonalcoholic Fatty Liver Disease and Nonalcoholic Steatohepatitis.....	17
ADME in the Liver.....	26
ADME Remodeling in NASH.....	34
Hepatocyte Hopping and NASH	38
Hepatic Iron Regulation and NASH.....	41
Current Study.....	44
CHAPTER TWO: GENE-BY-ENVIRONMENT INTERACTION OF BCRP-/- AND METHIONINE- AND CHOLINE-DEFICIENT DIET-INDUCED NONALCOHOLIC STEATOHEPATITIS ALTERS SN-38 DISPOSITION	
Introduction.....	47
Materials and Methods.....	49
Results.....	56

Discussion.....	62
CHAPTER THREE: INTERACTION OF OATP1B2 GENE DOSE AND NONALCOHOLIC STEATOHEPATITIS ON PLASMA CLEARANCE OF PRAVASTATIN	
Introduction.....	68
Materials and Methods.....	69
Results.....	73
Discussion.....	80
CHAPTER FOUR: NONALCOHOLIC STEATOHEPATITIS INCREASES PLASMA RETENTION OF SORAFENIB-GLUCURONIDE BY ALTERING THE MECHANISMS OF HEPATOCYTE HOPPING	
Introduction.....	85
Materials and Methods.....	86
Results.....	91
Discussion.....	98
CHAPTER FIVE: ALTERATION OF IRON REGULATORY PROTEINS IN NONALCOHOLIC STEATOHEPATITIS	
Introduction.....	103
Materials and Methods.....	104
Results.....	108
Discussion.....	115
CHAPTER SIX: CURRENT PERSPECTIVES AND FUTURE DIRECTIONS	

Summary of Studies	120
Future Directions	122
BIBLIOGRAPHY.....	127

LIST OF FIGURES

Figure 1.1. Variable platelet response to clopidogrel can associate with risk factors and outcomes.	15
Figure 1.2. Histology of human NAFLD.	19
Figure 1.3. “Multi—hit” hypothesis: pathogenesis of NAFLD	21
Figure 1.4. Hepatic uptake and efflux transporters.	27
Figure 1.5. Fraction of clinically used drugs metabolized by P450 isoforms and factors influencing variability.	30
Figure 1.6. Alteration to hepatic uptake and efflux transporters during NASH.	36
Figure 1.7. Hepatocyte hopping and recirculation of SG.	39
Figure 2.1. Liver histopathology of control and MCD-diet rats	57
Figure 2.2. Effects of MCD diet on systemic exposure of SN-38 and SN-38G.....	58
Figure 2.3. Effects of MCD diet on biliary excretion of SN-38 and SN-38G.	59
Figure 2.4. Alterations of Mrp2 and Mrp3 protein expression in MCD diet.	60
Figure 2.5. Mislocalization of Mrp2 in MCD diet.	61
Figure 2.6. Alterations of Bcrp protein and mRNA expression during MCD diet.	62
Figure 3.1. Effects of Oatp1b2 gene dose and NASH on plasma pravastatin concentration....	74
Figure 3.2. Effects of Oatp1b2 gene dose and NASH on biliary pravastatin concentration.	75
Figure 3.3. Effects of Oatp1b2 gene dose and NASH on tissue pravastatin concentrations....	76
Figure 3.4. Altered expression of Oatp transporters due to diet-induced NASH and Oatp1b2 gene dose.	77
Figure 3.5. Altered expression of Mrp2 and Mrp3 due to diet-induced NASH.....	78
Figure 3.6. Weight-adjusted Pravastatin Clearance.....	79
Figure 4.1. Liver histopathology of control and diet-induced NASH mice.	92
Figure 4.2. Effects of Oatp1a/1b cluster knockout and NASH on plasma sorafenib-glucuronide concentration.	92
Figure 4.3. Effects of Mrp2 knockout and NASH on plasma sorafenib-glucuronide concentration	93
Figure 4.4. Effects of Oatp1a/1b cluster knockout and Mrp2 knockout and NASH on liver tissue sorafenib-glucuronide concentration.	94
Figure 4.5. Altered mRNA expression of Oatp and Mrp transporters due to Oatp1a/1b cluster knockout and Mrp2 knockout and diet-induced NASH.	95

Figure 4.6. Altered protein expression of Oatp and Mrp transporters due to Oatp1a/1b cluster knockout and Mrp2 knockout and diet-induced NASH.	97
Figure. 5.1. Altered mRNA expression during the progression of NASH in human liver tissue	109
Figure 5.2. Altered protein expression during the progression of NASH in human liver tissue.....	110
Figure. 5.3. Perl's Prussian blue iron staining in liver tissue.	111
Figure. 5.4. Percent area of Perl's Prussian blue iron staining in liver tissue	112
Figure. 5.5. Altered mRNA expression in rodent diet-induced NASH.	113
Figure. 5.6. Altered protein expression in rodent diet-induced NASH.	114

LIST OF TABLES

Table 3.1. Peptide Fragments and MRM Transitions for LC-MS/MS Analysis	79
Table 4.1. Peptide Fragments and MRM Transitions for LC-MS/MS Analysis	98
Table 5.1. Peptide Fragments and MRM Transitions for LC-MS/MS Analysis	115

ABSTRACT

Nonalcoholic steatohepatitis (NASH) is the advanced form of nonalcoholic fatty liver disease and is the hepatic manifestation of metabolic syndrome. The overall rate of NASH is on the rise globally, and currently approximately 1.5-6.45% of the population is afflicted with this disease (Z. M. Younossi et al., 2016). The progression of NASH is known to result in the dysregulation of many genes, including those that are responsible for ADME processes. These changes can alter the disposition of xenobiotics and result in adverse drug reactions (ADRs). Since ADRs are becoming increasingly frequent, with nearly 1 in 20 hospital patients experiencing ADRs in the United States (Bourgeois, Shannon, Valim, & Mandl, 2010), determining the factors that contribute to variations in drug response is increasingly important. Additionally, genetic polymorphisms are known to cause pharmacokinetic variations, and many of them have been extensively researched for their impacts on patient response. Less known, however, is how genetic polymorphisms and chronic liver disease interact, and how that interaction may increase patient risk for ADRs. As the goal of precision medicine is to provide the right dose to the right person at the right time, determining how factors like disease state can interact with genetic polymorphisms to alter pharmacokinetics can provide a better basis for individualized dosing. The purpose behind this study was therefore to utilize a methionine- and choline-deficient (MCD) rodent model to determine the gene-by-environment interactions of hepatic xenobiotic transporter polymorphisms and NASH on the disposition and toxicity of pharmaceutical compounds.

To identify the impact of these gene-by-environment interactions, pharmacokinetic studies were designed to investigate the alterations to drug distribution that occurred with NASH in combination with disruptions of hepatic uptake and efflux transporters and to determine the underlying mechanism behind pharmacokinetic alterations during disease progression. The results in the MCD rodent model of NASH found a synergistic interaction between

polymorphisms of both hepatic uptake and efflux transporters and NASH that lead to changes in plasma retention and biliary excretion of probe substrates. The comparison between biliary excretion of SN-38 in wild-type and *Bcrp*^{-/-} rats demonstrated this synergistic interaction, as no alterations were found in biliary AUCs until the combination of the disease and genetic disruption, where biliary excretion significantly decreased. A similar interaction was demonstrated in a study investigating the gene dose of *Oatp1b2* and NASH on pravastatin disposition, where the combination of full genetic *Oatp1b2* knockout along with NASH was necessary to see dramatic increases in plasma AUC and tissue concentrations. Finally, in order to identify the underlying mechanism by which NASH alters pharmacokinetics, the disposition of sorafenib-glucuronide was determined in wild-type, *Oatp1a/1b* cluster knockouts, and *Mrp2* knockouts, with and without MCD diet. By comparing the changes to plasma AUC and liver concentrations in these groups, the disruption to hepatocyte hopping that occurs during NASH was made quantifiable.

In summation, these data identify synergistic gene-by-environment interactions of hepatic xenobiotic transporter polymorphisms and NASH, the alterations that these interactions cause to drug disposition, and the mechanism by which NASH causes pharmacokinetic changes through disruption of hepatocellular shuttling.

CHAPTER ONE: TRANSPORTER ALTERATIONS DURING NASH, GENE-BY-ENVIRONMENT INTERACTIONS, AND THEIR IMPACT ON ADVERSE DRUG REACTIONS

Adverse Drug Reactions

Adverse drug reactions (ADRs) are one of the leading causes of morbidity and mortality and represent 2.7-15.7% of hospital admissions. ADRs are defined as “an appreciably harmful or unpleasant reaction, resulting from an intervention related to the use of a medicinal product, which predicts hazard from future administration and warrants prevention or specific treatment, or alteration of the dosage regimen, or withdrawal of the product”(Edwards & Aronson, 2000). These adverse events can occur in in-patient or out-patient settings. Out of these admissions, 28.9% of them were considered preventable(Hakkarainen, Hedna, Petzold, & Hägg, 2012). Though many ADRs are not severe and will resolve when the patient is no longer exposed to the causative agent, others are debilitating and may result in permanent disability or death and represent a significant financial burden on hospital systems. In 1997, it was estimated that, due to the cost associated with increased hospital stays and additional required treatment, each ADR had a cost of \$2,500 per patient, with a total estimated cost burden of \$1.56 billion annually(Bates et al., 1997; Classen, Pestotnik, Evans, Lloyd, & Burke, 1997).

ADRs are classified into two types: pharmacologic or idiosyncratic. Pharmacologic ADRs are the most common type to appear in patients, comprising about 80% of all reported ADRs and are usually not life-threatening. They are also dose-dependent and predictable based on the known pharmacological properties of the compound. There are three major causes for this type of reaction: pharmaceutical, pharmacokinetic, and pharmacodynamic. Pharmacologic ADRs due to pharmaceutical formulations are generally due to differences in the bioavailability or release rate of the compound, while pharmacokinetic ADRs are usually due to

variations in ADME processes, and pharmacodynamic ADRs are usually due to variability in the sensitivity of drug targets, such as receptor density or affinity(Rawlins, 1981).

Idiosyncratic ADRs, however, are much less common and are neither dose-dependent nor predictable. Most of the reactions associated with idiosyncratic ADRs appear to be immune mediated, as there tends to be a delayed onset of symptoms, but a more rapid onset for patients who have been rechallenged(Utrecht, 2007). The duration of the delay between administration and appearance of symptoms varies depending on the type of reaction; dermatological symptoms, the most common kind of idiosyncratic ADRs, generally appear within a week, while more severe reactions such as liver injury may be delayed to one or two months. Additionally, drugs that are associated with high numbers of idiosyncratic ADRs often precipitate multiple types of reactions. As an example, carbamazepine can result in liver injury, mild skin rash, toxic epidermal necrolysis, agranulocytosis, aplastic anemia, and autoimmunity, among other reactions(Jain, 1991; Syn, Naisbitt, Holt, Pirmohamed, & Mutimer, 2005). It is difficult, however, to predict which patients may experience an idiosyncratic ADR, since the reactions are specific to the individual. There have been some weak genetic associations between variants of the glutathione-S-transferase enzyme and other metabolic enzymes with idiosyncratic drug toxicity, which may indicate that idiosyncratic ADRs are dependent on multiple genes(Pirmohamed, 2010). The exception to this, however, is abacavir hypersensitivity, which has been linked to patients with the HLA-B*57:01 variation; approximately 50% of these patients will develop an idiosyncratic ADR when given this drug(Mallal et al., 2008). Idiosyncratic ADRs increase the uncertainty involved in drug development and further investigation is needed into the potential immune mechanisms that govern these ADRs.

Pharmacogenomics and Precision Medicine

Genetic variation plays a significant role in the therapeutic effect of drug treatments, and the wide range of genetic diversity that occurs in the human population also results in high variability in patient response. Clinical trials can provide information on the average patient response to a drug therapy for a narrow population, but other patient subpopulations may experience adverse reactions or no therapeutic benefit from the same dose. Regardless as to whether the result is an ADR or no therapeutic benefit, the impact of these inter-individual variabilities can be both expensive and potentially life-threatening. In order to better predict patient response to therapy, pharmacogenomic studies have traditionally focused on variations in genes that impact ADME processes, like drug metabolizing enzymes and xenobiotic transporters; in recent years, however, due to advances in technology, the focus has shifted to a broader range of genetic contributions to ADRs. By understanding how genetic variations can impact the pharmacokinetics or pharmacodynamics of drug therapies, medication regimens and dosages can be more appropriately tailored for the individual patient's needs.

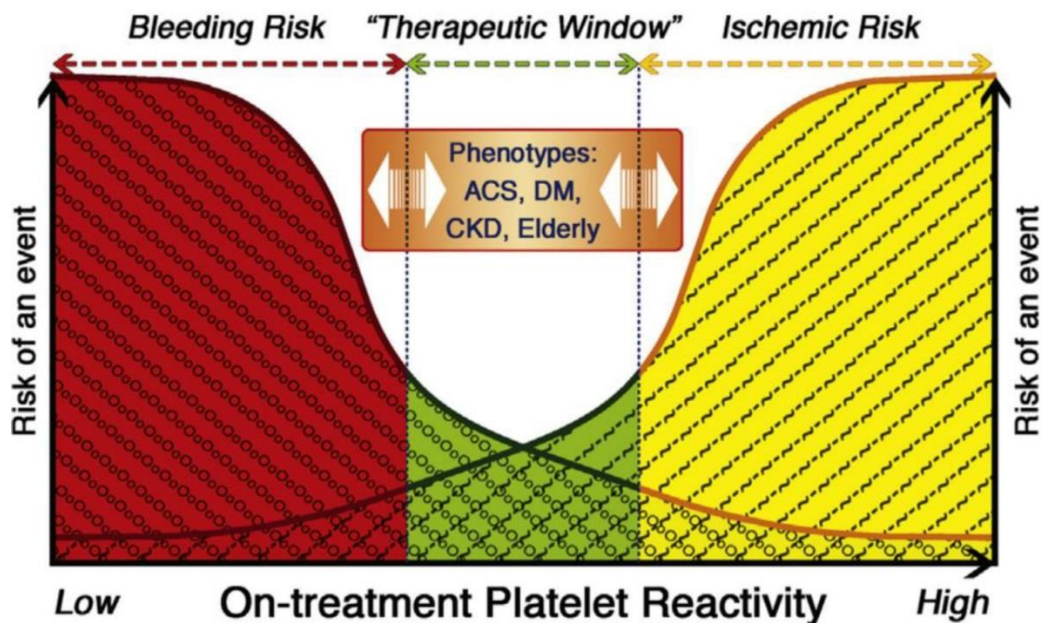


Figure 1.1. Variable platelet response to clopidogrel can associate with risk factors and outcomes.

On-treatment platelet reactivity in response to clopidogrel can associate with bleeding risk if low or ischemic risk if

high, with a therapeutic window. Various risk factors for ischemic heart disease can impact on-treatment platelet reactivity in individuals treated with clopidogrel. ACS: acute coronary syndrome; CKD: chronic kidney disease; DM: diabetes mellitus. Brown and Pereira, *Journal of Personalized Medicine*, **2018**, 8.1.

Genetics, however, are not solely responsible for all inter-individual variabilities seen in patient populations. Non-genetic factors that may impact patient response include lifestyle factors such as diet and smoking, as well as factors like concomitant disease, patient compliance, age, and ethnicity. There are many therapies that may have serious pharmacologic adverse reactions that can only partly explain their inter-individual variabilities through pharmacogenomics. Many antiplatelet therapies follow this trend; in particular, variants in *CYP2C19* are associated with an alteration in patient response to the commonly prescribed drug clopidogrel. Approximately one-quarter of patients display reduced response to clopidogrel therapy, leaving them at risk for cardiovascular events like heart attack or stroke, and poor response to clopidogrel therapy is highly heritable (Cappola & Margulies, 2011). *CYP2C19* is responsible for the hepatic bioactivation of clopidogrel, performing 45% of the first step and 20% of the second step in the biotransformation of this drug (Brown & Pereira, 2018). Patients with loss-of-function mutations of *CYP2C19* may present as poor metabolizers, leading to decreased sensitivity and increased risk of blood clots, while those with gain-of-function or multiple functional copies of the gene may present as hyper metabolizers, leading to increased sensitivity to treatment and a greater risk of hemorrhage. However, genetic factors, primarily involving *CYP2C19*, only account for approximately 20% of the pharmacokinetic variability and 65% of the pharmacodynamic variability of clopidogrel therapy (Frelinger et al., 2013). While genetic testing for polymorphisms of *CYP2C19* in the case of clopidogrel, or for other enzymes and transporters involved in ADME processes for other therapies, have their uses, pharmacogenomics cannot precisely predict patient response and a systems biology approach for precision medicine will be needed to accurately account for the additional factors that impact inter-individual variability.

Nonalcoholic Fatty Liver Disease and Nonalcoholic Steatohepatitis

Nonalcoholic fatty liver disease (NAFLD) is the hepatic manifestation of metabolic syndrome and consists of a spectrum of liver pathologies ranging from simple steatosis to cirrhosis. It is defined clinically as the presence of >5% of macrovesicular steatosis in the hepatocytes of individuals who do not consume much or any alcohol (Loomba & Sanyal, 2013). The disease is divided into two histological types: nonalcoholic fatty liver disease, which involves the presence of simple steatosis, and nonalcoholic steatohepatitis, which includes the presence of inflammation, fibrosis, and necrosis. Approximately 10-20% of the population is estimated to be affected by this NAFLD, and though it is primarily a disease of adults, it has been described in pediatric patients.

Considerable effort has been put into determining the prevalence of NAFLD worldwide, and current evidence indicates that it is highly prevalent in all populations. The highest rates of NAFLD are reported in South America and the Middle East (31% and 32%, respectively), Asia (27%), the United States (24%), and Europe (23%), with the lowest rates described in Africa (14%) (Lazo et al., 2013; Schneider, Lazo, Selvin, & Clark, 2014). In the United States, NAFLD prevalence can also vary significantly by ethnic group, with the highest reported rates of NAFLD in Hispanic Americans, followed by European-descent Americans, with the lowest reported rates in African Americans (Z. Younossi et al., 2018). While the root of these ethnic disparities is unclear, several genetic, environmental, and social factors may be responsible, including factors such as comorbid conditions and access to healthcare.

Even among ethnic groups, there may be differences in the prevalence of NAFLD based on the country of origin. In a study involving the Multi-Ethnic Study of Atherosclerosis (MESA) cohort, the prevalence of NAFLD in Hispanic Americans was found to vary significantly depending on their country of origin. Overall, the incidence of NAFLD was 29% among Hispanics, but Hispanics of Mexican origin were found to have higher rates of the disease

(33%), compared to Hispanics of Puerto Rican origin (19%) or Dominican origin (16%)(Fleischman, Budoff, Zeb, Li, & Foster, 2014). Given that the term Hispanic can refer to a collection of individuals that is culturally and genetically diverse, it is too non-specific to function as an umbrella term regarding the propensity to develop NAFLD and therefore assumptions of homogeneity cannot be made when performing risk assessment in Hispanic populations.

NASH, the advanced form of NAFLD, was originally coined in 1980 by Ludwig et al. in their groundbreaking paper that described the histological findings that are characteristic of the disease: steatosis, inflammatory infiltrates, fibrosis, cirrhosis, and Mallory bodies(Ludwig, Viggiano, McGill, & Oh, 1980). As NASH can currently only be definitively diagnosed through a liver biopsy, determining the prevalence of this disease in any given population has inherent challenges. In the United States, however, the estimated incidence of NASH is around 1-3%(Sayiner, Koenig, Henry, & Younossi, 2016a). In an autopsy study conducted in 1990, 18.5% of obese patients were found to have NASH, while only 2.7% of lean patients had evidence of the disease(Wanless & Lentz, 1990). Diabetes, dyslipidemia, hypertension, and obesity remain high risk factors for the development of NAFLD and NASH; in studies involving Italian and UK cohorts with type-2 diabetes, incidence rates of NAFLD were found to be 60-70% and 42.6%, respectively(Soresi et al., 2013; Williamson et al., 2011).

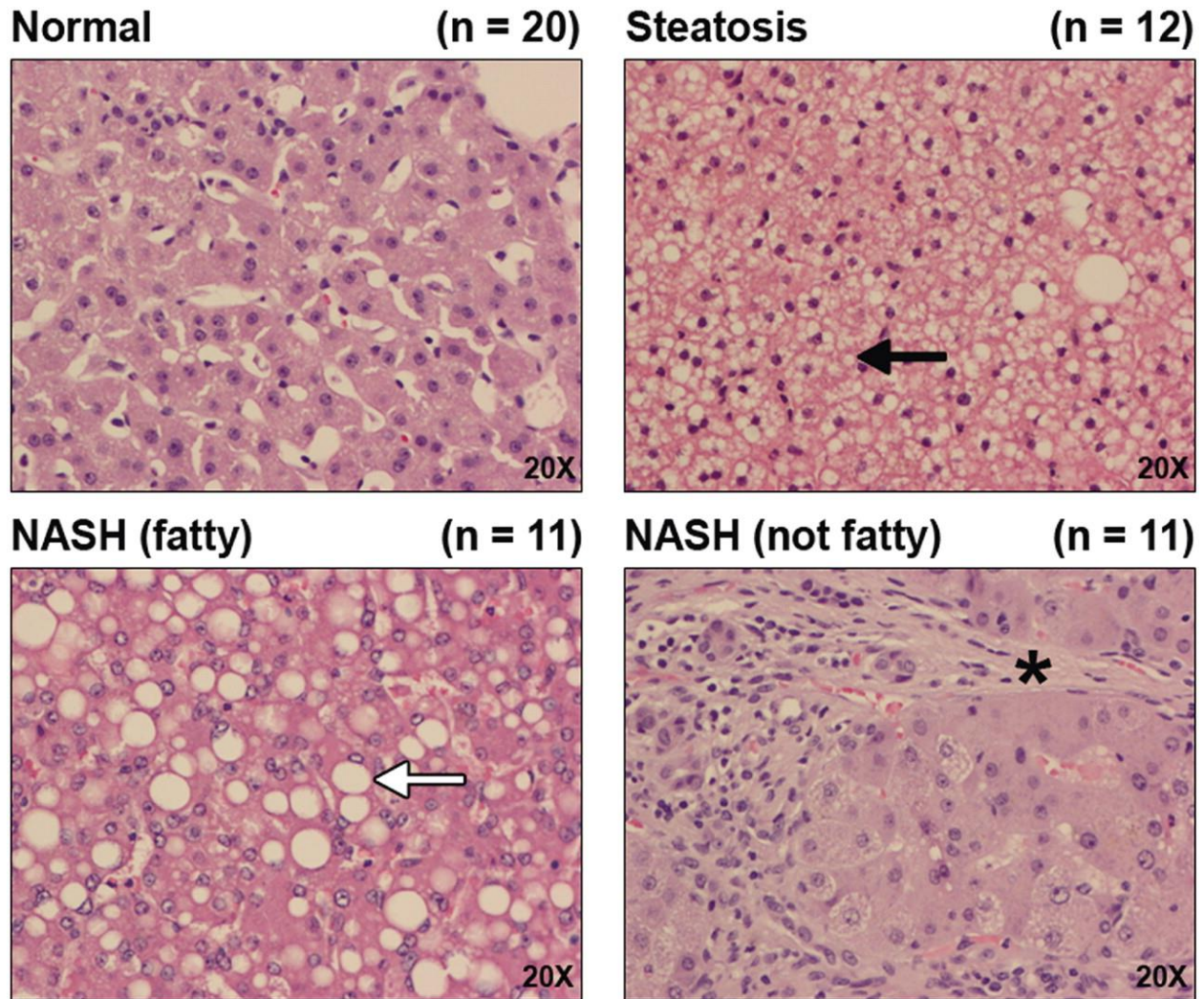


Figure 1.2. Histology of human NAFLD. H&E staining of FFPE human liver samples diagnosed as normal, steatotic, NASH (fatty), and NASH (not fatty), shown at magnification 20x. Diagnoses: steatosis, >10% fatty infiltration of hepatocytes with microvesicular steatosis (black arrow); NASH (fatty), >5% fatty infiltration with macrovesicular steatosis (white arrow), inflammation, and fibrosis; NASH (not fatty), <5% fatty infiltration with more significant inflammation and fibrosis (*). Hardwick *et al.*, *Drug Metab. Dispos.* **2011**, 39, 2395-2402.

NASH is considered a complex disease, as it has no one single genetic variation or origin that is associated with its pathogenesis. Several molecular mechanisms underlie the pathogenesis of NAFLD and NASH, including perturbations of free fatty acid (FFA) packaging, mitochondrial dysfunction, oxidative stress and inflammation, and fibrinogenesis.

Lipotoxicity

The liver is a major site of lipid metabolism, and is the major organ that imports, manufactures, stores, and packages lipids. Perturbation of any of these processes could lead to dysfunctional lipid processing and subsequently contribute to the development of NAFLD. While fatty acids (FAs) are important for regular cellular function and are required for processes such as forming lipid membranes and cellular signaling, chronically elevated FAs can cause disturbances in metabolic pathways and is highly associated with insulin resistance (Buzzetti, Pinzani, & Tsochatzis, 2016). Insulin resistance in the peripheral adipose tissue in particular increases lipolysis and the delivery of FFAs to the liver; this process can be exacerbated by obesity, which increases the expression of tumor necrosis factor α (TNF α) in adipocytes, enhances adipocyte insulin resistance, and increases the rate of lipolysis (Morigny, Houssier, Mouisel, & Langin, 2016). Under normal circumstances, excess FFAs would stimulate the synthesis of triglycerides (TGs), which would then be stored within hepatocytes in droplets or secreted into the blood as very-low-density-lipoprotein (VLDL) (Buzzetti et al., 2016). The excessive accumulation of hepatic triglycerides in NAFLD and NASH are associated with the increased pool of FFA from peripheral adipocytes and increased *de novo* lipid synthesis, as well as increased VLDL production and β -oxidation of FAs (Paglialunga & Dehn, 2016; Saponaro, Gaggini, & Gastaldelli, 2015). These abundant FFAs in NAFLD then causes lipotoxicity through the induction of ROS release, leading to inflammation, cell death, fibrosis, and the progression of the disease to NASH (Ibrahim, Kohli, & Gores, 2011).

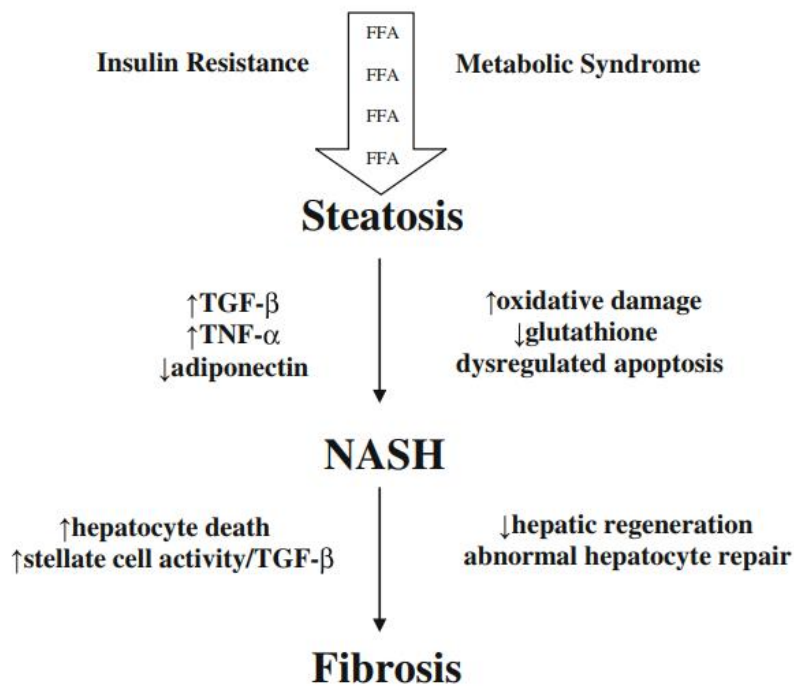


Figure 1.3. “Multi—hit” hypothesis: pathogenesis of NAFLD. In this model, dysregulated free fatty acid (FFA) metabolism (the “first hit”) results in lipid accumulation in the liver, producing steatosis. Inflammatory mediators, reactive oxygen species, and abnormal apoptotic mechanisms serve as “second hits” that result in superimposed inflammation (NASH). The interplay between inflammatory mediators and the activation of stellate cells can lead to fibrosis that, left unchecked, will overcome the regenerative capacity of the liver, producing cirrhosis.

Edmison *et al.*, Clin Liver Dis, **2007**, 11.1, 75–104.

In addition to the alterations to lipid metabolism that occur during NAFLD, hepatic mitochondria are structurally and molecularly altered, and the decline in mitochondrial function may exacerbate metabolic disturbances and drive disease progression (Simões, Fontes, Pinton, Zischka, & Wieckowski, 2018). FAs are oxidized within the mitochondria, peroxisomes, and the endoplasmic reticulum (ER), and while short and medium-chain FAs can pass the mitochondrial membrane, long-chain FAs (LCFA) require activation in the cytosol by acetyl-CoA and transport across the membrane via carnitine palmitoyltransferase-1 (CPT1) (Berlanga, Guiu-jurado, Porras, & Auguet, 2014). In NAFLD, the increased pools of FFA increases the burden of

oxidation and TCA cycle stimulation on hepatic mitochondria, promoting the formation of superoxides through the over-reduction of respiratory complexes(Aharoni-simon, Hann-obercyger, Pen, Madar, & Tirosh, 2011). Mitochondrial damage can occur once the superoxides are enzymatically converted into hydrogen peroxide. Additionally, during FA overload, ω -oxidation of LCFAs induces ROS formation and lipid peroxidation in the ER(Berlanga et al., 2014). To compensate for the increase in ROS formation, upregulation of PPAR α and UCP-2 occurs to increase fatty acid oxidation and increase the activity of the electron transport chain to limit the further production of ROS, respectively. This adaptive response, however, also decreases the proton gradient and hampers ATP production, leaving the hepatocytes vulnerable to ATP depletion and necrosis, as has been observed in NASH patients(Cortez-Pinto et al., 1999; Koek, Liedorp, & Bast, 2011).

Peroxisomal β -oxidation of FFAs are responsible for the formation of acetyl-COA, which is transported to the mitochondria for further degradation. Peroxisomal genes involved in lipid metabolism are controlled by PPAR α , and increased expression of these genes is associated with the induction of peroxisome proliferation. This increase in the number of peroxisomes in the hepatocyte increases the cell's capacity to oxidize FFAs, leading to a higher production of H₂O₂ that can be converted to highly reactive hydroxyl radicals.(Koek et al., 2011; Pawlak, Lefebvre, & Staels, 2015)

Lipid peroxidation is the oxidative degradation of lipids that occurs when an electron is stolen from an unsaturated fatty acid, resulting in lipid peroxides. This can result in membrane disruption and the formation of reactive products like malondialdehyde (MDA) and 4-hydroxy-2,3-transnonenal (4-HNE), which can themselves cause damage through the formation of deleterious DNA adducts(Koek et al., 2011). Both MDA and 4-HNE are used as biomarkers of lipid oxidation, and these biomarkers have been found in higher levels in up to 90% of NASH patients when compared to patients with steatosis. 4-HNE is primarily found in the cytoplasm of

hepatocytes and sinusoidal cells and correlates well with the histological grade of inflammation(Ucar et al., 2013).

Hepatic iron accumulation may contribute to disease progression through the production of reactive oxygen species. Iron can catalyze the conversion of peroxides into hydroxy and hydroperoxyl radicals, which are highly reactive and can cause significant oxidative damage in cells(Yang & Stockwell, 2016). Patients with chronic liver disorders such as chronic hepatitis C, NAFLD, NASH, and cirrhosis exhibit increased hepatic iron deposition even in the absence of mutations in the hemochromatosis gene (HFE). There are three primary patterns of hepatic iron deposition: exclusively in hepatocytes, exclusively in the reticuloendothelial system (RES) cells, or distributed throughout both hepatocytes and RES cells(Nelson et al., 2011). Hepatic iron accumulation in patients with cirrhosis or secondary iron overload generally begins in the RES cells, while deposition in patients with NAFLD, NASH, or chronic hepatitis C may occur in any pattern(Batts, 2007; Y., 2007). The role that iron plays in liver disease progression, if any, is unclear, though several studies have insinuated a relationship between hepatic iron loading and disease stage in hepatitis C patients and iron deposition in the RES cells and advanced fibrosis in alcoholic liver disease(Kohgo et al., 2005; Price & Kowdley, 2009). In NAFLD and NASH patients, those with the RES iron staining pattern were significantly more likely to have advanced fibrosis than those with the hepatocyte staining pattern were also more likely to have advanced histological features such as fibrosis, portal inflammation, and a definitive NASH diagnosis(Nelson et al., 2011). This indicates that the presence and pattern of iron deposition in patients with NAFLD and NASH plays a role in disease pathogenesis and may represent a potential avenue of therapeutic intervention.

Antioxidant Response

In normal physiological conditions, reactive oxygen species would be resolved by ROS detoxification mechanisms like SOD2, catalase, or GSH, or through reduction in substrate

delivery to the TCA cycle. However, there is evidence to suggest that antioxidant response pathways are dysfunctional in patients with NASH and other chronic liver diseases, resulting in unconstrained damage from ROS. The decreased expression of antioxidant factors such as coenzyme Q10, catalase, Cu/Zn superoxide dismutase (SOD1), glutathione, and glutathione S-transferase are shown to correlate with disease severity(LECLERCQ, 2004), and patients with NAFLD and NASH have been observed to have lower hepatic GSH:GSSG ratios than healthy patients, indicating a higher burden of oxidative stress(R. N. Hardwick, Fisher, Canet, Lake, & Cherrington, 2010). It should be noted that there does not appear to be dysfunctional GSH synthesis during the progression of the disease; NRF2 activation appropriately occurs in response to oxidative stress, as has been evidenced through nuclear immunohistochemical staining of NRF2, leading to increased expression of antioxidant response proteins like NQO1, GST isoforms, GCLC, and GCLM following disease progression. However, the activity of enzymes like GST appears to be decreased in NAFLD and NASH patients(R. N. Hardwick et al., 2010), indicating that the impairment of the antioxidant response may lie in the dysfunction of particular antioxidant defense enzymes rather than in dysregulation of expression.

Inflammatory Response

Liver inflammation leads to hepatic damage and the formation of fibrosis and is one of the major drivers of NASH disease progression. The presence of inflammatory cytokines may play a central role in the progression of NAFLD to NASH. Evidence suggests a correlation between the circulating levels of tumor necrosis factor- α (TNF α) and the severity of steatosis, inflammation, necrosis, and fibrosis(Marra, Gastaldelli, Svegliati Baroni, Tell, & Tiribelli, 2008). Similarly, interleukin-6 (IL-6) levels in the blood and liver of NASH patients was significantly elevated when compared to those with steatosis or normal biopsies, and positively correlated to the degree of inflammation, stage of fibrosis, and degree of systemic insulin resistance(Wieckowska et al., 2008). Chronic IL-6 exposure will also cause chronic activation of

the JAK-STAT pathway, which is controlled through a negative feedback loop via the suppressors of cytokine signaling (SOCS) family. SOCS family members also can interfere with insulin-receptor and leptin-receptor signaling, thus depicting a potential link between liver inflammation, insulin resistance, and obesity(Howard & Flier, 2006). ROS and lipid peroxides are factors that can contribute to the generation of inflammatory signals that ultimately result in neutrophil chemotaxis and the hepatic lesions associated with NASH(Marra et al., 2008). These ROS can also activate the NF- κ B pathway, thus inducing the expression of TNF α and also resulting in an elevation of the levels of other cytokines, such as the transforming growth factor- β (TGF β), IL-6, IL-8, and Fas ligand(Rolo, Teodoro, & Palmeira, 2012). Additionally, this activation of TNF α can further exacerbate oxidative stress in the liver by causing additional lipid peroxidation of mitochondrial membranes and also induces NADPH oxidase (NOX) activity, which leads to an inflammatory response through tumor necrosis factor receptor-1 (TRF-1) expression and NF- κ B activation(Koek et al., 2011). TNF α and TGF- β are also involved in the formation of Mallory bodies, a common histological feature of NASH, and in the activation of stellate cells that induce fibrotic formation(Mehta, Van Thiel, Shah, & Mobarhan, 2002). Fibrosis formation by stellate cells can also be up-regulated through glucose and insulin, indicating a possible link between diabetes, hyperinsulinemia, and liver fibrosis in NASH(Koek et al., 2011).

Other proinflammatory factors that may contribute to the inflammatory response in the fatty liver include the pattern-recognition receptor (PRR) family. These receptors consist of Toll-like receptors (TLRs) and other receptors that can recognize bacterial products and activate a variety of pathways, including the NF- κ B pathway, further exacerbating and maintaining the presence of inflammatory mediators and fibrosis formation(Schwabe, Seki, & Brenner, 2006; Seki et al., 2007).

NALFD and NASH is rapidly becoming the most common chronic liver condition worldwide due to the rising rates of obesity in both adult and pediatric patients. The progression of this disease is a complex interplay between lifestyle, the environment, and genetic factors, though there is not yet a full understanding of its pathogenesis. No drug therapies currently exist to ameliorate NASH, though the presence of NASH has significant implications for the drug therapies involved in the management of conditions that are comorbid with the disease.

ADME in the Liver

The liver is the major organ of metabolism of endogenous and xenobiotic compounds through phase 1 modification and phase 2 conjugation reactions and subsequent elimination through xenobiotic transporter proteins. While some compounds are capable of diffusing across the membrane, many large, polar compounds can only enter the hepatocyte through active transport. Endogenous substrates of hepatic transporters include coproporphyrins, bile acids, bilirubin, and hormones such as estrone sulfate, while exogenous substrates include statin drugs, chemotherapeutics such as methotrexate and paclitaxel, and antimicrobials such as caspofungin and rifampin(König, 2011; Takehara et al., 2018). Hepatic uptake is mainly mediated through transporters of the SLC (solute carrier) family, including the organic anion transporting polypeptides OATP1B1, OATP1B3, OATP1A2, and OATP2B1; the organic anion transporter OAT2; the sodium/bile acid cotransporter NTCP; and the organic cation transporter OCT1 in humans(Giacomini et al., 2010) (fig.1.4).

The liver plays an important role in protecting against chemical insults via its ability to convert lipophilic compounds into more hydrophilic metabolites that can be excreted into urine or bile. Its capacity for these detoxification steps is due to the expression of a large number of drug metabolizing enzymes which allow for the oxidation, reduction, and hydrolysis in the case of phase 1 metabolism, and conjugation in the case of phase 2 metabolism. Phase 1 metabolism is mostly mediated by cytochrome P450 (CYP) enzymes, but may also involve other

enzymes like oxidases, peroxidases, hydrolases, and esterases. The end result of phase 1 metabolism is usually either the exposure or addition of a functional group that may later become the target of phase 2 conjugation. During conjugation reactions, the labile functional groups, usually carboxyl, hydroxyl, amino, or sulfhydryl groups, will be modified by a charged species such as GSH, sulfate, or glucuronic acid, resulting in the detoxification of reactive electrophiles and also a large, polar metabolite that cannot diffuse across plasma membranes. These conjugated metabolites generally require active transport to be excreted into bile or urine.

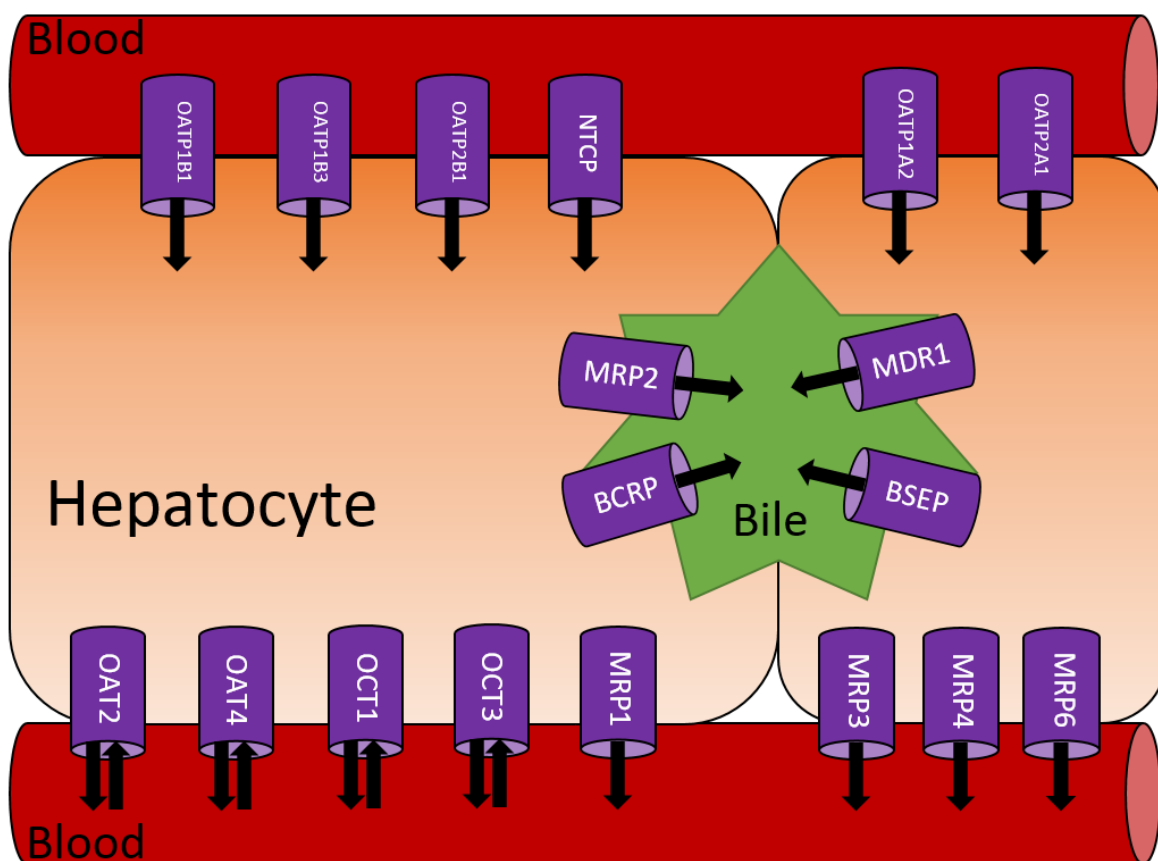


Figure 1.4. Hepatic uptake and efflux transporters. Compounds are taken into hepatocytes from the blood via the sinusoidal uptake transporters. Transporters on the bile canalicular export compounds and their metabolites into the bile for excretion. Sinusoidal efflux transporters export compounds metabolites from hepatocytes into blood.

The active transport of compounds into bile or urine is usually facilitated through transporter proteins of the ATP binding cassette transporter family. Among the many functionally diverse transporters contained within this group, however, only some of them are relevant to the transport of pharmaceutical drugs: P-glycoprotein (P-gp), breast cancer resistance protein (BCRP), and the multidrug resistance proteins 1-5 (MRPs). These transporters are localized to either the plasma membrane or the bile canaliculuar membrane, where they participate in the export of compounds either into blood or into bile in an active, ATP-dependent manner (fig.1.4).

Drug efflux transporters can be divided into four classes based on predicted two-dimensional structure and amino acid sequence homology. The first of these classes is based on the structure of P-gp, which consists of two domains of six transmembrane segments each with two nucleotide binding domains, *N*-glycosylated at the first extracellular loop. The second class contains MRP1, 2, and 3, which have an additional 5-member transmembrane domain at the N-terminus, with *N*-glycosylation at the sixth extracellular loop and the N-terminus. The third class contains MRP4 and 5, which lack the extra 5-member transmembrane domain of MRP1, 2, and 3 and instead are *N*-glycosylated at the fourth extracellular loop. The fourth class contains BCRP, which is a half-transporter that consists of a single six-member transmembrane domain and one nucleotide binding domain at the N-terminus. (Schinkel & Jonker, 2012)

While the function of drug metabolizing enzymes and xenobiotic transporters is important for the timely detoxification and elimination of compounds, they can also be the site for drug-drug interactions when multiple compounds compete for enzymatic activity or transport. DMEs may also be responsible for the production of reactive metabolites that can result in off-target effects, including toxicities. Some drugs are also activated through hepatic metabolism, a process known as bioactivation, and a lack of timely bioactivation could result in decreased therapeutic effect. Alterations to the expression of DMEs and xenobiotic transporters, whether

via transcriptional, translational, or post-translational means, could therefore have a significant impact on the metabolism and elimination of compounds.

Regulation of DMEs

Drug metabolizing enzymes, such as those within the cytochrome P450 family (CYPs), are particularly relevant for clinical pharmacology, and significant pharmacokinetic and pharmacodynamic variability stems from the expression and function of these enzymes (fig.1.5). While polymorphisms explain some of the variability seen in enzymatic activity, other factors are also involved in the regulation of DMEs, including polymorphisms of regulatory genes, age, sex, xenobiotic exposure, and disease state. Though many CYP450 enzymes have overlapping substrate specificity, many clinically relevant compounds are only metabolized to a significant degree by a few enzymes, which limits the redundancy in the phase I oxidation system and increases the importance of enzyme expression, function and activity on predicting drug response(Zanger & Schwab, 2013).

There have been decades of research into the heritable genetic variation in DMEs, and there are many examples of clinically relevant variants. In *CYP* genes, the majority of variants that impart a loss of function do not impact transcription or protein structure, but rather cause aberrations in splicing and expression(Sadee et al., 2011). Variations that induce a gain of function in these enzymes generally involve an increase in copy number variants, promoter variants, and amino acid variants with increased substrate turnover, while few involve aberrations in substrate selectivity or pathway inducibility(Johansson & Ingelman-Sundberg, 2008; Zanger & Schwab, 2013). Clinically, polymorphisms of DMEs can have significant impacts on pharmacokinetics and pharmacodynamics; loss-of-function variants may result in prolonged exposure while gain-of-function variants may result in decreased efficacy of any given therapeutic, and vice-versa in the case of prodrugs that require bioactivation.

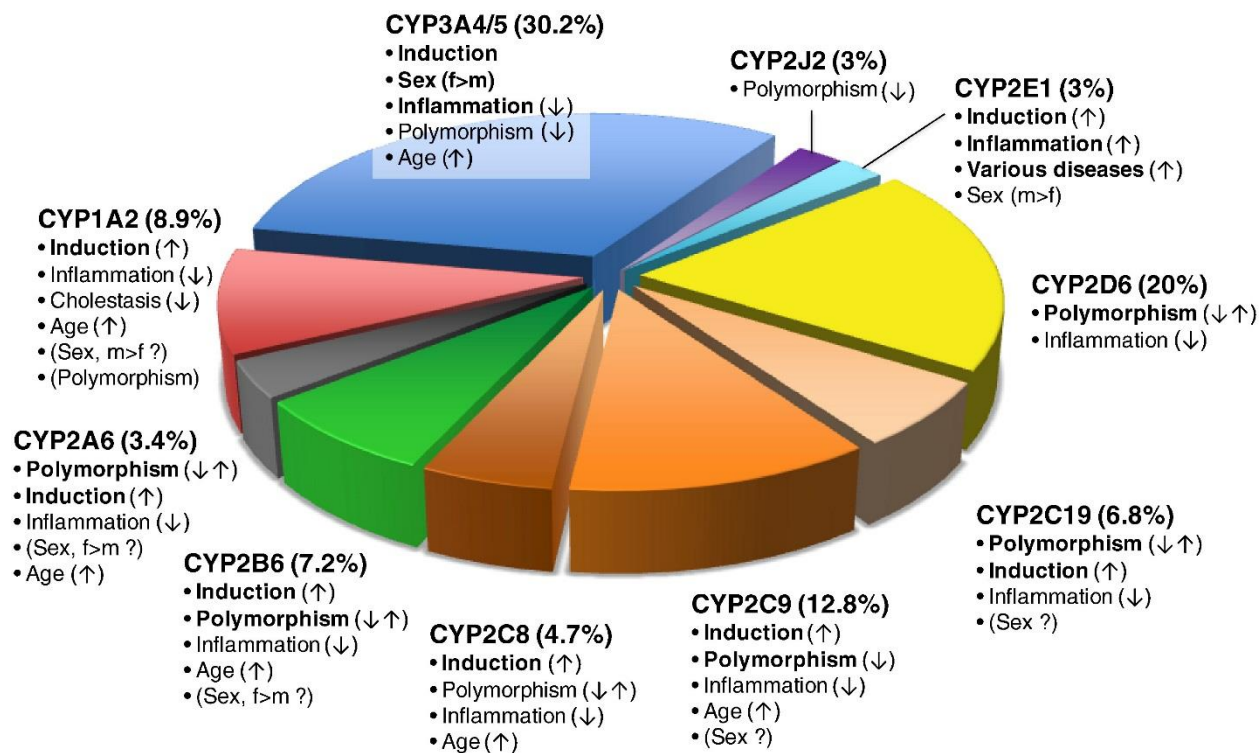


Figure 1.5. Fraction of clinically used drugs metabolized by P450 isoforms and factors influencing variability.

Important variability factors are indicated by bold type with possible directions of influence indicated (↑, increased activity; ↓, decreased activity; ↑↓, increased and decreased activity). Factors of controversial significance are shown in parentheses. Zanger and Schwab, *Pharmacology and Therapeutics*, 2013, 138.1, 103-141.

Not all heritable variations involve an alteration to the DNA sequence of a gene. Epigenetic variations can control gene expression through DNA methylation, histone modification, and through microRNA (miRNA) regulation. In general, DNA methylation of promoter regions suppresses the expression of the target gene by inhibiting transcription factor binding or recruiting methyl-CpG-binding proteins that alter chromatin structure. For many DMEs, there is an inverse correlation between mRNA expression and DNA methylation, including with *CYP1A2*, *CYP2C19*, *CYP2D6*, *GSTA4*, *GSTM5*, *GSTT1*, and *SULT1A1*, as observed in adult human liver (Habano et al., 2015). For certain enzymes, such as *CYP3A4*, hepatic expression is highly variable in humans, but there are few genetic variations that contribute significantly to this variability. While it has been previously shown that methylation of

the promoter site of *CYP3A4* has little impact on gene expression, methylation at CpG sites near or within transcription factor binding sites does correlate with the expression of *CYP3A4* in adult human liver (Fisel, Schaeffeler, & Schwab, 2016; Habano et al., 2015; Kacevska et al., 2012). In addition to DNA methylation, miRNA can also regulate gene expression, usually through binding to a section of the 3'UTR segment of a target gene, causing an inhibition of translation or cleavage of the target mRNA and reduced expression of the protein. miRNA posttranscriptional regulation has been observed in DMEs; the broadly conserved miR-27b targets, among others, the 3'UTR of *CYP3A4* and *CYP1B1*, downregulating the protein and mRNA expression of these enzymes, while *CYP2E1* is negatively regulated by miR-378, but through translational repression rather than mRNA degradation. (Pan, Gao, & Yu, 2009; Yokoi & Nakajima, 2013). Even outside of direct modulation of gene expression, miRNAs can indirectly modulate expression by regulating nuclear receptors and other transcription factors like PXR, NRF2, and PPARs (Y. Chen, Xiao, Zhang, & Bian, 2016; Yokoi & Nakajima, 2013).

DME expression at the transcriptional level is largely mediated through various transcription factors. These regulatory proteins generally contain a highly conserved DNA binding domain that allows for binding to promoter regions of target genes, and a variable ligand-binding domain that allows for the interaction between the protein and a wide range of endogenous or exogenous compounds. A number of nuclear receptor transcription factors, notably farnesoid X receptor (FXR), liver X receptor (LXR), peroxisome proliferator activation receptors (PPARs), constitutive androstane/active receptor (CAR), pregnane X receptor (PXR), nuclear factor-erythroid 2-related factor 2 (NRF2), and aryl hydrocarbon receptor (AhR), bind xenobiotics such as pharmaceuticals and environmental toxicants, and their activation results in the upregulation of genes that encode for phase I and phase II DMEs (Tolson & Wang, 2010).

Regulation of Transporters

Similar to DMEs, hepatic transporter expression is regulated by a number of different mechanisms, including transcription factors, genetic polymorphisms, epigenetic modifications, and miRNAs. A solid understanding of the mechanisms of transporter regulation is of potential importance to more accurately predict pharmacokinetics and variable drug responses in human populations.

Genetic polymorphisms of hepatic uptake and efflux transporter proteins have been extensively studied with regards to their potential impact on the pharmacokinetics of xenobiotics. There are multiple variants of OATP uptake transporters that are known to cause alterations to the pharmacokinetics or drug responses of substrates, including the reduction-of-function c.521T>C variant of *SLCO1B1*, which increases the risk of statin-induced myopathy, and the c.1683-5676A>G reduction-of-function variant of *SLCO1B3*, which has been associated with an increased risk of docetaxel-induced neutropenia (Franke, Gardner, & Sparreboom, 2010; Maeda, 2015). Polymorphisms of efflux transporters can also result in significant pharmacokinetic alterations; the c.24C>T variant of *ABCC2* alters the volume of distribution and clearance rate of methotrexate in human patients, and the c.421C>A variant of *ABCG2* is significantly correlated with altered erlotinib clearance in Japanese lung cancer patients (Fukudo et al., 2013; Simon et al., 2013).

Beyond DNA sequence variation, epigenetic control mechanisms like methylation of genomic DNA, histone modification, and regulatory noncoding RNAs can alter gene expression of hepatic transporter proteins. Methylation of the *ABCB1* promoter region has been shown to inversely correlate with mRNA expression. Similarly, methylation of the *ABCG2* promoter region also decreases mRNA expression in myeloma patients, and also the binding of methyl-CpG binding domain proteins to CpG islands of this gene alters acetylation and therefore modulates gene expression (Kim, Han, Burckart, & Oh, 2014). Additionally, miRNAs participate in the posttranscriptional regulation of uptake and efflux transporters. Over a dozen miRNAs

are known to regulate the expression of *ABCB1*, including miR-27a and miR-451 and the expression of *ABCC2* is regulated through miR-297, miR-379, and let-7c. *SLC16A1* has also shown to be regulated by miR-124 and miR-29a/b (Yu, Tian, Tu, Ho, & Jilek, 2016). These miRNAs alter the mRNA and protein expression of these genes, as well as the protein function.

Transcription factors are a major factor in the transcriptional regulation of hepatic xenobiotic transporter genes. The activation of transcription factors such as the aryl hydrocarbon receptor (AhR), constitutive androstane receptor (CAR), pregnane X receptor (PXR) and nuclear factor E2-related factor 2 (Nrf2) plays a significant role in the expression of efflux and uptake transporters in the liver. Many ADME-related genes, including some xenobiotic transporters, contain antioxidant response elements (AREs) and therefore are impacted by the redox-sensing NRF2 transcription factor, including *Abcg2*, *Abcc2*, *Abcc3*, and *Abcc4*, which show significant downregulation of mRNA expression in *Nrf2*-null mice (Reisman, Csanaky, Aleksunes, & Klaassen, 2009). This is supported in human primary hepatocyte cell culture assays, where Jigorel et al. determined that the mRNA expression of *MDR1* (P-gp), *ABCG2*, *ABCC2*, and *ABCC3* were upregulated by incubation with oltipraz (OPZ), a known NRF2 activator. In addition to NRF2 inducers, *ABCG2* and *MDR1* were upregulated by treatment with dioxin (TCDD, an AhR activator) and rifampicin (RIF, a PXR activator), and *ABCC3* was also upregulated after exposure to RIF. The bile acid transporters *ABCB11* and *SLC10A1* and the sinusoidal uptake transporter *SLC22A7*, conversely, were downregulated after exposure to OPZ, RIF, TCDD, and phenobarbital (PB, a CAR activator). Other uptake transporters also become downregulated in the presence of transcription factor activators, including *SLC22A1* and *SLCO1B3* via PB, TCDD, RIF, and OPZ and *SLCO2B1* via PB and TCDD. (Jigorel, Le Vee, Boursier-Neyret, Parmentier, & Fardel, 2006) Transporter regulation through transcription factor activation is a complicated process, and many transporters can be

regulated through multiple pathways, allowing for significant inter-individual variability among humans.

ADME Remodeling in NASH

A 2011 study involving human liver biopsies from patients who had confirmed diagnoses of steatosis, fatty NASH, or non-fatty NASH were analyzed using an AffyMetrix GeneChip to determine altered mRNA expression when compared to normal patients. This study found that 11,633 genes were dysregulated during the progression of NASH, including a variety of genes that are important to ADME processes, such as drug metabolizing enzymes and xenobiotic transporters(Lake et al., 2011). Many different pathways were found to be altered during the progression of this disease, including those involved in endoplasmic reticulum stress, antioxidant response, and N-linked glycosylation of proteins(Clarke, Novak, Lake, Hardwick, & Cherrington, 2016; R. N. Hardwick et al., 2010; Lake et al., 2013). While previous studies have examined the gene expression of various pathological groups related to NAFLD and NASH, this study notably compares all three pathological groups (normal, steatosis, and NASH), and therefore is able to determine global gene expression alteration patterns across disease progression. In this way, the study was able to identify that the majority of gene expression alterations occur during the progression from steatosis to NASH, and not from the progression of normal to steatosis(Lake et al., 2011). In particular, the pairwise comparison of over 500 transporter genes revealed significant trends in the expression of uptake and efflux transporters in NASH. The hepatic uptake transporter genes showed significant enrichment for downregulation, which may represent a protective mechanism in the liver by which it attempts to prevent the accumulation of toxic compounds or metabolites by limiting hepatic uptake; this is bolstered by studies in mouse models that reveal similar transporter alterations in the presence of toxic doses of acetaminophen and carbon tetrachloride(Aleksunes et al., 2004; Lake et al.,

2011). Conversely, the hepatic efflux transporters showed significant upregulation during the progression of NASH, further coinciding with other research that determined that there is a concomitant upregulation of efflux transporter mRNA during hepatotoxicant exposure in mouse models(Aleksunes, Scheffer, Jakowski, Pruiomboom-Brees, & Manautou, 2005; Lake et al., 2011).

The Cherrington group has put a significant amount of effort into determining the specific alterations to drug metabolizing enzymes that occur during the progression of NASH and their potential impact on pharmacokinetics. As the cytochrome P450 enzyme family is responsible for the majority of xenobiotic metabolism in the liver, alterations to the mRNA and protein expression of these enzymes during the progression of NASH could have significant pharmacokinetic consequences. As the CYP1, CYP2, and CYP3 families are responsible for about 75% of the biotransformation of pharmaceuticals in humans, determining the impact of disease state on their function is of particular importance. In adult human patients, CYP1A2, 2C19, and 2E1 show decreased mRNA expression, while CYP2A6, 2B6, and 2C9 show increased mRNA expression with respect to disease progression. Following mRNA expression, CYP2A6 protein expression is also increased during the progression of NAFLD; CYP2B6 and CYP2C9 show no significant changes, however. CYP1A2, 2C19, and 2E1 show decreased protein expression following the mRNA trend, and additionally, CYP2C8, 2D6, and 3A4 also had decreased expression(Fisher, Lickteig, Augustine, Ranger-Moore, et al., 2009). When probe substrates were used to determine enzymatic activity, CYP1A2, 2C19, 2D6 and 3A4 exhibit decreased function, while CYP2A6 and 2C9 showed increased function(Fisher, Lickteig, Augustine, Ranger-Moore, et al., 2009). The discrepancies between alterations to mRNA expression and protein expression are likely due to post-translational and other forms of regulation. In pediatric populations, though there are similar cardiovascular and metabolic risk factors, there are differences certain histological features, potentially due to differences in

toxicant exposures and pubertal hormone levels that may result in alterations to pathogenesis(Crespo, Lappe, Feldstein, & Alkhoury, 2016). The activity of CYP enzymes was determined in a pediatric population, and the only enzyme that was significantly changed during the progression of the disease was CYP2C19, which was significantly decreased in NASH pediatric patients(Li, Canet, et al., 2017). This is different from the enzyme alterations found in adult NASH patients, implying that pediatric and adult NASH are distinct and adolescent populations should be treated as a separate at-risk group from adults.

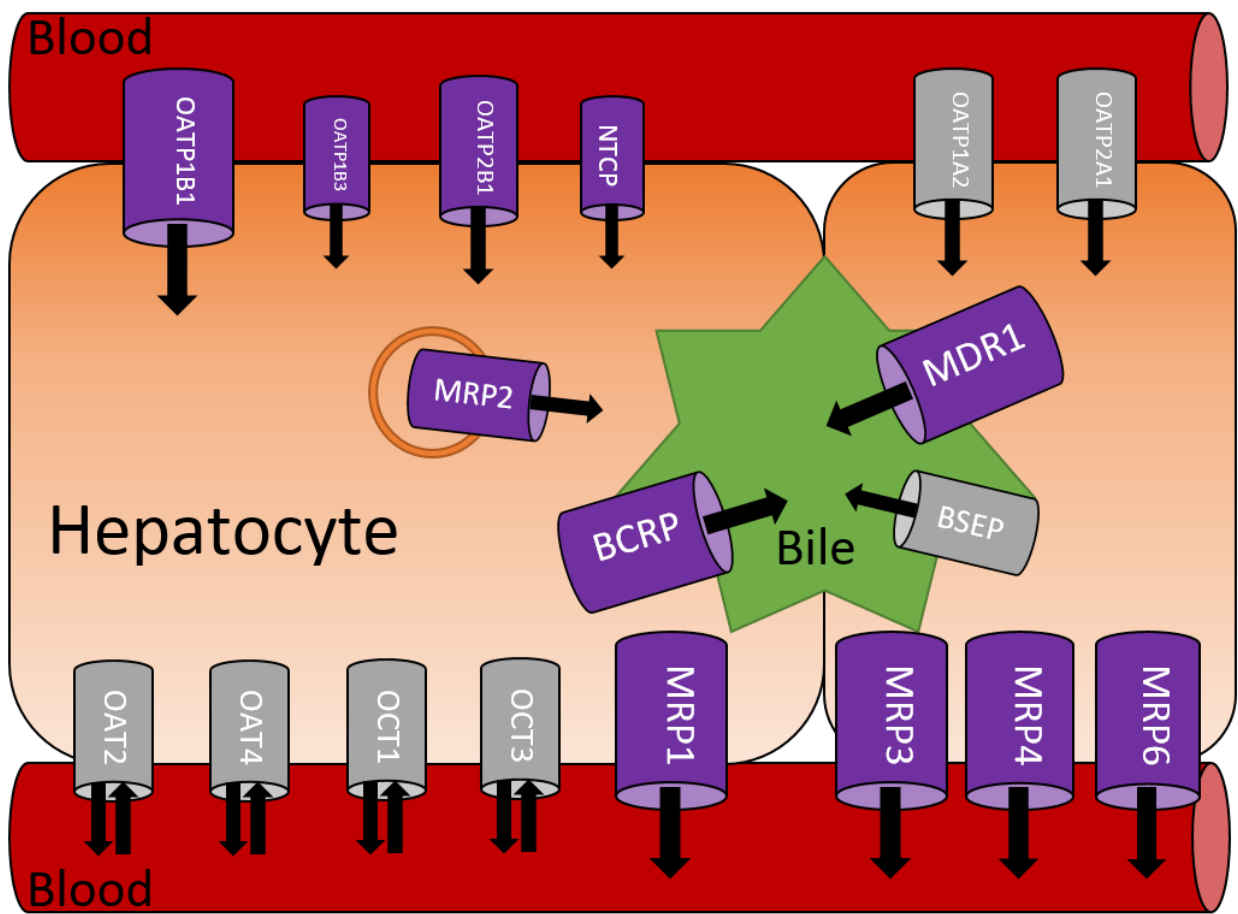


Figure 1.6. Alteration to hepatic uptake and efflux transporters during NASH. Protein expression for hepatic uptake transporters experience a general downregulation during NASH, while efflux transporters are generally upregulated. MRP2 protein becomes mislocalized from the bile canalculus during NASH. No human protein data available for gray transporters.

Drug transporter proteins modulate the movement of endo- and xenobiotics and their metabolites into and out of cells; significant alterations to these proteins on the transcriptional or translational level could therefore cause potentially detrimental changes to the pharmacokinetics and pharmacodynamics of compounds. The Cherrington lab has extensively mapped the alterations that occur to clinically relevant xenobiotic transporters of the *SLC* and *ABC* transporter families and the impact that these changes have on drug distribution and toxicity (fig.1.6). Many of the *SLC* transporters, such as OATPs, OATs, and OCTs, are located on the plasma membrane of hepatocytes and facilitate the uptake of compounds from circulation into the cell. A single SNP in one of these transporters can significantly impact the pharmacokinetics of its substrates; during the progression of NASH, not one, but multiple transporters are dysregulated. Previous research found that in human patients, the protein expression of OATP1B1 was significantly increased during the course of the disease, while OATP1B3 was significantly decreased and OATP2B1 remained unchanged (Clarke et al., 2014). For the *ABC* efflux transporters, a general trend of upregulation was observed; the mRNA expression of *ABCB1*, *ABCC1*, *ABCC3*, *ABCC4*, *ABCC5*, and *ABCG2* were significantly increased in the progression of the disease, while only *ABCC6* showed downregulation and *ABCC2* remained unchanged. The protein expression, however, increases for all of these transporters. (R. N. Hardwick, Fisher, Canet, Scheffer, & Cherrington, 2011) This trend of decreased hepatic uptake transporters and increased hepatic efflux transporters that has been found in human patients bolsters the concept that ADME remodeling during the progression of NASH is a protective mechanism to try to prevent further hepatic injury.

As remodeling during NASH impacts the expression of various hepatic transporter proteins, there is ample evidence that these changes the pharmacokinetics of substrate xenobiotics. In animal models of NASH, the pharmacokinetics of ezetimibe, morphine-glucuronide, pemetrexed, metformin, and methotrexate have altered metabolism and excretion

during the progression of the disease(Clarke et al., 2015; A. L. Dzierlenga et al., 2015; Anika L Dzierlenga et al., 2016; R. Hardwick et al., 2014; R. N. Hardwick, Fisher, Street, Canet, & Cherrington, 2012). These changes generally resulted in an increase in plasma concentrations of xenobiotics and a shift from biliary excretion to urinary excretion; this can also result in a similar shift in toxicity. This toxicity profile shift can be seen with methotrexate; rats with MCD diet-induced NASH that were given a dose of methotrexate experienced decreased biliary excretion and increased plasma retention when compared to controls. These rats also exhibited less intestinal injury, but had increased renal toxicity(R. Hardwick et al., 2014). When normal mechanisms of metabolism and elimination become dysregulated, the risk of toxicity significantly increases.

Hepatocyte Hopping and NASH

Under normal physiological conditions, a blood-to-hepatocyte-to-blood shuttling mechanism known as hepatocyte hopping allows for efficient detoxification of compounds via multiple changes at metabolism and excretion. This mechanism, which was first described by the Schinkel group in 2012, involves three main processes: 1) MRP3 sinusoidal efflux, 2) MRP2 biliary efflux, and 3) OATP sinusoidal uptake. By exporting metabolites back into hepatic blood through MRP3 to allow for downstream reuptake through OATPs, the liver maintains a salvage pathway by which it can circumvent the retention of potentially toxic compounds or their metabolites in the event of saturated excretion processes in upstream hepatocytes(Iusuf, Steeg, & Schinkel, 2012).

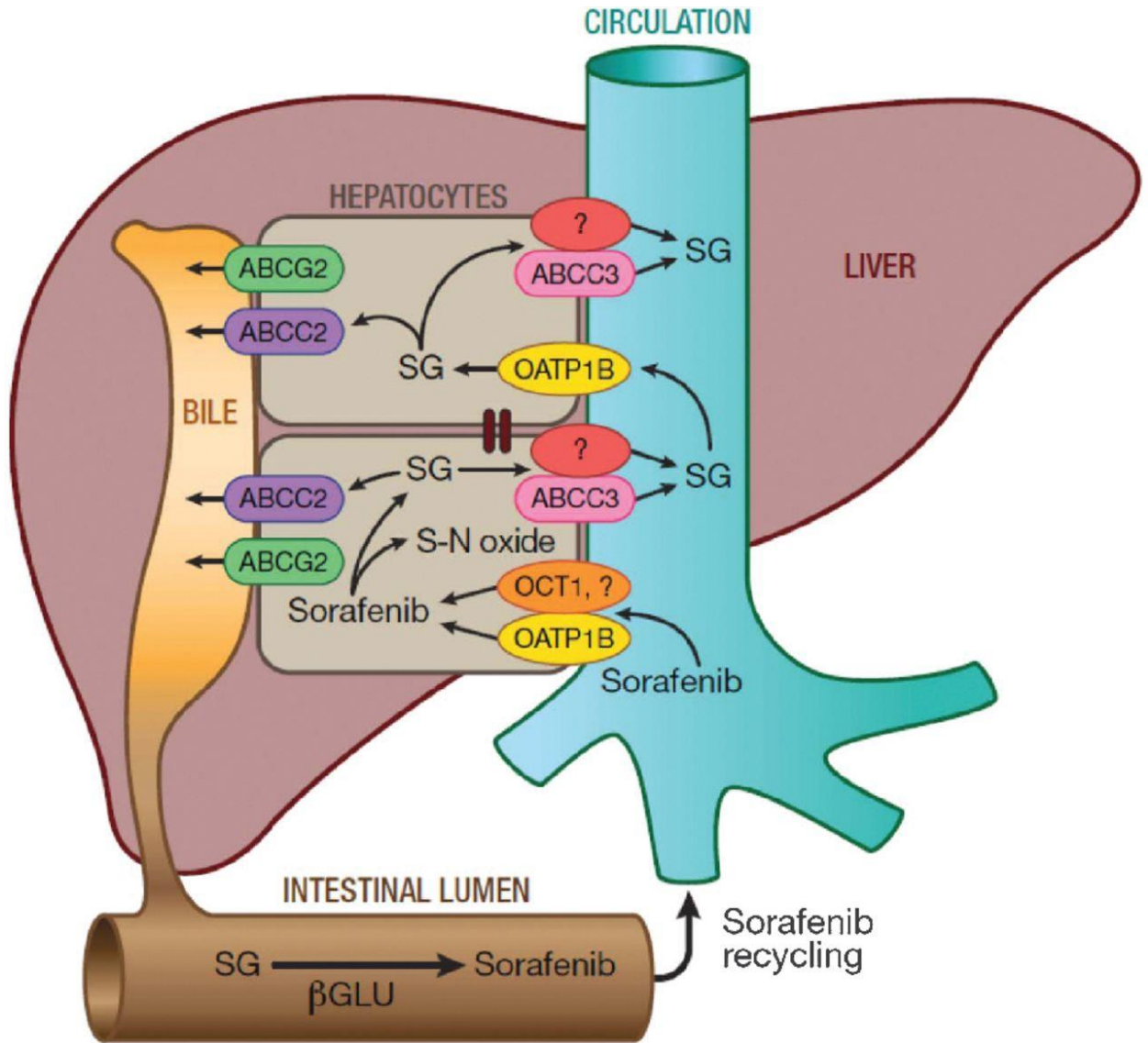


Figure 1.7. Hepatocyte hopping and recirculation of SG. After oral administration, sorafenib enters the hepatocytes by incompletely defined transporters mechanisms, including OATP1B-type carriers and OCT1, and undergoes CYP3A4-mediated metabolism to sorafenib-N-oxide (s-N-oxide) and conjugation by UGT1A9 to form SG. After conjugation, SG is extensively secreted into the bile by a process that is mainly mediated by ABCC2. Under physiologic conditions, a fraction of the intracellular SG is secreted by ABCC3 and at least one other transporter back to the blood, from where it can be taken up again into downstream hepatocytes via OATP1B1-type carriers (Oatp1a and Oatp1b in mice). This secretion-and-reuptake loop may prevent the saturation of ABCC2-mediated biliary excretion in the upstream hepatocytes, thereby ensuring efficient biliary elimination and hepatocyte detoxification. Once secreted into bile, SG enters the intestinal lumen where it serves as a substrate for as yet unknown bacterial β -

glucuronidases (β GLU) that produce sorafenib, which subsequently undergoes intestinal absorption and reenters the systemic circulation. Vasilyeva *et al.*, *Therapeutics, Targets, and Chemical Biology*, **2015**, 75.13, 2729-2736.

Previous studies by the Schinkel group have found that OATP1B1/1B3, MRP3, and MRP2 function play significant roles in hepatocyte hopping. The plasma concentrations of bilirubin, a heme degradation product, drastically increases in *Oatp1a/1b* cluster knockout mice, mostly through an increase in its metabolite, bilirubin-mono-glucuronide (BMG). This increase is reversed, however, in combination *Oatp1a/1b* cluster and *Abcc3* knockout mice, indicating that the plasma accumulation was due to Mrp3 efflux of the metabolite and that Oatp transporters and Mrp3 form a hepatocellular shuttling route for bilirubin (Iusuf *et al.*, 2012). It was also determined in later studies that sorafenib-glucuronide followed the same hepatocellular shuttling loop, and it is likely that a number of substrates would be impacted by the hepatocyte hopping pathway (Vasilyeva *et al.*, 2015) (fig.1.6). As hepatocyte hopping relies on transporter function to shuttle compounds to downstream hepatocytes, liver conditions such as NASH that cause drastic alterations to ADME processes would be detrimental to this pathway, and disruption of normal hepatocellular shuttling could be the underlying mechanism behind the altered pharmacokinetics seen in NASH.

Hepatocyte hopping as an underlying mechanism of pharmacokinetic alteration in NASH is supported by changes to drug disposition observed in both human and rodent models of disease. The three mechanisms involved in hepatocyte hopping are correspondingly regulated in both the human disease and MCD-diet induced NASH, as has been shown with both APAP/APAP-glucuronide and morphine. In the case of APAP and APAP-glucuronide, the biliary concentrations of APAP and its metabolites were significantly decreased in NASH, while the Mrp3 substrate APAP-glucuronide was elevated in NASH rat plasma and urine when compared to the other metabolites (Lickteig *et al.*, 2007). This pattern was also identical to the one found in human patients dosed with APAP (Canet *et al.*, 2015), indicating that the changes to the

MRP2/MRP3 axis are the same between the MCD diet and human NASH. Similarly, the changes to morphine pharmacokinetics follow the same trend in the MCD rat model and human patients, showing an increase in systemic morphine-glucuronide exposure, and an increase in serum exposure of M3G due to decreased biliary efflux and increased sinusoidal efflux of the metabolite (A. L. Dzierlenga et al., 2015; Ferslew et al., 2015; Pierre, Johnston, Ferslew, Brouwer, & Gonzalez, 2017). Alterations to OATP uptake transporters are also known to be concordant between the MCD diet and human NASH (Clarke et al., 2014). As NASH is known to disrupt the three cooperative transport mechanisms involved in hepatocyte hopping, this forms the basis for a potential underlying mechanism for altered drug disposition in human NASH patients.

Hepatic Iron Regulation and NASH

Iron is regulated in the liver in multiple ways, but one of the major methods of controlling iron levels is through iron transport proteins. Ferroportin, a transmembrane protein found in various cell types, including hepatocytes and enterocytes, functions to move iron from the inside of a cell to the bloodstream. As the only known mammalian iron exporter, ferroportin plays a key role in the retention of iron, and dysregulation of the transporter can be the root cause of iron accumulation (D. Chen et al., 2007; Ward & Kaplan, 2012). The hormone hepcidin is the main regulator of ferroportin function, and therefore is one of the principal regulators of iron metabolism as a whole. Hepcidin regulates ferroportin activity by binding to its active site and catalyzing its internalization, removing it from the membrane (Bogdan, Miyazawa, Hashimoto, & Tsuji, 2016; Nemeth & Ganz, 2006), and is itself regulated by intracellular iron concentrations and Nrf2 (Silva-Gomes et al., 2014; Tanaka, Ikeda, Yamamoto, Ogawa, & Kamisako, 2012).

Iron homeostasis is particularly important in humans, as iron cannot be excreted from the body by any means other than hemorrhaging or enterocyte sloughing (Nemeth & Ganz, 2006). Under normal conditions, iron levels are strictly maintained to prevent the deleterious

effects of overload or deficiency; however, conditions like liver disease have been known to disrupt iron homeostasis through dysregulation of hepcidin (Bekri et al., 2006; Nemeth et al., 2004). In iron overloaded mice, hepcidin mRNA and protein expression is significantly upregulated, reducing intestinal iron uptake but also preventing iron release from hepatocytes. Concordant results are found with multiple models of iron overload in rodents, indicating that the increase in hepcidin could be attributed to iron accumulation and not to other factors (Pigeon et al., 2001). In humans, hepcidin levels are correlated with hepatic iron accumulation and hemoglobin, as well as decreased liver function. Hepcidin is also significantly upregulated during inflammation, and can rise to levels far higher than what is seen for normal iron regulatory function (Nemeth & Ganz, 2006). In patients with NAFLD and NASH, serum hepcidin levels are positively associated with increased triglycerides, cholesterol, and inflammation, and worsened NAS scores (Senates et al., 2011; Zimmermann et al., 2011). Elevated triglyceride and cholesterol levels and inflammation are all well-known hallmarks of NASH; this association suggests the possibility of iron accumulation via the inability to remove iron from hepatocytes, and thus indicates a potential link between hepcidin levels, iron accumulation, and hepatic injury.

Transferrin receptor-1 (TfR1) is a ubiquitously expressed iron uptake protein that imports iron into cells. It facilitates the transport of the glycoprotein transferrin, which contains two high-affinity Fe(III) binding sites and modulates the amount of free iron in blood. In addition to TfR1, TfR2 is a homolog of TfR1 that is located in specific tissues like hepatocytes and hematopoietic cells, and can also internalize diferric-transferrin. The exact function of TfR2 is not fully known, but it is postulated that it acts in a regulatory fashion, whereas TfR1 is the main transporter for iron uptake (Goswami & Andrews, 2006). TfR1 is controlled post-transcriptionally by intracellular iron levels through the interaction of iron response proteins (IRP1/2) and the iron response element (IRE) on mRNA. TfR1 is the only known protein to contain multiple IRE hairpins; it has

5 of these motifs located in its 3' UTR, and binding of the IRPs to these motifs stabilizes the mRNA and allows for translation(PANTOPOULOS, 2004). Regulation of IRP1 comes through post-translational alterations in structure in response to the presence or absence of iron. IRP1 contains an iron-sulfur cluster that acts as a kind of 'switch' in the presence of iron, changing the protein to a cubane structure that prevents it from binding to mRNA(Haile et al., 1992; PANTOPOULOS, 2004). However, IRP1 is not solely modulated by iron, as it has also been shown to become rapidly activated in the presence of ROS and capable of binding to IRE(Mueller, Pantopoulos, Hübner, Stremmel, & Hentze, 2001; Pantopoulos & Hentze, 1998). IRP2 is homologous to IRP1, except for a unique 73 amino acid iron-dependent 'degradation domain'; this domain contains 3 critical cysteine residues that, when oxidized by iron, allow for recognition of the protein by proteasomes and rapid degradation, and is the main means of regulating the protein(Iwai, Klausner, & Rouault, 1995; PANTOPOULOS, 2004).

The ROS produced by iron accumulation may also have an effect on ferritin, the main intracellular protein for the cellular storage of iron. Ferritin is a globular protein composed of 24 subunits of either heavy or light isoforms, and is responsible for containing iron in a soluble and nontoxic form(ten Kate, Wolthuis, Westerhuis, & van Deursen, 1997). Ferritin production is mediated post-translationally by a mechanism similar to TfR1, but in a negative fashion. While the binding of IRPs to the IRE sites on TfR1 stabilizes the protein, the binding of IRP to the single IRE motif in the 5' UTR of ferritin mRNA inhibits its translation(PANTOPOULOS, 2004). Different cell types also produce ferritin with different heavy to light subunit ratios; the liver and spleen contain ferritin with higher proportions of light subunits. The isoforms of the ferritin subunits are particularly important, as the heavy subunits have ferroxidase activity to convert iron from the ferrous to the more stable ferric form for storage. When antioxidants are depleted, as in conditions of high oxidative stress, ferroxidase activity becomes downregulated, preventing the removal of ferrous iron from iron pools in the cell. Additionally, a rapid release of

iron from ferritin occurs during these conditions due to increasing reducing potential and anaerobiosis.(Manuel Fernandez-Real, Lopez-Bermejo, & Ricart, 2002) Overall, this results in a decrease in ferric iron within ferritin proteins and an increase in ferrous iron in intracellular iron pools, with a greater abundance of iron available for deleterious ROS generation.

The deleterious effects of iron accumulation is well understood and has significant support from the literature; the liver's role as the main organ for iron metabolism, the incidence of hepatic iron accumulation in fatty liver diseases, the beneficial effects of iron removal seen in chronic liver disease patients and the effects of ROS and chronic liver diseases on iron storage mechanisms suggests that iron plays an exacerbating role in disease progression.

Current Study

The alterations to pharmacokinetics that occur due to genetic polymorphisms of DMEs and hepatic transporters and the progression of NASH has been well documented in various studies; the interaction of genetic variants with the alterations that occur during NASH, however, has not been greatly explored. As NASH is rapidly becoming one of the most prevalent chronic liver diseases and polymorphisms of DMEs and hepatic transporter proteins are relatively common in human populations, it has become increasingly likely that patients with some form of genetic variation in a key ADME gene will present with NASH. Previous research with a rodent model of NASH and pravastatin has indicated that there can be synergistic relationships between genetic polymorphisms of xenobiotic transporters and NASH, resulting in dramatic increases in plasma and tissue concentrations and an increased risk of toxicity(Clarke et al., 2014). Though full genetic knockout resulted in significantly increased plasma and tissue retention of the compound, the question still remained as to whether full disruption was necessary to observe this change, or whether the accumulation would be affected by gene dose. Additionally, while that particular study focused on the genetic loss of Oatp1b2/OATP1B1 and NASH on the disposition of statins, other transporter proteins also significantly impact drug

disposition, and thus the combination of polymorphisms of these critical transporters and chronic disease may result in increased risk of toxicity. Polymorphisms of BCRP, an efflux transporter located on the bile canaliculus, have been implicated in altered pharmacokinetics of sunitinib, imatinib, and other chemotherapeutics; pharmacokinetic changes have also been found with polymorphisms of MRP2 for docetaxel, mycophenolic acid, lumefantrine, and pravastatin (Patel, Taskar, & Zamek-Gliszczyński, 2016; Terada & Hira, 2015; Vos et al., 2017). As NASH results in the dysregulation of other compensatory transporter pathways, the interaction between the disease and polymorphisms of hepatic efflux transporters may result in pharmacokinetic changes that are greater than the sum of their parts, and identifying these synergistic interactions is important to precision medicine. Additionally, it would be important to determine the underlying mechanism by which the interplay of hepatic uptake and efflux transporter alteration causes the pharmacokinetic changes observed in NASH.

Given these research questions, the purpose of this study was to identify the impact of gene-by-environment interactions of hepatic xenobiotic transporter polymorphisms and nonalcoholic steatohepatitis on drug disposition and toxicity via the studies described in the following aims:

Aim 1 (Chapter 2): Determine the gene-by-environment interaction of hepatic efflux transporter polymorphisms and NASH using probe substrates of Bcrp and Mrp2.

Using *Bcrp* knockout and wild-type rats and the probe substrates SN-38 and SN-38-glucuronide, this study identified the interaction of deleterious *Bcrp* polymorphisms and NASH on drug disposition. These data were valuable in determining the synergistic interaction of hepatic efflux transporter polymorphisms and NASH on pharmacokinetics.

Aim 2 (Chapter 3): Determine the impact of hepatic uptake transporter gene dose and NASH on drug disposition using a probe substrate of Oatp1b2.

Using *Oatp1b2* heterozygous, knockout, and wild-type mice with the probe substrate pravastatin, this study identified the impact of hepatic uptake transporter gene dose and NASH on drug disposition. These data were necessary for determining the extent of genetic disruption to hepatic uptake transporters that is required to observe a synergistic gene-by-environment interaction.

Aim 3 (Chapter 4): Determine the impact of hepatic xenobiotic transporter alteration during NASH on hepatocyte hopping.

Using *Oatp1a/1b* cluster knockout, *Mrp2* knockout, and wild-type mice with the probe substrate sorafenib-glucuronide, this study described the process of hepatocyte hopping in a rodent model of NASH, which pinpointed the underlying mechanism of pharmacokinetic alteration in NASH.

Aim 4 (Chapter 5): Identify the alterations to iron regulatory proteins, iron transporters, and iron storage during NASH.

Using human and MCD diet-induced NASH rat liver tissue, this study investigated the alterations to hepatic iron storage in hepatocytes via histological iron staining with Perls' Prussian blue, as well as the changes in the mRNA and protein expression of key mediators of iron regulation.

CHAPTER TWO: GENE-BY-ENVIRONMENT INTERACTION OF BCRP^{-/-} AND METHIONINE- AND CHOLINE-DEFICIENT DIET-INDUCED NONALCOHOLIC STEATOHEPATITIS ALTERS SN-38 DISPOSITION

Toth EL, Hui L, Dzierlenga AL, Clarke JD, Vildhede A, Goedken M, Cherrington NJ

Published in *Drug Metab. Disp.*

Introduction

Adverse drug reactions (ADRs) are becoming increasingly frequent, and approximately 1 in 20 hospital patients experience an ADR in the United States (Bourgeois et al., 2010; Stausberg, 2014). Variations in drug response can occur due to a variety of factors, including alterations to drug metabolizing enzymes and transporters. Understanding the mechanistic basis behind inter-individual variability can potentially identify at-risk populations.

Many variations in drug response can be attributed to genetic polymorphisms in genes that are responsible for the absorption, distribution, metabolism, and excretion (ADME) processes that determine the pharmacokinetics of drugs. Single nucleotide polymorphisms (SNPs) in SLCO1B1 have been linked to increases in statin plasma concentrations as well as increases in statin-induced myopathy (Yee et al., 2018). Variations in multidrug resistance proteins have been known to influence therapeutic outcomes of anti-cancer treatments such as difluomotecan (Sparreboom et al., 2004) and doxorubicin (Lal et al., 2008). Genetic variations, however, are not the sole factor involved in variable response; alterations in response to disease pathogenesis may also affect ADME processes and contribute significantly to ADRs. Transient alterations in transporter function due to disease can alter drug disposition in a manner that closely resembles the loss of function due to genetic variations. These alterations create a phenotype that is incongruent with genotype; a phenomenon referred to as phenoconversion.

Nonalcoholic steatohepatitis (NASH) is the hepatic manifestation of metabolic syndrome. Disease progression to NASH presents with hepatocellular injury, inflammation, and fibrosis (Marra et al., 2008) and the prevalence of NASH is overall about 1.5-6.45% (Sayiner, Koenig, Henry, & Younossi, 2016b). In addition to the histological changes, there are also significant alterations to hepatic enzyme and transporter mRNA, protein expression, and function that are important to ADME processes, such as the ATP-binding cassette transporter (ABC) family (Anika L Dzierlenga et al., 2016; R. N. Hardwick et al., 2013). A global transcriptional study among NASH patients showed that the effect of NASH progression on transporters is a phenocopy event; many uptake transporters are significantly downregulated, and efflux transporters like MRP2, MRP3, and BCRP are significantly upregulated (Lake et al., 2011). Both MRP2 and BCRP are members of the ABC family and are located on the bile canalculus of the liver, where they efflux endo- and xenobiotics. MRP3 is an ABC transporter located on the sinusoidal membrane, where it transports compounds back into the blood. Mislocalization of MRP2 during NASH significantly decreases its function (A. L. Dzierlenga, Clarke, & Cherrington, 2016), and alterations to the MRP2/MRP3 transport system can result in significantly altered drug disposition such as the increase in plasma retention of pemetrexed in rodent models of NASH (Anika L Dzierlenga et al., 2016). mRNA analyses of human NASH liver tissue have also shown an increase in BCRP expression during the disease (R. N. Hardwick et al., 2011). Alterations in BCRP function have not been explored, and it is important to understand changes to BCRP in the context of other transporters.

Irinotecan is a camptothecin-derivative chemotherapeutic that is used to treat colorectal cancers, the third leading cause of cancer death (Siegel, Desantis, & Jemal, 2014). It undergoes hepatic metabolism to a variety of metabolites, only one of which, SN-38, is active. SN-38 is a known substrate of BCRP (Houghton et al., 2004; Tuy et al., 2016), and SN-38G, like many glucuronides, is thought to be mainly exported through MRP2 (Kroetz, 2006). Patient

response to irinotecan, however, is highly variable and carries a significant risk of life-threatening side effects (Falcone et al., 2007). Enzyme polymorphisms, such as UGT1A1*28, account for only a portion of this variability (Sadée & Dai, 2005). Hepatobiliary efflux of SN-38 and SN-38G facilitates the toxic effects in the intestine (Kato, Suzuki, & Sugiyama, 2002). Additionally, SN-38G in the intestine is converted back into SN-38 by β -glucuronidase and is then reabsorbed into systemic circulation, which is vital to irinotecan therapy as it prolongs circulation time (Hasegawa et al., 2006). Given the previous data on the effects of NASH on hepatobiliary transport of xenobiotics, it was hypothesized that functional alterations of BCRP and MRP2 during NASH would alter the disposition of SN-38 and SN-38G, potentially contributing to variable response. It was postulated that alterations to BCRP during NASH would significantly alter biliary elimination of SN-38 and lead to decreased plasma concentrations; it was similarly proposed that mislocalization of MRP2 could significantly reduce biliary elimination of its substrate, SN-38G, and lead to plasma accumulation. This study aimed to determine the effect of Bcrp polymorphic loss of function and NASH alone, and in a gene-by-environment interaction, on the disposition of SN-38 and SN-38G. The observations made through comparison of these models may provide mechanistic insight into inter-individual variability, and a basis for response prediction in human NASH patients.

Materials and Methods

Reagents

SN-38 and camptothecin were purchased from Sigma-Aldrich (St. Louis, MO), and SN-38-glucuronide was purchased from Toronto Research Chemicals (Toronto, Ontario, Canada). Urethane, UPLC-grade acetonitrile, and UPLC-grade water were obtained from Sigma-Aldrich. Heparin was purchased from Alfa Aesar (Ward Hill, MA). ReadyScript® cDNA synthesis kit, KiCqStart™ SYBR® green qPCR with low ROX™ master mix, and PCR primers for Bcrp and β -

actin (Actb) were obtained from Sigma-Aldrich. RNA Bee isolation reagent was obtained from Amsbio (Cambridge, MA).

Animals

Male *Bcrp* knockout and wild-type Sprague-Dawley rats of at least 8 weeks of age were purchased from Horizon Discovery (Saint Louis, MO). Animals were housed in a University of Arizona Association for Assessment and Accreditation of Laboratory Animal Care–certified animal facility with a 12-hour light-dark cycle and allowed to acclimatize for at least one week before experiments. A methionine and choline deficient diet (MCD) or control diet from Dyets, Inc (Bethlehem, PA) was given *ad libitum* for 8 weeks when the animals were 16 weeks of age. After 8 weeks of diet, the animals underwent disposition studies. All handling, maintenance, care, and testing of the animals was in accordance with NIH policy, and experimental protocols were approved by the University of Arizona Institutional Animal Care and Use Committee.

SN-38 and SN-38G Disposition Studies

A stock solution of 10 mg/mL of SN-38 was prepared in DMSO. From this stock solution, a 0.8 mg/mL SN-38 co-solvent solution was prepared for injection. This solution was made by adding the SN-38 stock solution to a solution of ethanol, propylene glycol and Tween-80, then diluting in water. The final proportion of each component was as follows: 14% ethanol, 40% propylene glycol, 3% Tween-80, 10% DMSO and 33% water. No more than 5 mL/kg of solution was administered.

Animals were anesthetized for cannulation surgery using an intraperitoneal bolus dose of urethane (1g/kg, up to 10 mL/kg in saline). In order to assess the disposition of SN-38 and SN-38G, cannulas were inserted into the jugular vein for drug and saline administration, carotid artery for blood collection, and bile duct for bile collection. Prior to dosing, blood was collected from the arterial cannula as a baseline. A bolus dose of 0.8mg/kg SN-38 was then administered

intravenously over a period of 90 seconds. After drug administration, blood was collected at 2, 7, 12, 20, and 40 minutes, while bile was collected at 0, 15, 30, and 45 minutes. Terminal liver and kidney was collected at 90 minutes. A portion of collected tissue was prepared for histological analyses by fixing in 10% neutral-buffered formalin for 24 hours, then exchanging for 70% ethanol until embedded in paraffin by the University of Arizona Histology Service Laboratory. The remaining tissue was flash-frozen in liquid nitrogen for storage at -80°C. Blood was collected in heparin-coated microcentrifuge tubes and was spun down for 10 minutes at 10,000xg to separate plasma from blood cells. Plasma and bile samples were also stored at -80°C.

SN-38 and SN-38G Quantification

Sample clean-up for blood and bile samples was performed using the Bond Elut 96 Plexa solid-phase extraction plates (Agilent, Santa Clara, CA) according to the manufacturer's protocol. 40µL of plasma and 10µL of bile were used in the sample preparation process. The eluent was then evaporated to dryness and reconstituted in 120 uL of mobile phase for injection onto the LC-MS/MS. The tissue homogenates were made from 300mg of tissue and then cleaned up via protein precipitation in a 1:3 solution of homogenate to UPLC-grade acetonitrile. The samples were vortexed and kept on ice for 10 minutes, then centrifuged at 13,000 rpm for 10 minutes. The supernatant was collected in a new microcentrifuge tube and evaporated to dryness. The sample was reconstituted in 120 uL of mobile phase, centrifuged at 10,000 rpm for 5 minutes, and the supernatant was collected for injection onto the LC-MS/MS, as previously described(Khan et al., 2005).

The method for quantification of SN-38 and SN-38G in plasma, bile, and tissue was adapted from previously published methods(D'Esposito, Tattam, Ramzan, & Murray, 2008; Khan et al., 2005). The Arizona Laboratory for Emerging Contaminants at the University of Arizona provided a Waters (Milford, MA) Micromass Quattro Premier XE tandem mass

spectrometer coupled to an Acquity UPLC. The mobile phase consisted of a gradient of water (solvent A) and acetonitrile (solvent B) with 0.1% formic acid at a flow rate of 0.3mL/min through a Waters Acquity UPLC BEH C19 column (1.7 μ m, 2.1 \times 50 mm). The mobile phase was composed of A:B 90:10 (v:v) running to A:B 10:90 (v:v) over 1.0-6.0 minutes, then returned to A:B 90:10 over 60 seconds with two minutes of equilibration, for a total run time of 9.0 minutes. Multiple reaction monitoring in positive mode was used to detect SN-38 at m/z 393>349, SN-38G at m/z 569.0>393.2 and camptothecin at m/z 349.1>305.2. The retention times for SN-38, SN-38G, and camptothecin were 3.6 minutes, 3.1 minutes, and 3.8 minutes, respectively. Recovery determination was done using four replicates, and the recovery in plasma and bile respectively were: 76.3% and 86.8% for SN-38, 81.3% and 77.4% for SN-38G, and 80.6% and 81.8% for internal standard. The linear range of SN-38 and SN-38G in plasma was from 50ng/mL to 1000 ng/mL, and the range in bile was from 50ng/mL to 5 μ g/mL. The lower limit of quantification (LLOQ) in plasma was found to be 15ng/mL for SN-38 and 20ng/mL for SN-38G; in bile, it was found to be 20ng/mL for both SN-38 and SN-38G. Peak analysis was done in MassLynx Mass Spectrometry software and data analysis and processing was done using GraphPad Prism 5.0.

Quantitative Reverse Transcription-PCR

RNA was isolated from liver tissue using the RNA Bee isolation reagent. Between 200-300 mg of tissue was added to 4 mL of RNA Bee and homogenized. The manufacturer's protocol was followed and the resulting RNA pellet was reconstituted in 250 μ L of DEPC water per 100 mg of tissue, then was stored at -80°C. RNA concentration was determined using a NanoDrop 2000 UV-visible spectrophotometer (Thermo Fisher Scientific). Final preparations of RNA had a 260/280 quality ratio between 1.6 and 1.9. cDNA was prepared from the isolated RNA using the ReadyScript® cDNA synthesis kit from Sigma-Aldrich. Each reaction well contained 1x KiCqStart™ SYBR® green master mix, 100nM of forward and reverse primers,

2 μ L of cDNA template, and nuclease-free water up to 20 μ L, run in duplicate. Reactions were run on an ABI StepOnePlus Real Time PCR system with the standard SYBR® green PCR cycling profile. Fold change was determined using the delta-delta C_T method.

Histopathology

Paraffin-embedded liver sections were stained with hematoxylin and eosin then examined by a board-certified veterinary pathologist. Tissues were incidence and severity scored using an established rodent NASH system (Kleiner et al., 2005) with endpoints including steatosis, necrosis, inflammation, hyperplasia and biliary hyperplasia. Representative digital images were acquired. Rank-order statistical methods and one-way ANOVA were used to determine differences between groups.

IHC

Immunohistochemistry staining was performed on formalin-fixed paraffin-embedded tissue slides. The slides were deparaffinized in 100% xylene and hydrated in 100% ethanol. Antigen retrieval was performed in boiling pH 9.0 Tris-EDTA. Endogenous peroxidases were blocked using 0.3% (v/v) H₂O₂ in phosphate buffered saline (PBS) for 20 minutes. MRP2 was stained by incubating the slides overnight at 4°C with anti-MRP2 antibody (Sigma-Aldrich, M8163), followed by the Mach 4™ staining kit protocol (Biocare Medical). Images were taken using a Leica DM4000B microscope with a DFC450 camera.

Protein Preparation

Crude membrane fractions were obtained from liver samples. Approximately 500mg of tissue was homogenized in 5mL of cold ST buffer (Sucrose Tris buffer, 10mM tris base and 250mM sucrose with 1 Protease Inhibitor Cocktail tablet (Roche, Indianapolis, IN) per 25 ml, pH 7.5). Homogenates were centrifuged at 10,000xg for 20 minutes to remove nuclei; the supernatant was decanted into a second set of ultracentrifuge tubes. The supernatant was

spun at 100,000xg for 60 minutes to pellet the membranes. Membrane pellets were rinsed with buffer before being resuspended in 200µL of buffer and stored at -80°C. Protein concentrations were determined by BCA assay (Thermo Fisher Scientific).

Immunoblotting

Immunoblotting for MRP2 and MRP3 was performed using crude membrane preparations. Membrane preparations (60µg/lane) were separated by SDS-Page on 7.5% polyacrylamide gels. The proteins were transferred to polyvinylidene difluoride membranes, and then blocked with 5% nonfat dry milk in Tris-buffered saline/Tween-20 for at least one hour. The membranes were probed with MRP2 (Sigma-Aldrich, M8163) or MRP3 (Santa Cruz Biotechnology, SC-5775) primary antibody at a dilution of 1:500 in 2.5% blocking solution. Image processing and analysis through the ImageJ software (National Institutes of Health, Bethesda, MD) determined relative protein density and the proteins were normalized to the housekeeping protein ERK2 (Santa Cruz Biotechnology, SC-125).

Targeted Proteomic Quantitation of Bcrp Surrogate Peptide

Homogenization of liver tissues was done in a FastPrep 24 bead mill homogenizer (MP Biomedicals, Santa Ana, CA) with 1.4 mm ceramic beads. The ProteoExtract™ Native Membrane protein extraction kit (EMD Millipore, Billerica, MA) was used to prepare membrane fractions according to the manufacturer's protocol, and protein concentrations were subsequently determined by BCA assay (Pierce, Rockford, IL). 300 µg aliquots of membrane protein fraction were prepared in 100 mM ammonium bicarbonate with 3.7 w/v% sodium deoxycholate, and then were reduced using 6 mM dithiothreitol (DTT) for 5 minutes at 95°C. The samples were alkylated with 15 mM iodoacetamide for 20 minutes at room temperature, protected from light. Matrix for calibration curves was obtained from human serum albumin processed under the same conditions. Protein digestion was performed over 24 hours at 37°C

with a protein:trypsin ratio of 1:20. The reaction was quenched with 0.2% formic acid. Bcrp peptide labeled with a stable isotope (SIL) was added as internal standard to each sample post digestion and unlabeled peptide standard was added into the matrix samples in known concentrations. The acid-precipitated sodium deoxycholate was pelleted out of the samples by centrifugation at 16,000xg and 4°C. The supernatant was transferred to a LoBind plate (Eppendorf, Hamburg, Germany) and evaporated under nitrogen to concentrate, then reconstituted in 0.1% formic acid for injection onto the LC-MS/MS.

Peptide quantification was performed on an API-6500 triple quadrupole mass spectrometer operating in ESI mode with a Shimadzu LC-30AD interface. The mobile phase consisted of solution A, 0.1% FA in water and solution B, 0.1% FA in 90:10 acetonitrile:water set to a flow rate of 0.2 mL/min. 10 µL of sample was injected onto a Kinetex C18 core-shell column (1.7 µM, 100Å, 100 x 2.1 mm), and separation occurred along the following solvent gradient: 5.5% mobile phase B for 5 minutes, linear gradient of 5.5 to 33.3% mobile phase B over 40 minutes, hold at 33.3% for 5 minutes, wash at 100% mobile phase B for 5 minutes, then re-equilibration for 4 minutes. Multiple reaction monitoring was used to detect the analyte peptide (SLLDVLAAR) at transition 523.1>757.5 and the SIL peptide at 528.1>767.5. The mass spectrometer settings were: 500°C source temperature, 5 kV ion spray voltage, 10eV entrance potential, 50 V declustering potential, 25 V collision energy, and 15 V collision cell exit potential. Data were processed in Analyst 1.6.2 (SCIEX, Ontario, Canada) and the external peptide calibration curve was used to determine BCRP peptide concentration in the samples.

Statistical Analyses

All results are represented as the mean ± standard deviation (SD). Two-way ANOVA statistical analyses with Bonferroni post-test were used to compare between control and NASH animals of each genotype group. Each group consisted of n=3 animals, except for KO-MCD

group, which consisted of n=4.

Results

Effects of MCD Diet-Induced NASH on the Disposition of SN-38 and SN-38G

Hemotoxylin- and eosin-stained liver sections were examined under a light microscope at 40x magnification for histological analysis (Fig. 2.1).

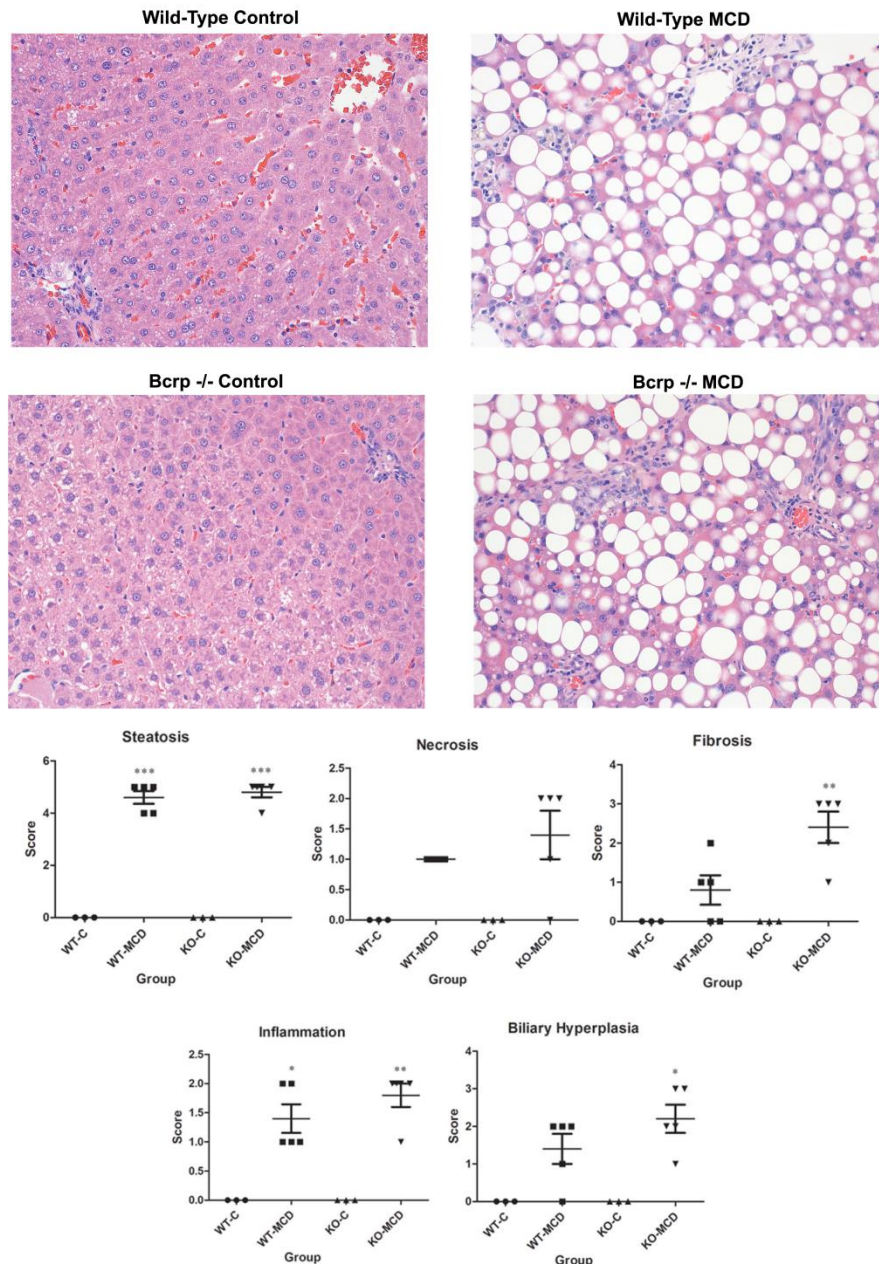


Figure 2.1. Liver histopathology of control and MCD-diet rats. Hematoxylin and eosin stained liver sections of control rats and rats fed 8 weeks of MCD diet, wild-type and Bcrp knockouts. Hallmark characteristics of NASH were found in MCD rats, while control group animals showed no signs of NASH pathology. Original magnification, 40x. 2-way ANOVA, * $P \leq 0.05$, ** $P \leq 0.01$, *** $P \leq 0.001$, $n=3$, $n=4$ (KO-MCD) .

NASH hallmarks were observed in rats fed an MCD diet for 8 weeks, including steatosis, inflammation, necrosis, fibrosis, and biliary hyperplasia. This is consistent with previous observations using an established NASH scoring system and recapitulates the histological

findings in human disease(Canet et al., 2014; Kleiner et al., 2005). There was no significant interaction between the genetic knockout and disease in the severity of NASH hallmarks, except for fibrosis; in KO-MCD animals, fibrosis was more severe than in KO-C animals. The effects of NASH on SN-38 and SN-38G disposition were observed over 90 minutes. The plasma AUC of SN-38 and SN-38G showed no significant alterations between MCD groups and their controls (Fig 2.2).

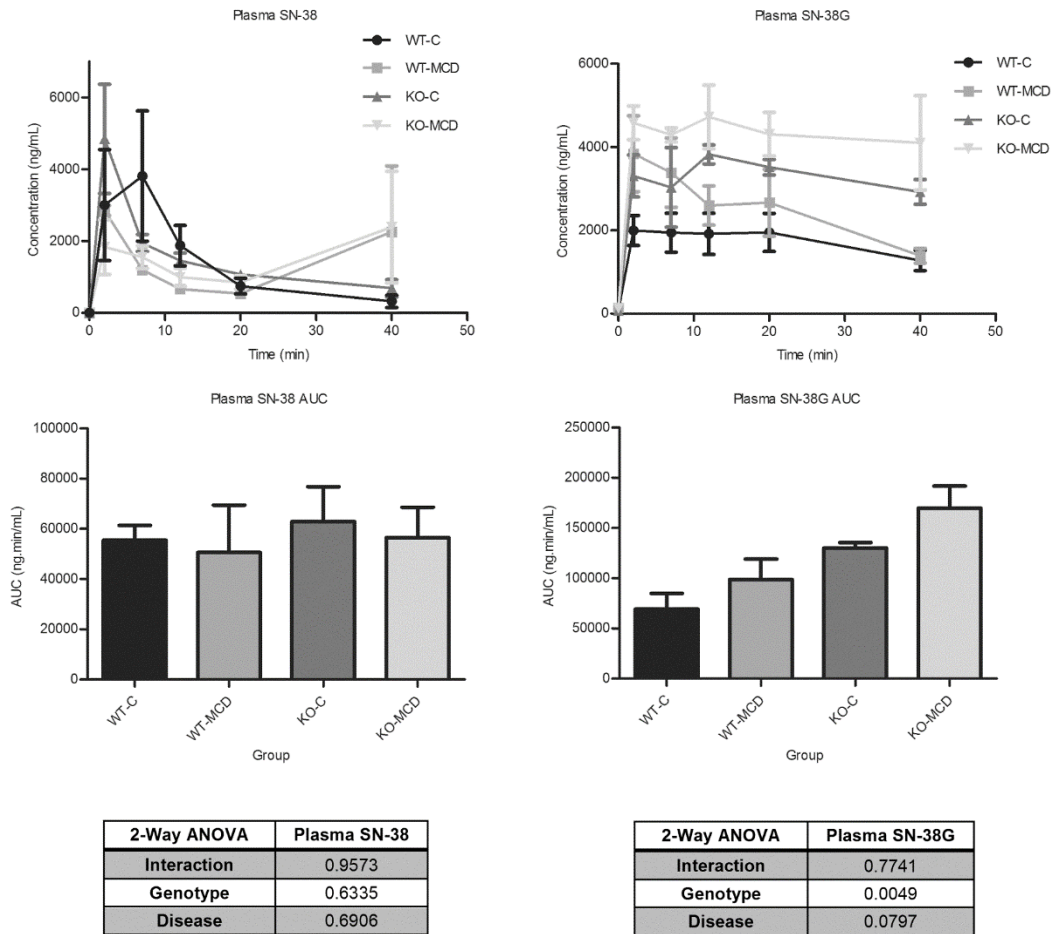


Figure 2.2. Effects of MCD diet on systemic exposure of SN-38 and SN-38G. Plasma concentrations were taken over 40 minutes after intravenous infusion of 0.8mg/kg SN-38. Graphs represent mean \pm S.D., n=3, n=4 (KO-MCD)

Significant reductions in biliary efflux were seen for SN-38 and SN-38G between the KO-C and KO-MCD groups (Fig 2.3 A and B).

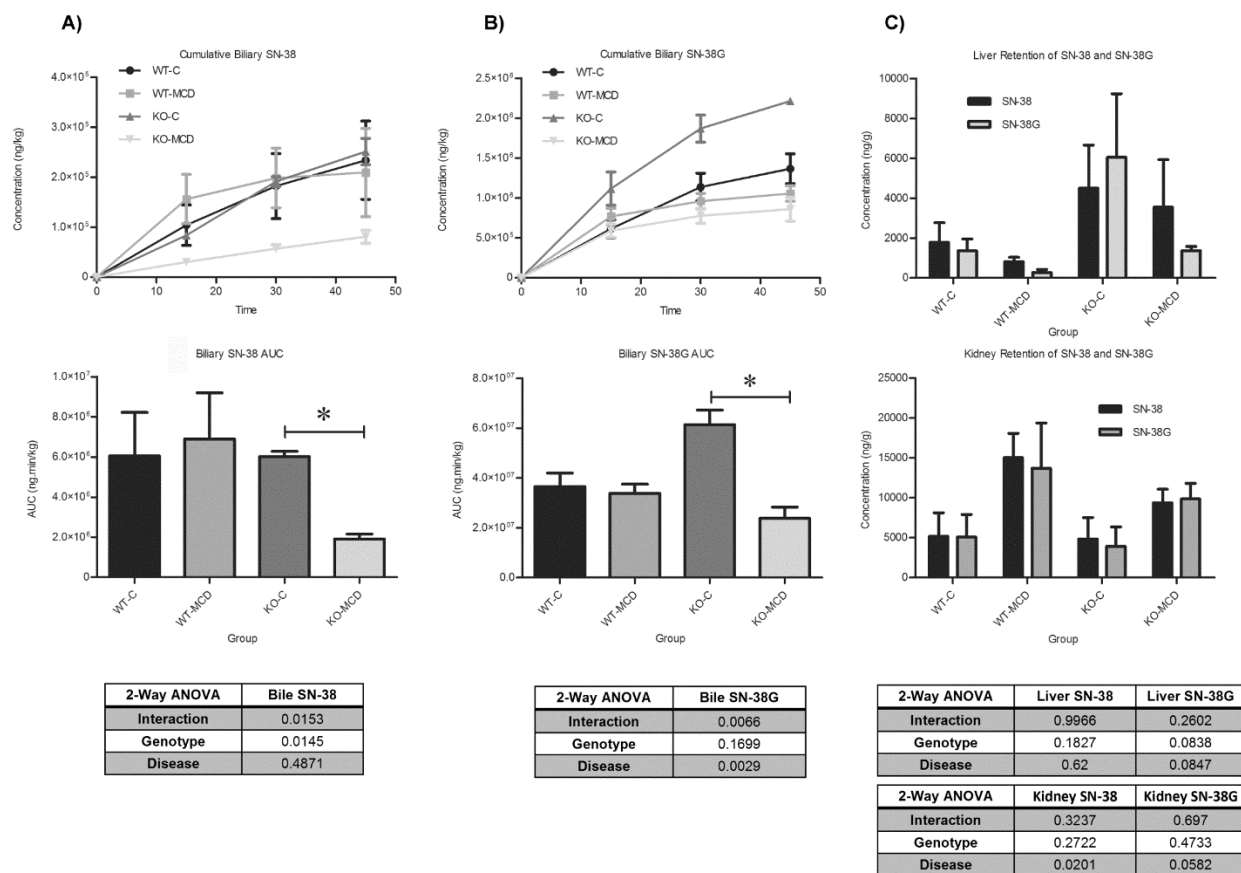


Figure 2.3. Effects of MCD diet on biliary excretion of SN-38 and SN-38G. Bile concentrations were taken over 45 minutes after intravenous infusion of 0.8mg/kg SN-38. Graphs represent mean \pm S.D. 2-way ANOVA, * $P \leq 0.05$, $n=3$, $n=4$ (KO-MCD) .

Biliary efflux of SN-38 in the KO-MCD group decreased to 31.9% of control (from $5.59 \pm 0.102 \mu\text{g}/\text{min}$ to $1.79 \pm 0.058 \mu\text{g}/\text{min}$), and efflux of SN-38G decreased to 38.7% of control (from $49.18 \pm 0.944 \mu\text{g}/\text{min}$ to $19.15 \pm 2.04 \mu\text{g}/\text{min}$).

The hepatic and renal tissue concentrations of SN-38 and SN-38G showed high variability and no statistically significant differences between the MCD groups and their controls (Fig. 2.3 C).

Effects of MCD Diet-Induced NASH on *Mrp2* and *Mrp3* Protein Expression

Relative protein concentrations of MRP2 and MRP3 and localization of MRP2 were determined by Western blotting and immunohistochemistry (IHC), respectively. Densitometric analysis was used to compare relative protein expression between groups (Fig. 2.4).

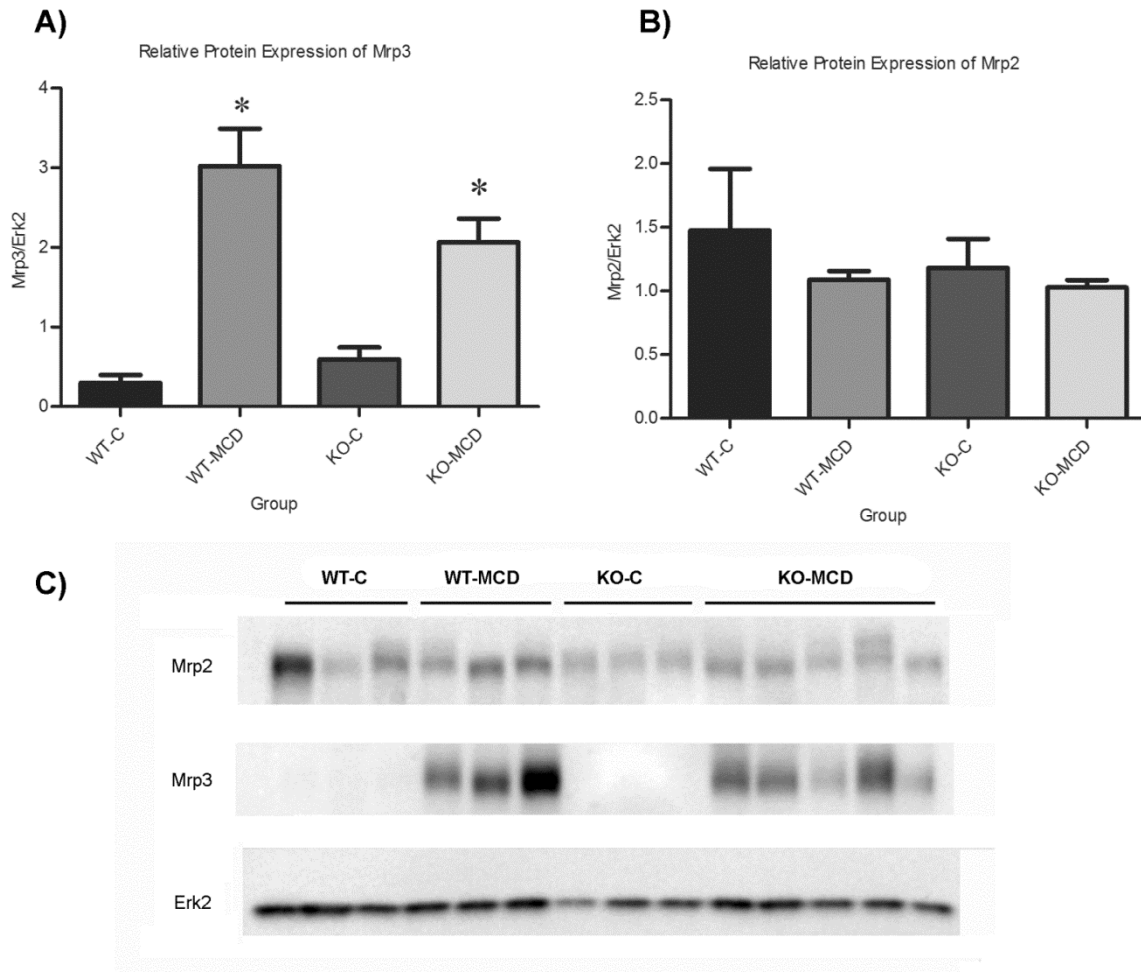


Figure 2.4. Alterations of Mrp2 and Mrp3 protein expression in MCD diet. Relative protein expression of (A) Mrp2 and (B) Mrp3 between control and MCD groups. (C) Relative protein expression was determined by immunoblot analysis. Graphs represent mean \pm S.D. 2-way ANOVA, $*P \leq 0.05$, $n=3$, $n=4$ (KO-MCD)

MRP3 increased by 10-fold in the WT-MCD group when compared to control, and increased by 3.5-fold in the KO-MCD group when compared to control. Protein concentrations of MRP2 remained relatively unchanged between the WT-C and WT-MCD groups and the KO-C and KO-MCD groups. Immunohistochemical staining of MRP2 revealed normal localization at the canalicular membrane in the control groups, while MCD groups showed pockets of internalized

staining, indicating mislocalization consistent with previous observations(A. L. Dzierlenga et al., 2015; Anika L Dzierlenga et al., 2016) (Fig 2.5).

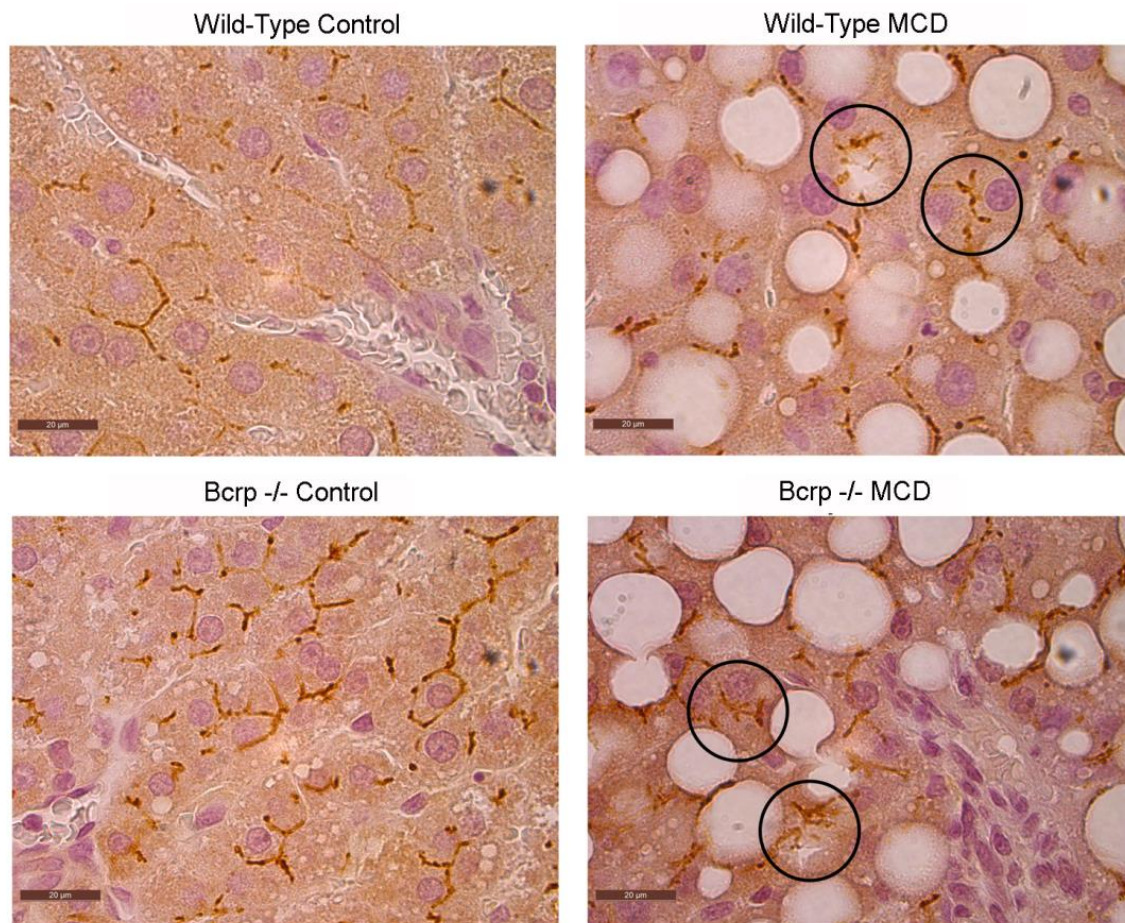


Figure 2.5. Mislocalization of Mrp2 in MCD diet. Protein localization of Mrp2 was visualized by immunohistochemistry in paraffin-embedded liver tissue of controls and MCD groups. Representative images were taken at 100x magnification.

Effects of MCD Diet-Induced NASH on Bcrp Expression

mRNA expression of Bcrp was determined by qRT-PCR and relative protein concentration was determined by LC-MS/MS analysis of BCRP surrogate peptide (Fig. 2.6).

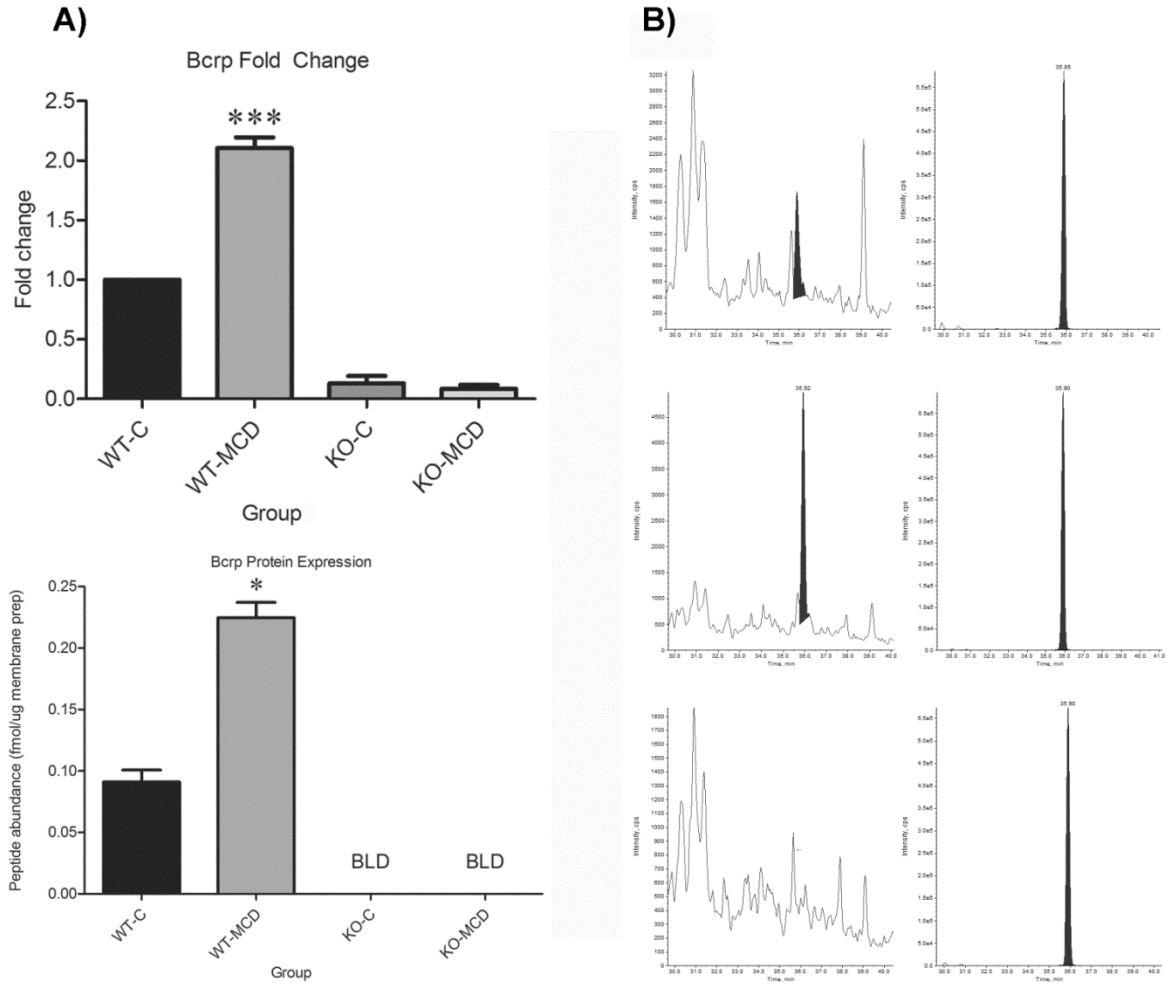


Figure 2.6. Alterations of Bcrp protein and mRNA expression during MCD diet. (A) mRNA expression was determined by qRT-PCR analysis and fold change was determined using the delta-delta CT method. Protein expression was determined by proteomic analysis using LC-MS/MS. Graphs represent mean \pm S.D. 2-way ANOVA, $*P \leq 0.05$ and $***P \leq 0.01$, $n=3$, $n=4$ (KO-MCD). (B) Representative chromatograms of WT-C, WT-MCD, and KO groups. Left chromatogram depicts native protein concentration and right chromatogram depicts internal standard peptide.

Bcrp mRNA increased by two-fold in the WT-MCD group when compared to its control, while both knockout groups showed no expression. Protein expression of BCRP increased in keeping with mRNA expression, showing a 1.6-fold increase in the MCD group when compared to controls, and no expression in the knockout groups.

Discussion

The hepatobiliary disposition of SN-38 and SN-38G is mediated by BCRP and MRP2 transport, and during NASH, alterations to BCRP function can significantly impact systemic drug exposure. It has been previously established that alterations of hepatobiliary efflux pathways can affect the distribution of xenobiotics in bile and plasma, potentially increasing patient exposure and the risk of toxicity. The MRP2/MRP3 hepatobiliary efflux pathway has been found to play a significant role in the distribution of various xenobiotics, including the chemotherapeutics pemetrexed and methotrexate, and analgesics like morphine (A. L. Dzierlenga et al., 2015; Anika L Dzierlenga et al., 2016; Ferslew et al., 2015; R. Hardwick et al., 2014). The participation of other transport proteins can also affect the distribution and toxicity of xenobiotics. Uptake transporters contribute significantly to the uptake and clearance of various drugs, including SN-38. In human patients, the hepatic uptake of ^{99m}Tc-mebrofenin (MEB), a substrate for OATP1B1 and OATP1B3, was significantly decreased in NASH due to disease-related impairment (I. Ali et al., 2017). *Oatp1a/1b*^{-/-} mice exhibit increased SN-38 concentrations in plasma and have more pronounced neutropenia (Iusuf et al., 2014). Although hepatic uptake transporters can cause alterations in xenobiotic disposition, efflux transporters are generally considered to have the most significant impact (Köck & Brouwer, 2012). SN-38 and its metabolite SN-38G are substrates for MRP2, MRP3, and BCRP, and their disposition is significantly affected by the functional status of these transporters (Kato et al., 2002). While it has been previously noted that SN-38 is a substrate for Bcrp and SN-38G is a substrate for MRP2 (Chu et al., 1997; Kawabata et al., 2001), our data confirm that both compounds are substrates for both transporters. The data herein indicate that biliary efflux of SN-38 and SN-38G is unchanged either by genetic disruption of Bcrp or the NASH-related disruption of MRP2 function alone, but the combination of disease and genetic disruption significantly impedes biliary efflux.

The disposition of SN-38 and its metabolite will also be influenced by the activity of UDP-glucuronosyltransferases. UGT1A1 is one of the major isoforms responsible for the glucuronidation of SN-38(Etienne-Grimaldi et al., 2015), and variants of UGT1A1 have been shown to increase the risk of neutropenia in human patients taking irinotecan(Liu, Cheng, Kuang, Liu, & Xu, 2014). The impact of NASH on UGT expression has been explored in previous research; in human patients, there is no change in either the mRNA or protein expression of UGT1A1 in when compared to normal(R. N. Hardwick et al., 2013; Lake et al., 2011). Similarly, the MCD diet model of NASH had no impact on the mRNA or protein expression of UGT1A1 in rats, making it unlikely that alterations to the disposition of SN-38 glucuronide would be due to the effects of the disease on this enzyme(R. N. Hardwick et al., 2012).

Uptake transporters may also have an effect on the disposition of SN-38. SN-38 is known to be transported by human OATP1B1, OATP1B3, and OATP2B1(Fujita, Saito, Nakanishi, & Tamai, 2015; Kalliokoski & Niemi, 2009), and rodent transporters OATP1B2, OATP2B1, and OATP1A4(Wang et al., 2016), though other transporters of organic anions may also be involved. The MCD diet has been shown to alter the mRNA and protein expression of various hepatic uptake transporters, including rat OATP1A1, OATP1A3, OATP1B2, and OATP2B1. Decreases have been observed in the mRNA expression of *Oatp1a1*, *1a4*, *1b2*, and *2b1*, while protein expression of *Oatp1A1*, *1B2*, and *2B1* decreases and *1A4* does not change(Fisher, Lickteig, Augustine, Oude Elferink, et al., 2009). While mRNA and protein expression of transporters significantly impact drug disposition, the glycosylation status of these transporters will also play a role. The N-linked glycosylation of transporters has multiple functions, including protein maturation, stability, and function, and membrane bound proteins in particular rely on proper glycosylation for protein folding and trafficking to the appropriate membrane(Tannous, Brambilla, Hebert, & Molinari, 2015; Urquhart, Pang, & Hooper, 2005). In

human NASH, it has been observed that genes involved in N-glycan synthesis are down-regulated, indicating a perturbation of N-linked glycosylation. This perturbation is reflected in the increase in unglycosylated OATP1B1, OATP1B3, OATP2B1, and NTCP protein found in human NASH patients (Clarke et al., 2016). Disruption of normal glycosylation may be one mechanism by which NASH alters the function of transporter proteins.

Inter-individual variability can be accounted for in some cases by genetic polymorphisms; the function of hepatic transport proteins, however, can be affected not only by genetic variation, but also by disease state. NASH has been known to cause alterations in multiple efflux transporters, including MRP2 and MRP3. There is a trend towards increased efflux transporter expression in NASH in both the human disease and rodent MCD models (Canet et al., 2014; R. N. Hardwick et al., 2011). The interactions of these disease-induced alterations with genetic polymorphisms and their functional consequences, however, have not been fully determined. Previous studies have shown gene-by-environment interactions between NASH and genetic loss of OATP transporters that affects the disposition of statins (Clarke et al., 2014). The plasma and muscle concentrations of pravastatin were synergistically increased in *Oatp1b2*^{-/-} mice with NASH, indicating an increased risk for statin toxicity. Myopathy is the major adverse effect of statin therapy, and it is known to be dose dependent and related to plasma concentrations; this synergistic increase between the genotype and disease indicates a potential at-risk patient group of those with OATP1B1 polymorphisms and NASH. We found that NASH causes an alteration to the normal hepatobiliary efflux of SN-38 and SN-38G by perturbing the MRP2/MRP3 efflux pathway through mislocalization of MRP2 and increased expression of MRP3. Compensation, however, occurs in the form of upregulated BCRP, restoring sufficient biliary efflux and leading to no significant alteration in SN-38 or SN-38G elimination in the MCD rodent model. There is a significant gene-by-environment effect observed with the addition of a genetic *Bcrp* knockout to the MCD diet, whereby removal of the

compensatory BCRP upregulation results in a sharp decrease in biliary elimination of both parent compound and metabolite. There was no significant increase in plasma AUC over the observed time points, though alteration to the plasma retention may only be observable at points after the final 40 minute time point. Similarly, there was no statistically significant difference in SN-38 or SN-38G retention in kidney or liver tissues when compared with controls. We can therefore conclude that Bcrp plays a role in the disposition of SN-38 and SN-38G along with MRP2 and MRP3, and that its function as a compensatory transporter is of increased importance in NASH. As BCRP can compensate for the loss of other transporter function during NASH, disrupting its function can restrict the biliary excretion of SN-38 and SN-38G. Systemic retention of SN-38 may increase the risk of toxicity. It has been previously seen that decreased SN-38/SN-38G ratios in plasma are a predictor of the severity of neutropenia in irinotecan therapy, though not all irinotecan toxicity could be accounted for by UGT activity(Hirose et al., 2012; Iyer et al., 2002). Diminished efflux of SN-38G may also decrease the therapeutic efficacy of irinotecan by preventing the intestinal conversion of SN-38G to SN-38 and enterohepatic recycling.

These findings provide a mechanistic basis for variable response to irinotecan therapy and identify potential risk in vulnerable populations. NASH has only recently been identified as a factor in drug disposition and ADRs, and due to the invasive liver biopsy required for definitive diagnosis, susceptible patients may not be readily identified. Additionally, genetic variants of BCRP are relatively common, and the C421A variant can be found in 39% of Japanese and 30% of Caucasian populations, producing a transporter with a nonfunctional ATP-binding domain(Imai et al., 2002; Kobayashi et al., 2005). A less abundant variant, G34A, exists in 18% of Japanese populations, 6% of African-American populations, and 3% of Caucasian populations(Imai et al., 2002; Noguchi, Katayama, Mitsuhashi, & Sugimoto, 2009). Genetic variation in BCRP has also been shown to cause alterations to the pharmacokinetics and

pharmacodynamics of drugs on its own(Mizuno, Fukudo, Terada, Kamba, & Nakamura, 2012; Zhang et al., 2006), and the combination of genetic polymorphisms and disease could potentially compound these changes as demonstrated herein with SN-38. With the increasing prevalence of NASH, the importance of phenoconversion in patients who also have genetic polymorphisms is significant. These data provide a possible mechanistic basis for previously unidentified causes of variability and toxicity to BCRP substrates in NASH patients.

Acknowledgements

The authors would like to thank Dr. Leif Abrell for his assistance with LC-MS/MS method development.

CHAPTER THREE: INTERACTION OF OATP1B2 GENE DOSE AND NONALCOHOLIC STEATOHEPATITIS ON PLASMA CLEARANCE OF PRAVASTATIN

Introduction

In the United States, nearly 1 in 20 hospitalized patients have adverse drug reactions (ADR)(Stausberg, 2014). Various factors may contribute to altered drug responses, including genetic polymorphisms of drug-metabolizing enzymes and hepatic transporter proteins that are involved in absorption, distribution, metabolism, and excretion (ADME) processes, as well as liver diseases.

Variants of *SLCO1B1*, the gene encoding the transporter protein OATP1B1, has been shown to result in increased plasma concentrations and risk of statin-induced myopathy (SEARCH Collaborative Group, 2008; Shitara & Sugiyama, 2006). Statin drugs, including pravastatin, are the first-line therapy for hyperlipidemia and for reducing the risk of heart disease and stroke(Mortensen & Falk, 2018). Although these drugs are incredibly effective, it is estimated that up to 40% of eligible patients are not prescribed statins, with one of the major barriers being intolerance due to myopathy (Joy & Hegele, 2009). According to the Prediction of Muscular Risk in Observational conditions (PRIMO) study, the incidence of myopathy in high-dose statin patients was 10.5%, while 5-18% of patients experienced some muscular symptoms (Bruckert, Hayem, Dejager, Yau, & Bégaud, 2005). As statin toxicity is dose-dependent based on plasma concentrations, understanding the mechanisms behind variable drug response can identify populations who are at risk for myopathy while on statin therapy (Newman & Tobert, 2018).

Although genetic polymorphisms are one of the most commonly investigated mechanisms of inter-individual variability in statin response, other factors may also modify the pharmac- and toxicodynamic responses of patients. Liver diseases have been previously found to affect phase I and II enzymes and transporters involved in absorption, distribution, metabolism, and excretion

(ADME) leading to altered drug disposition (Farrell, Cooksley, & Powell, 1979; Pacifici et al., 1990; Thakkar, Slizgi, & Brouwer, 2017). Nonalcoholic steatohepatitis (NASH), the hepatic manifestation of metabolic syndrome, is known to change the activity of xenobiotic transporters and significantly influence the disposition of various drugs, including morphine, ezetimibe, and pemetrexed (A. L. Dzierlenga et al., 2015; Anika L Dzierlenga et al., 2016; R. N. Hardwick et al., 2012). In rodents, the MCD–diet model of NASH recapitulates the observed alterations of hepatic transporters, including the downregulation of multiple Oatp transporters resulting elevated prolonged plasma concentrations of xenobiotics (Canet et al., 2014; Fisher, Lickteig, Augustine, Oude Elferink, et al., 2009). In Oatp1b2-null mice, MCD diet (NASH) synergistically increases the concentrations of pravastatin in plasma and muscle compared to WT mice (Clarke et al., 2014). A significant patient population may be at risk for statin-induced myopathy because of the comorbidity of compromised function of OATP1B1 (e.g. due to rs4149056 polymorphism of OATP1B1, 10-20% in European and Middle-Eastern populations and 10-15% in East Asian populations, MAF: 0.24 (Liutkeviciene et al., 2018)) and of NASH (5-17% of the general population) (Stewart, 2013). Based on these observations we hypothesized that the combination of this liver disease with a partial genetic loss of Oatp1b2 (the rodent analog of human OATP1B1) would also result in increased systemic exposure of pravastatin. To test this hypothesis, we examined the pharmacokinetic changes of pravastatin after MCD diet in Oatp1b2-null, Oatp1b2-heterozygote and WT mice.

Materials and Methods

Chemicals and Reagents

Urethane, formic acid, acetontirile, bovine serum albumin, UPLC-grade water, iodoacetamide, dithiothreitol, methanol, chloroform, ammonium bicarbonate, sucrose, and Tris base were purchased from Sigma Aldrich (St. Louis, MO). Pravastatin (sodium salt) was purchased from Cayman Chemical Company (Ann Arbor, MI). Protease Inhibitor Cocktail tablets

and sequencing-grade trypsin were purchased from Roche (Indianapolis, IN) and Promega (Madison, WI) respectively. 3- α -isopravastatin and pravastatin-d3 were purchased from Toronto Research Chemicals (Toronto, ON, Canada).

Animal Breeding and Housing

Breeders of wild-type C57BL/6 (WT) mice were purchased from Charles River Laboratories, Inc. (Wilmington, MA). Oatp1b2-null mice were engineered in the laboratory of Dr. Curtis D. Klaassen and backcrossed (>99% congenic) on C57BL/6 background (Csanaky et al., 2011; Lu et al., 2008) Male WT, Oatp1b2-/+ (Het), and Oatp1b2-/- (KO) were bred and housed in a standard temperature-, light-, and humidity-controlled facility at the University of Kansas Medical Center. At four months of age, male WT, Het, and KO mice (6-9 mice per group) were fed either a methionine and choline sufficient control diet (# 518810), or a methionine and choline-deficient diet (MCD, 518810) for six weeks to induce NASH (Dyets Inc, Bethlehem, PA).

In Vivo Pharmacokinetic Studies of Pravastatin

After the six weeks of MCD or control diet feeding, the mice were anesthetized with urethane (1.2g/kg), and subsequently, the right carotid artery was cannulated with PE-10 tubing, and the common bile duct was cannulated through a high abdominal incision with the shaft of a 30-gauge needle attached to PE-10 tubing. Throughout the experiment body temperatures of mice were maintained at 37°C by rectal probe-controlled heating pads. Depth of anesthesia was monitored by pinching the footpad before and throughout surgery, and if necessary, additional anesthetic drugs were administered during sample collection. After collection of 5-min pre-bile, pravastatin (10 mg/kg/10 ml) was injected via the carotid cannula (0 min). Thirty to 40 μ l of blood was collected into heparinized tubes at 2, 7.5, 22.5, 37.5, 52.5 and 90 min after pravastatin administration. Bile samples were then collected on ice in 15 min periods into pre-weighed 0.6 ml microcentrifuge tubes. The volumes of bile samples were determined gravimetrically, taking 1.0

as specific gravity. At 90 min after pravastatin administration the mice were exsanguinated via cardiac puncture and liver, kidneys, and gastrocnemius muscle were collected. All blood samples were immediately centrifuged at 5,000 x g for 10 min. All samples were snap-frozen in liquid nitrogen and stored at -80°C until analysis. The experimental protocol was approved by the University of Kansas Medical Center Institutional Animal Care and Use Committee (IACUC), and humane care of the animals followed the criteria outlined in the *Guide for the Care and Use of Laboratory Animals*.

Pravastatin Quantification

Pravastatin extraction and quantification were according to previously established methods (Anika L Dzierlenga et al., 2014; Sparidans, Iusuf, Schinkel, Schellens, & Beijnen, 2010). Plasma (20 µl) and bile (20 µl) samples were extracted using the Bond Elut 96 Plexa solid-phase extraction plates (Agilent, Santa Clara, CA), according to the manufacturer's protocol. The solvent was then evaporated and the pellets were reconstituted in 120 µl of mobile phase for injections. The solid tissues (~300 mg) were homogenized in three volumes of 4% bovine serum albumin. Then the proteins in the homogenate were precipitated with UPLC-grade acetonitrile (1:3). The samples were vortexed and kept on ice for 10 minutes, and then centrifuged at 13,000 rpm for 10 minutes. The supernatants were collected in a new microcentrifuge tube and evaporated to dryness. The pellets were reconstituted in 120 µl of mobile phase and centrifuged at 10,000 rpm for 5 minutes, and the supernatants were used for injections into the LC-MS/MS, as previously described (Khan et al., 2005).

A Waters (Milford, MA) Micromass Quattro Premier XE tandem mass spectrometer coupled to an Acquity UPLC was used in the Arizona Laboratory for Emerging Contaminants at the University of Arizona. The chromatographic separations were performed on a Waters Acquity UPLC BEH C18 column (1.7 µm, 2.1 × 50 mm) (Milford, MA). The mobile phase consisted of 0.1% formic acid in UPLC-grade water (A) and acetonitrile (B) at a flow rate of 0.3 ml/min. The UPLC gradient

ran from 20% to 36% B over four minutes, then equilibrated back to 20% B for one minute before the next injection. Pravastatin was detected at m/z 423.3 $>$ 303.3, 3- α -isopravastatin at m/z 423.3 $>$ 303.3, and pravastatin-d3 at m/z 426.3 $>$ 303.3.

Membrane Protein Preparation

Crude membrane fractions were prepared from liver samples based off of a protocol adapted from Hirohashi et al (Ogawa et al., 2000). Approximately 100mg of tissue was homogenized in 1 ml of ice-cold ST buffer (sucrose tris buffer, 10mM Tris, 250mM sucrose, pH 7.5) with one Protease Inhibitor Cocktail table (Roche, Indianapolis, IN) per 50 ml. The homogenates were centrifuged at 10,000xg for 20 minutes to remove nuclei. The supernatant was decanted into 1ml ultramicrocentrifuge tubes and centrifuged at 100,000xg for 30 minutes. The resulting pellet was resuspended in ST buffer and stored at -80°C. Protein concentrations were determined by Pierce BCA assay kit (Thermo Fisher, Waltham, MA).

LC-MS/MS Quantification of Transporter Proteins by Surrogate Peptides

300 μ g of crude membrane fraction was diluted into 12 mM dithiothreitol and 15 mM ammonium bicarbonate and proteins were denatured by heating at 95°C for 5 minutes. Proteins were then alkylated by incubation with 20 mM iodoacetamide in the dark at room temperature followed by precipitation with 0.5 ml ice cold methanol, 0.2 ml chloroform, and 0.2 ml water, sequentially. Proteins were then pelleted at 16,000 x g at 4°C for 5 minutes, washed with 0.5 ml methanol, and resuspended in 100 μ l of 3.7% sodium deoxycholate and 50 mM ammonium bicarbonate. Protein samples were then digested with sequencing-grade trypsin (Promega, Madison WI) at an enzyme:substrate ratio of 1:100 in a water bath at 37°C overnight. The next day, the reaction was quenched using 0.4% formic acid in water. Samples were centrifuged at 16,000 x g for 30 minutes and the supernatant was collected, then desalted on a Waters Oasis strong cation exchange solid phase extraction cartridge (Milford, MA) per the manufacturer's

instructions. The eluted peptides were dried using a centrivap, reconstituted in mobile phase, and 10 μ l was separated on a Waters Acquity UPLC BEH C18 column (1.7 μ m, 2.1 x 50 mm) using an Agilent 1290 Infinity II UPLC (Agilent Technologies, Santa Clara CA). UPLC separation was achieved by binary gradient flow of water with 0.1% formic acid (mobile phase A) and 90:10 acetonitrile:water with 0.1% formic acid (mobile phase B) at 0.2 ml/min as follows: 5.5%B (0-2 minutes), 5.5-33%B (2-22 minutes), 33%B (22-24 minutes), 100%B (24-26 minutes), 5.5%B (26-28 minutes). The UPLC was connected to a Sciex Qtrap 6500+ triple quadrupole mass spectrometer (Framingham, MA) and operated in positive electrospray ionization mode with a source voltage of 5.5 kV, curtain gas of 20 psi, nebulizer gas of 50 psi, and turbo gas of 25 psi. Surrogate peptide parent (doubly charged, [M+2H]²⁺) and fragment (singly charged, [M+H]⁺) ions were detected by multiple reaction monitoring (MRM) using a declustering potential of 50 V, entrance potential of 10 V, collision energy of 25 V, and collision cell exit potential of 15 V for all analytes. Surrogate peptide sequences and mass transitions were selected using Skyline software (MacLean et al., 2010) and unique tryptic peptides were filtered against homologous sequences within the host genome by NCBI Protein BLAST; selected MRM transitions can be found in Table 1. Raw data were analyzed using Analyst 1.6.2 (SCIEX, Ontario, Canada). Statistical analyses were performed using GraphPad Prism 7.

Statistics

All results are represented as the mean \pm standard deviation (SD). The differences amongst groups (control and NASH animals of each genotype group) were determined by two-way ANOVA with Bonferroni post-test, with significance set at $P < 0.05$.

Results

Effect of MCD Diet on Plasma Elimination of Pravastatin in Oatp1b2-WT, -HET, and -KO Mice

The plasma elimination of pravastatin in the six study groups is depicted in Fig. 3.1. The plasma elimination of pravastatin was not significantly influenced by the genotype of the Oatp1b2 transporter in control-fed mice. However, the plasma concentrations of pravastatin were significantly higher in MCD-fed KO mice compared to all other control and MCD fed groups. MCD diet increased plasma AUC by 4.4-fold in null-mice. In contrast, MCD feeding did not significantly alter the plasma elimination of pravastatin in either WT or HET mice after MCD feeding.

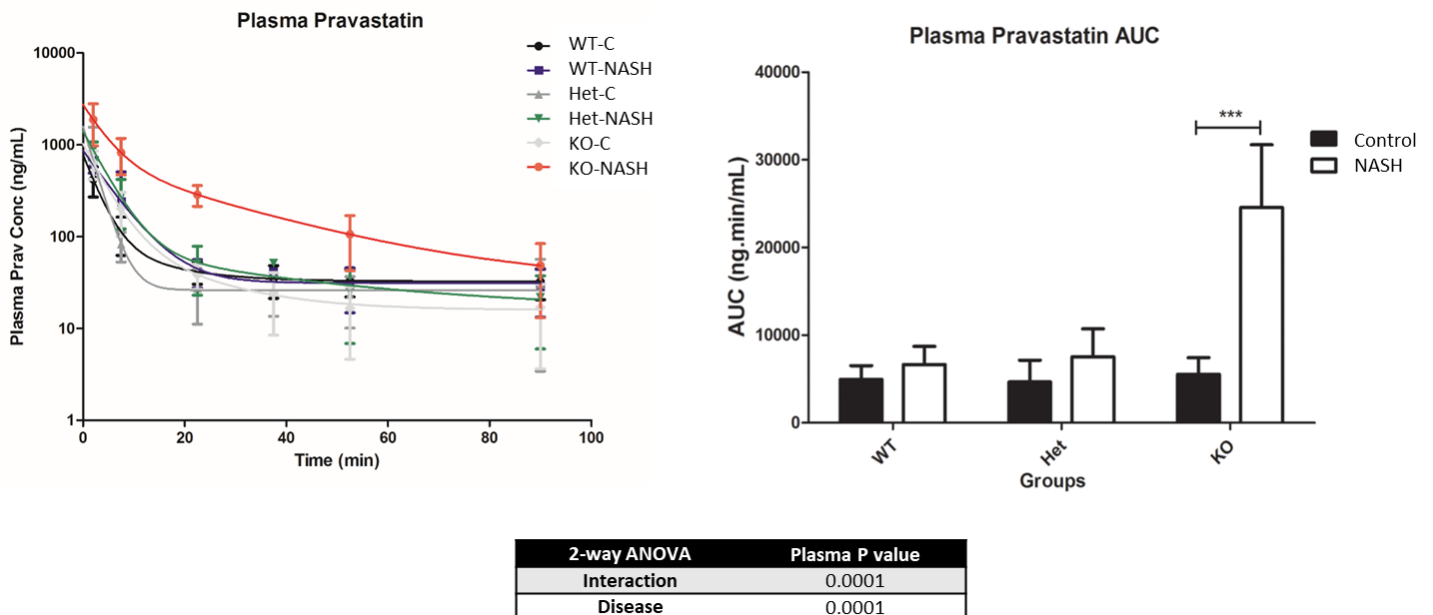


Figure 3.1. Effect of MCD diet on plasma elimination of pravastatin in Oatp1b2-WT, -HET, and -KO mice.. Plasma concentrations of pravastatin were quantified over 90 minutes after 10 mg/kg dose of pravastatin. Left panel, plasma pravastatin concentration over time for WT-C, WT-MCD, OH-C, OH-MCD, KO-C, and KO-MCD groups. Right panel, AUC graph of all groups. Plasma AUC represents mean \pm SD, n=6. *** $P \leq .001$.

Effect of MCD Diet on Biliary Excretion of Pravastatin in Oatp1b2-WT, -HET, and -KO Mice

Fig. 3.2 demonstrates the biliary excretion of pravastatin in mice with various genotypes of Oatp1b2 fed with control or MCD diet. The genotype of Oatp1b2 did not significantly alter the biliary excretion of pravastatin. Similarly, MCD diet did not alter the course of the biliary excretion significantly in WT and HET mice; however the peak (-76%) and consequently cumulative

excretion (-54%) of pravastatin was significantly decreased in KO mice after MCD feeding. It is important to note that the MCD diet decreased the biliary excretion of pravastatin only in the first 15 min after administration, but not in later periods.

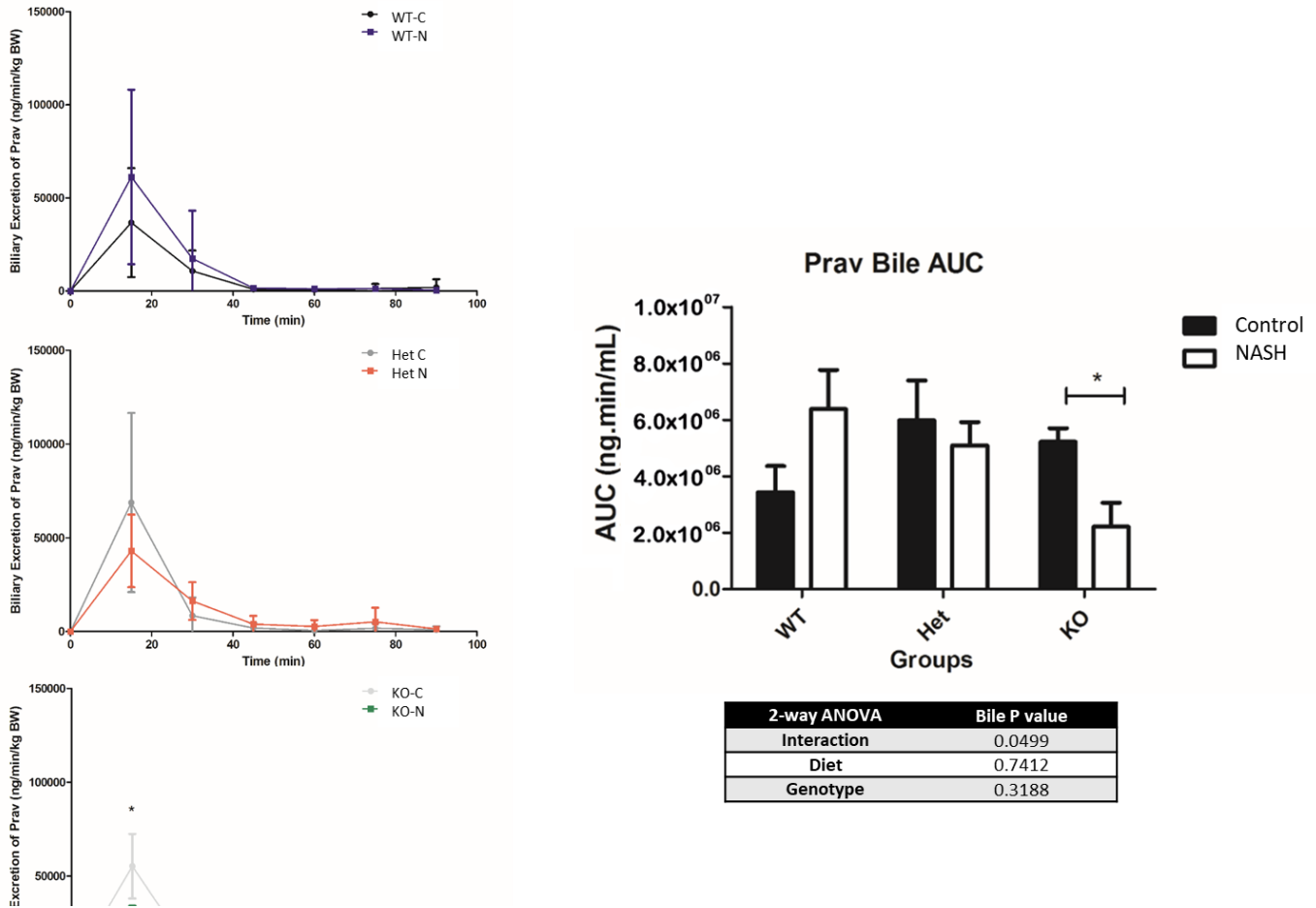


Figure 3.2. Effect of MCD diet on biliary excretion of pravastatin in Oatp1b2-WT, -HET, and -KO mice. Left panel, bile concentrations of pravastatin were quantified in 15-min periods over 90 minutes after 10 mg/kg dose of pravastatin.

Right panel, cumulative biliary AUC of pravastatin. Cumulative biliary AUC represents mean \pm SD, n=6. * $P \leq .05$.

Effect of MCD Diet on Tissue Concentrations of Pravastatin in Oatp1b2-WT, -HET, and -KO Mice

Tissue concentrations of pravastatin in liver, kidney, and muscle are shown in Fig 3.

Neither the genotype nor the MCD-diet significantly influenced the hepatic concentration of

pravastatin. The various genotype of *Oatp1b2* did not significantly change the renal and concentration of pravastatin; however the MCD diet dramatically increased the pravastatin concentration in kidney (4-fold) and muscle (21-fold) in KO, but not in HET and WT mice.

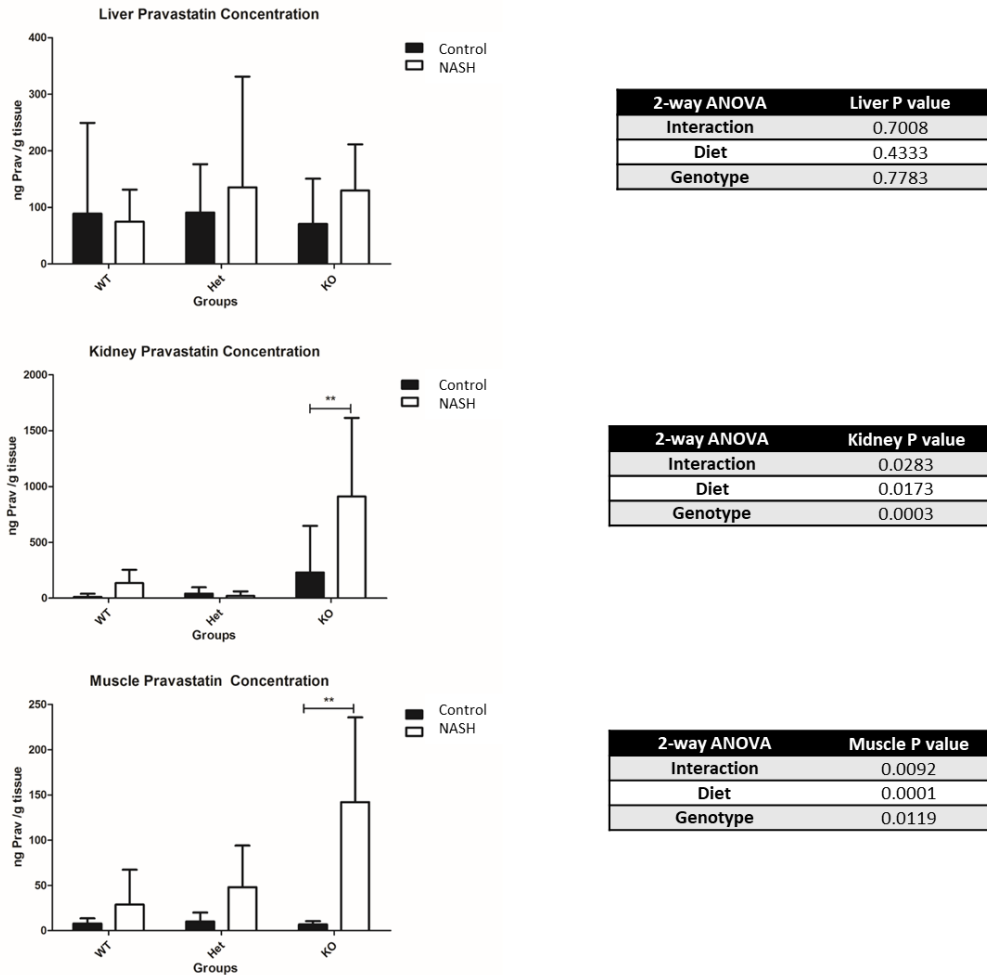


Figure 3.3. Effect of MCD diet on tissue concentrations of pravastatin in *Oatp1b2*-WT, -HET, and -KO

mice. Pravastatin concentrations per gram of tissue in liver, kidney, and muscle tissue. Data represents

mean \pm SD, n=6. ** $P \leq .01$.

*Effect of MCD Diet on Protein Abundance of Basolateral Oatp Uptake Transporters in Livers of *Oatp1b2*-WT, -HET, and -KO Mice*

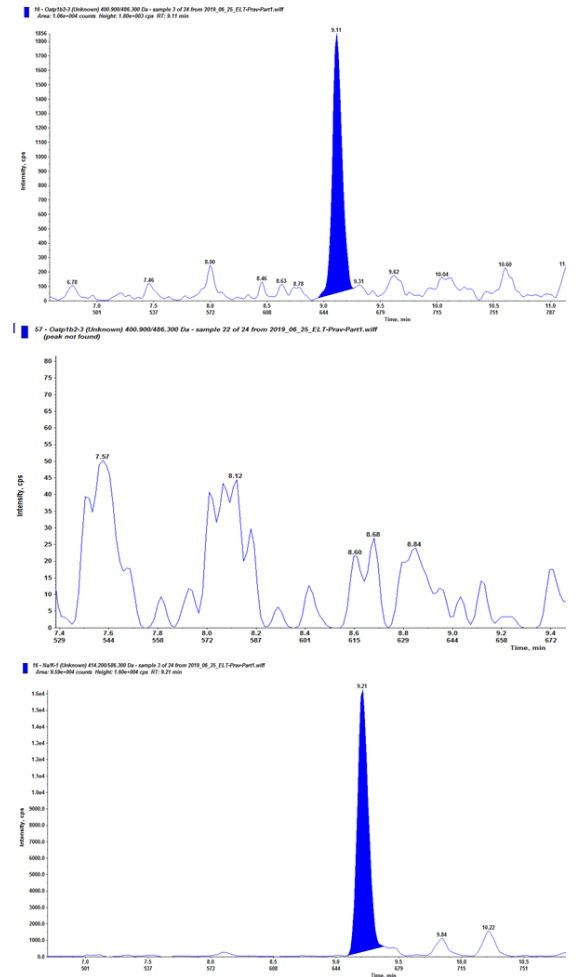
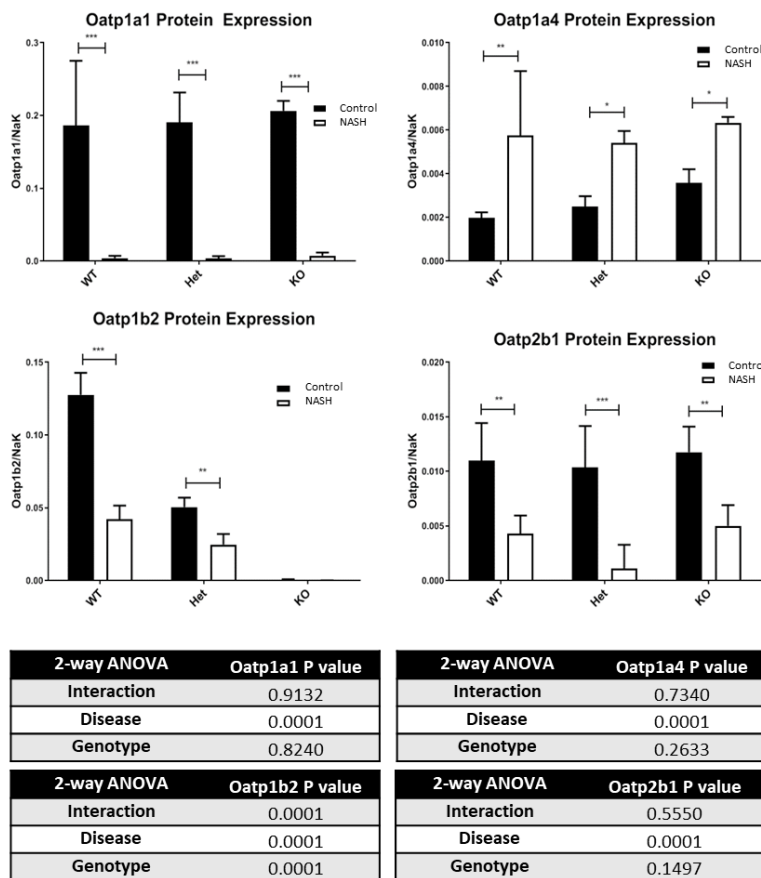


Figure 3.4. Effect of MCD diet on protein abundance of Oatp uptake transporters in livers of Oatp1b2-WT, -HET, and -KO mice. A) Relative protein expression of Oatp uptake transporters in wild-type, Oatp1b2-HET (+/-), and Oatp1b2-null (-/-) mice was determined by proteomic analysis using LC-MS/MS and normalized to Na⁺/K⁺-ATPase. B) Representative chromatograms of Oatp1b2 in WT-C and KO-C groups. Top two chromatograms depict native protein concentration, and bottom chromatogram depicts housekeeping protein Na⁺/K⁺-ATPase. Data represents mean ± SD, n=6. * P≤.05, ** P≤.01, *** P≤.001.

The effect of MCD diet on Oatp1a1, 1a4, 1b2, and 2b1 transporters are shown in Fig 3.4. The amount of Oatp1a1 and 1a4 proteins were not changed by the Oatp1b2 genotype. However, the MCD diet almost abolished the male predominant Oatp1a1 transporter protein [REF] and significantly increased the female predominant Oatp1a4 in all genotypes (WT:+200%; HET: +116%; KO: +80%). The abundance of Oatp1b2 protein was proportional to the Oatp1b2 genotype. The Oatp1b2 protein was 61% lower in HET than in WT, and practically no Oatp1b2

protein expression was detected in KO mice. The MCD diet decreased the Oatp1b2 protein by 67% and 48% in WT and HET mice compared to their corresponding control fed mice, respectively. The abundance of Oatp2b1 protein was similar in all genotypes. However, MCD diet decreases the amount of Oatp2b1 in all WT (-66%), HET (-51%) and KO (-55%) mice.

Effect of MCD Diet on Protein Abundance of Pravastatin Efflux Transporters in Livers of Oatp1b2-WT, -HET, and -KO Mice

The effect of MCD diet on hepatic efflux transporters are presented in Fig 3.5. The genotype of Oatp1b2 did not alter the protein abundance of either the canalicular Mrp2 or the basolateral Mrp3. MCD diet had an effect only on the amount of Mrp3 protein, but not on Mrp2 in all of the Oatp1b2 genotypes. Mrp3 was significantly increased in MCD fed WT (+166%), HET (+189%) and KO (+191%), compared to the respective control fed mice.

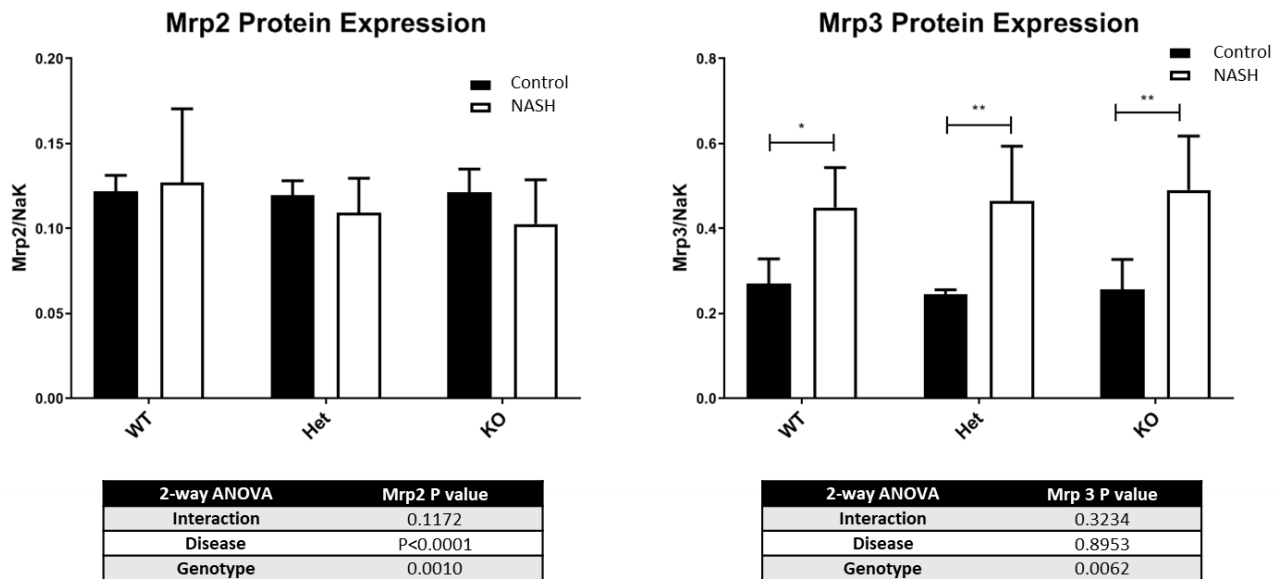


Figure 3.5. Effect of MCD diet on protein abundance of Mrp2 and Mrp3 efflux transporters in livers of Oatp1b2-WT, -HET, and -KO mice. Relative protein expression of Mrp2 and Mrp3 efflux transporters in wild-type, Oatp1b2-HET (+/-), and Oatp1b2-null (-/-) mice was determined by proteomic analysis using LC-MS/MS and normalized to Na⁺/K⁺-ATPase. Data represents mean ± SD, n=6. * P≤.05, ** P≤.01.

The clearance of pravastatin from plasma was calculated to determine alterations that occurred due to diet and Oatp1b2 gene dose (fig 3.6). Clearance was determined as $CL = \text{Dose}/AUC$. MCD diet significantly reduced the clearance of pravastatin across all genotypes. However, when the clearance is normalized per body weight, the MCD diet decreased the plasma clearance of pravastatin only in KO mice (-88%).

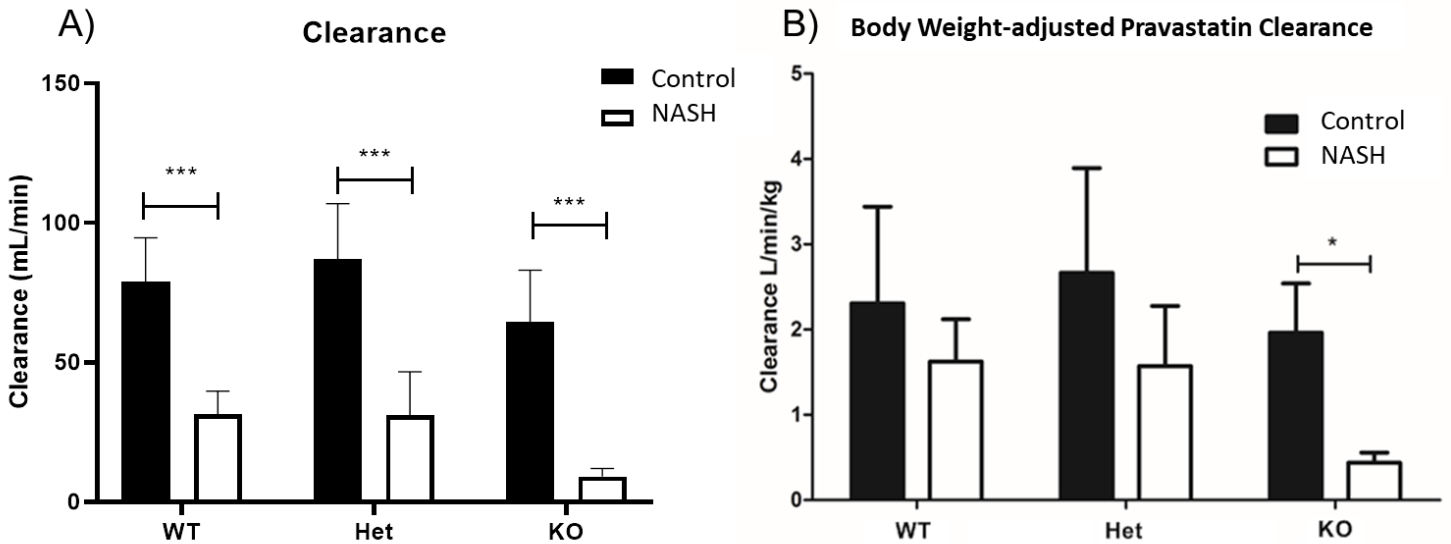


Figure 3.6. Pravastatin Clearance. Pravastatin A) clearance and B) weight-adjusted clearance in wild-type, Oatp1b2-HET (+/-), and Oatp1b2-null (-/-) mice. Data represents mean \pm SD, n=6. * $P \leq .05$, ** $P \leq .01$, *** $P \leq .001$.

Protein	Surrogate Peptide Sequence	Q1 [M+2H] ²⁺ (Da)	Q3 [M+H] ⁺ (Da)	Retention Time (min)
Na/K ATPase	AAVPDAVGK	414.2	586.3	9.2
Oatp1a1	GVQHPLYGEEK	564.3	706.3	11.1
Oatp1a4	YLEQQYGGK	514.8	495.2	4.0
Oatp1b2	ALGGVIMK	400.9	486.3	9.1
Oatp2b1	VVQEALGK	422.3	517.3	13.4
Mrp2	INEYINVDNEAPWVTDK	1010.4	1174.5	10.2
Mrp3	ILSALAEKGK	451.3	588.3	9.8

Table 3.1. Peptide Fragments and MRM Transitions for LC-MS/MS Analysis.

Discussion

The cholesterol-lowering, HMG-CoA reductase inhibitor statins are valuable drugs in primary and secondary prevention of cardiovascular diseases. While statin drugs are generally considered to be well-tolerated, muscle and consequential kidney toxicities are the primary reasons for the exceptionally high rate of discontinuation and low adherence (up to 75%) within the first two years of treatment (Stroes et al., 2015). Discontinuation of statins have significant impacts on patient health and mortality, as it has been found that removal of statin therapy negatively influences the long-term mortality after a stroke (Colivicchi, Bassi, Santini, & Caltagirone, 2007) and after acute myocardial infarction (Rasmussen, Chong, & Alter, 2007). Because there are a large number of patients being prescribed this class of drug, it is crucial to identify the groups of individuals who may be at higher risk of muscle and kidney toxicities from statin therapy.

Significant groups of potential risks for statin-induced myopathy are pharmacogenetic variants of drug transporters, especially *SLCO1B1*. OATP1B1 is a hepatic uptake transporter that is known to play an essential role in the disposition and elimination of statin drugs (Hsiang et al., 1999). Over 45 variants of OATP1B1 have been identified, some of which have functional consequences (Lee & Ho, 2017). The rs4149056 variant has been associated with increases in plasma concentrations of pravastatin in Caucasian and Japanese patients (Niemi et al., 2004; Nishizato et al., 2003). A SEARCH study conducted in 2008 found an association between this polymorphism and increased risk of myopathy with high-dose simvastatin (SEARCH Collaborative Group, 2008). Currently, only high-dose simvastatin and cerivastatin have strong evidence supporting an increased risk of myopathy with the rs4149056 SNP, and some studies have shown no association between this variant and muscle toxicities with other statin drugs (Brunham et al., 2012; Carr et al., 2013; Stewart, 2013). This suggests that additional factors other than genetic variation of OATP1B1 alone must be contributing to myopathy in statin therapy.

The data presented in this paper elucidate several aspects of the mechanisms behind the interaction between Oatp1b2 polymorphism and NASH on pravastatin pharmacokinetics. There is a clear synergistic interaction between diet-induced NASH and the genetic knockout of Oatp1b2, which results in delayed elimination of pravastatin. This effect is the result of the disruption of compensatory transport by other Oatp transporter proteins; as pravastatin is a substrate of several Oatps, the genetic loss of one transporter protein can be compensated for by others, as has been seen in previous studies (Clarke et al., 2014). Liver diseases such as nonalcoholic steatohepatitis are known to downregulate hepatic uptake transporters, such as OATPs, which is recapitulated in the rodent MCD model (Canet et al., 2014; Lake et al., 2011). This disruption of compensatory transport could explain the modest and inconsistent association of rs4149056 with muscle toxicity and statin pharmacokinetics and also indicates that the overlap between NASH patients and patients with specific OATP1B1 polymorphisms may be at increased risk of myopathy. Though the Oatp uptake transporters play a distinct role in the disposition of statin drugs, efflux transporters are a significant mediator of disposition and have an impact on pravastatin concentrations. Although MCD diet (NASH) minimally alters the plasma AUC of pravastatin in WT and HET mice, there is a synergistic effect between the total loss of functional Oatp1b2 and MCD diet in KO mice. The pravastatin AUC increased 4.4-fold in KO mice as the consequence of 78% decrease in plasma clearance (Fig 2). In MCD-,fed HET mice the single copy of functioning Oatp1b2 (high capacity/high affinity) and the alternative compensatory transport processes seem to still effectively sustain the elimination of pravastatin, avoiding the toxic accumulation of pravastatin in muscle and kidneys. However, in case of total functional loss of Oatp1b2 in mice with NASH, the compensatory mechanisms are not enough to substitute for the lost capacity of Oatp1b2, causing a 21-fold and 4-fold increase in pravastatin concentrations in the muscle and kidneys, respectively.

Protein and mRNA expression of Oatp transporters, however, may not be the only factor impacting their function. Transporter proteins are often glycosylated for stability, as well as for proper folding, trafficking, and localization (Tannous et al., 2015; Urquhart et al., 2005). A downregulation of N-glycan synthesis genes has been noted in human NASH, which may then disrupt N-linked glycosylation; this is evidenced by an increase in unglycosylated OATP1B1, OATP1B3, OATP2B1, and NTCP in human NASH patients (Clarke et al., 2016). This represents one potential mechanism for how NASH alters the function of transporter proteins outside of protein or mRNA expression.

It is also important to mention that besides basolateral uptake transporters, changes in canalicular transporters may also alter the pharmacokinetics of pravastatin. In Mrp2-null rats, the plasma AUC of pravastatin increased after both oral and intravenous administration due to decreased biliary efflux (Kivistö et al., 2005). The MCD diet that was used in our study to induce NASH also decreases Mrp2 function due to mislocalization from the canalicular membrane (Anika L Dzierlenga et al., 2016). MCD diet decreased the cumulative biliary excretion only in Oatp1b2-null mice (Fig 2). It is important to emphasize that this difference was due to the significant decrease in the early peak excretion of pravastatin (0-15 min), but no later effects on later excretion. This finding suggests that the hepatic uptake of pravastatin via Oatp1b2 is the key rate-limiting factor for the peak biliary excretion of pravastatin, contrary to the decreased abundance of canalicular efflux transporter Mrp2. In addition to decreases in Mrp2, the MCD diet is known to decrease the mRNA expression of Bsep, a membrane-associated ATP-binding cassette transporter that is a major mediator of bile formation and flow (Lickteig et al., 2007). Although Bsep has a high degree of homology with Mdr1, the transporter does not share the same broad substrate specificity as Mdr1 and mainly exports bile acids. While it has been shown that pravastatin is a substrate for Bsep using membrane microsomes expressing rodent and human BSEP (Hirano, Maeda, Hayashi, Kusuhara, & Sugiyama, 2005), the contribution of Bsep to the

biliary clearance of pravastatin *in vivo* is questionable, because in Bsep-null rats the pharmacokinetics of pravastatin is not altered (Cheng et al., 2016). MCD diet also increased the abundance of Mrp3 in the basolateral membrane, which potentially contributes to the back transport of the pravastatin from the liver to the blood. The increase in Mrp3 protein may become an important factor only when the function of Oatp1b2 is entirely lost (Fig 5). This hypothesis is also supported by the observation that MCD diet (NASH) did not alter the hepatic pravastatin concentration in any of the genotypes.

In conclusion, it is important to carefully interpret the present results, because the direct translation of these data to humans is difficult due to the differences in the expression and substrate specificity of human and rodent Oatps orthologs. However, these data are valuable in the modeling of important mechanisms impacting the pharmacokinetics of pravastatin and sheds light on essential factors, affecting the disposition and potential toxicity of statin drugs in NASH patients. These data demonstrate that under certain circumstances confounding factors like NASH and genetic polymorphism have a significant impact on drug disposition and toxicity, and the difficulties associated with definitively diagnosing NASH presents issues with identifying at-risk patients. Based on these findings, NASH patients with heterozygous polymorphisms with one functional copy of the gene may not be at higher risk of muscle toxicity but administering statins may require special cautions for homozygous populations.

Funding

This research was supported by National Institutes of Health grants ES006694, ES027351, HD062489 to NJC; ES009649, and the CMH Startup Fund to ILC.

Acknowledgments

The authors thank Mrs. Brittany Arce (KUMC) and Mrs. Melissa Cobb (KUMC) for their excellent help with the animal experiments, and Dr. Leif Abrell (UA) for his assistance in the UPLC-MS/MS works.

CHAPTER FOUR: NONALCOHOLIC STEATOHEPATITIS INCREASES PLASMA RETENTION OF SORAFENIB-GLUCURONIDE BY ALTERING THE MECHANISMS OF HEPATOCTE HOPPING

Introduction

Nonalcoholic steatohepatitis (NASH) is the hepatic manifestation of metabolic syndrome, and disease progression from nonalcoholic fatty liver disease (NAFLD) to NASH presents with fibrosis, inflammation, and hepatocellular injury (Marra et al., 2008). The overall prevalence of NASH is approximately 1.5-6.45% (Z. M. Younossi et al., 2016). The progression to NASH also presents with significant alterations to gene expression, including genes that are responsible for ADME (absorption, disposition, metabolism, excretion) processes, such as xenobiotic transporters and drug metabolizing enzymes (Lake et al., 2011). These alterations can drastically change the disposition and toxicity of xenobiotics, potentially resulting in adverse drug reactions. As nearly 1 in 20 hospital patients experience ADRs in the United States (Bourgeois et al., 2010), identifying the factors that contribute to variations in drug response is of increasing importance.

Sorafenib (SFB) is a kinase inhibitor chemotherapeutic used in the treatment of renal cell carcinoma, hepatocellular carcinoma, and radioactive iodine-resistant thyroid cancer. Patient response to sorafenib treatment, however, is variable (Rimola et al., 2018; Takeda et al., 2014), even though the metabolic pathways through CYP3A4-mediated formation of sorafenib-N-oxide and UGT1A9-mediated formation of sorafenib-glucuronide (SFB-G) have been reasonably well characterized (Edginton, Zimmerman, Vasilyeva, Baker, & Panetta, 2016; Ye et al., 2014). This presents difficulties in predicting patients who are at risk for adverse events. Previously, it has been observed that *Oatp1a/1b* cluster knockout mice, which lack several basolateral hepatic uptake transporters, experience increased SFB-G plasma concentrations after an oral dose of SFB (Vasilyeva et al., 2015). Conjugated glucuronide compounds like SFB-G and bilirubin-

glucuronide have been found to undergo a shuttling process into and out of hepatocytes, mediated through basolateral OATP uptake transporters and basolateral excretion via MRP3 and other unidentified transporters. This process, described by Vasilyeva et al. as 'hepatocyte hopping', is a normal physiological process that allows for relatively efficient hepatic elimination through multiple opportunities at excretion (Vasilyeva et al., 2015). In the hepatocyte hopping process, 1.) metabolites are either returned to sinusoidal blood through MRP3, or 2.) secreted into bile through MRP2. Finally, each subsequent hepatocyte that the compound encounters through downstream OATP uptake will afford another chance at MRP2 excretion. Thus, if biliary secretion in upstream hepatocytes is saturated, either due to incidental inhibition or overload, biliary secretion is distributed more evenly across the entire lobule and glucuronidated substrates can still be eliminated (Iusuf et al., 2012).

Nonalcoholic steatohepatitis has been known to alter the disposition of drugs through alteration of hepatic xenobiotic transporter expression and function (Anika L Dzierlenga et al., 2016; Toth et al., 2018). Among the affected transporters are OATP uptake transporters, MRP2, and MRP3, all of which play critical roles in the hepatocyte hopping of glucuronidated substrates. Given previous data on the effects of NASH on xenobiotic disposition, it was hypothesized that hepatocyte hopping of SFB-G would be disrupted by NASH, resulting in increased plasma concentrations. This study aimed to determine the impact of NASH on the three molecular mechanisms of SFB-G hepatocyte hopping using the MCD diet model of NASH in combination with rodent knockout models to isolate the effect of disease on hepatocellular shuttling.

Materials and Methods

Reagents

Sorafenib was purchased from Sigma Aldrich (St Louis, MO). Sorafenib-methyl-d3 was purchased from Santa Cruz Biotechnology (Dallas, TX). Sorafenib-glucuronide standard was

generously donated by Dr. Sharyn Baker from Ohio State University (Columbus, OH). Cremophor EL, UPLC-grade acetonitrile, and UPLC-grade water were purchased from Sigma Aldrich. ReadyScript® cDNA synthesis kit, KiCqStart™ SYBR® green qPCR master mix, and PCR primers for *Oatp1a1*, *Oatp1a4*, *Oatp2b1*, *Oatp1b2*, *Mrp2*, *Mrp3*, and β -actin (*Actb*) were obtained from Sigma-Aldrich. RNA Bee isolation reagent was obtained from Amsbio (Cambridge, MA). Synthetic peptides for targeted proteomic analysis were purchased from AnaSpec Inc (Fremont, CA).

Animals

Male FVB wild-type and *Oatp1a/1b*^{-/-} mice from Jackson Laboratory (Bar Harbor, ME) at 8 weeks of age were housed in a standard 12-hour light/dark cycle in the University of Arizona animal care facility. Male C57Bl6J and *Mrp2*^{-/-} mice at 8 weeks of age from the Aleksunes lab (Piscataway, NJ) were housed in the Rutgers University animal care facility. The mice were given either a methionine and choline sufficient (control) diet or a methionine and choline deficient (MCD) diet from Dyets, Inc (Bethlehem, PA) for 6 weeks to induce NASH. After the 6 weeks of diet, a stock solution of 2.5 mg/mL of sorafenib was made by dissolving sorafenib in a 1:1 mixture of Cremophor EL and 100% ethanol, then diluting 1:4 in deionized water. The animals were given an oral gavage of 10 mg/kg of sorafenib (5 mL/kg). Blood collections were taken at 20 minutes, 1, 2, 4, and 8 hours via submental bleed after sorafenib administration into heparinized tubes. Plasma was obtained via centrifugation. After the final time point, the animals were euthanized by CO₂ box and terminal liver was collected. Plasma samples were stored at -80°C, and tissue samples were flash-frozen in liquid nitrogen before being stored at -80°C. The animal study was approved by the University of Arizona Animal Care and Use Committee and the Rutgers University Animal Care and Use Committee.

Sorafenib Quantification

The method for quantification of sorafenib-glucuronide was adapted from previously established methods (Sparidans et al., 2009; Vasilyeva et al., 2015). The Arizona Laboratory for Emerging Contaminants provided a Waters (Milford, MA) Micromass Quattro Premier XE tandem mass spectrometer coupled with an Acquity UPLC. The mobile phase consisted of UPLC-grade water with 0.1% formic acid (A) and acetonitrile with 0.1% formic acid (B). A Waters Acquity UPLC BEH C19 column (1.7 μ m, 2.1 x 50 mm) was used for separation and set to a flow rate of 0.3 mL/min. The UPLC gradient began at 60% A, then decreased to 35% A from 1.0-1.70 minutes and held until 2.50 minutes. After 2.50 minutes, A decreased to 5% and held until 4.50 minutes before returning to 60% A and equilibrating for 1 minute. Sorafenib was detected at 465.1>270, Sorafenib-glucuronide was detected at 641.2>465.1, and Sorafenib-methyl-d3 (internal standard) was detected at 468>255. The assay was validated between 10-10,000 ng/mL for sorafenib and 10-30,000 ng/mL for sorafenib-glucuronide, with the lowest limit of these ranges being the lower limit of quantification (LLOQ). Raw data were processed using the Waters MassLynx software and statistical analyses were done using GraphPad Prism 7 (GraphPad Software, San Diego, CA).

Tissue Preparation

Liver tissue was prepared for LC-MS/MS quantification of sorafenib-glucuronide. 200 mg of tissue was homogenized in 400 μ L of cold 4% (w/v) bovine serum albumin in UPLC-grade water. 20 μ L of homogenate was placed into a 1.5 mL microcentrifuge tube and combined with 5 μ L of internal standard. 40 μ L of acetonitrile was added to precipitate proteins and then the mixture was vortexed vigorously. The homogenate was centrifuged at 10,000xg and the supernatant was pipetted into a 250 μ L glass insert and diluted to a total volume of 120 μ L with mobile phase.

Protein Preparation

Crude membrane preparations were prepared from liver tissue samples. Approximately 100 mg of tissue was homogenized in 1 mL of cold ST buffer (sucrose Tris buffer; 10 mM Tris base and 250 mM sucrose) with protease inhibitor (Roche, Indianapolis, IN). Homogenates were centrifuged at 10,000xg for 20 minutes to remove nuclei and the supernatant was decanted into a second set of ultracentrifuge tubes. The supernatant was spun at 100,000xg for 60 minutes to pellet the membranes. Membrane pellets were rinsed with buffer, then resuspended in 100 μ L buffer and stored at -80°C. Protein concentrations were determined via BCA assay (Thermo Fisher, Waltham, MA).

Proteomic Quantification of Transporter Proteins

Denaturing buffer was prepared, consisting of 3.7% sodium deoxycholate in 100mM of ammonium bicarbonate. Crude membrane preparations were diluted to 300 μ g in 100 μ L of denaturing buffer. Samples were reduced by adding DTT to a final concentration of 6 mM and incubated for 5 minutes at 95°C. The samples were then alkylated by adding iodoacetamide to 15 mM and incubating for 30 minutes at room temperature. Protein digestion was then performed using sequencing-grade trypsin at an enzyme:substrate ratio of 1:100. Proteins were digested in a water bath at 37°C overnight. The next day, the reaction was quenched using 0.4% formic acid. Samples were centrifuged at 16,000 xg for 30 minutes and the supernatant was collected, then desalted on a Waters Sep Pak C18 solid phase extraction cartridge (Milford, MA) as per the manufacturer's instructions. The eluted peptides were dried down using a centrivap. Samples were then reconstituted in mobile phase and run on a Sciex Qtrap 6500 with triple quad LC-MS/MS system (Framingham, MA) using a Waters Acquity UPLC BEH C19 column (1.7 μ m, 2.1 x 50 mm). Mobile phase consisted of 0.1% formic acid in water (A) and 0.1 % formic acid in 80% acetonitrile (B). Runs were 30 minutes long at 0.2 mL/min with a 10 μ L injection volume. The UPLC gradient ran at 5.5% B from 0-2 minutes, then increased to 33.3% B from 2-22 minutes, held at 33% B until 24 minutes, then increased to 100% B from 24-26

minutes. The gradient then returned to 5.5% B from 26-28 minutes and maintained for 2 minutes before the start of the next run. Raw data were analyzed using Analyst 1.6.2 (SCIEX, Ontario, Canada). Protein fragments and MRM transitions can be found in table 1. Statistical analyses were performed in GraphPad Prism 7.

Quantitative Reverse Transcription-PCR

RNA was isolated from liver tissue using RNA Bee isolation reagent (Amsbio, Cambridge, MA). 200-300 mg of tissue was added to 4 mL of RNA Bee and homogenized. Following the manufacturer's protocol, the RNA pellet was reconstituted in 250 μ L of DEPC water per 100 mg of tissue, then stored at -80°C. RNA concentration was determined via NanoDrop 200 UV-Vis spectrophotometer (Thermo Fisher Scientific, Waltham, MA) and final RNA preparations had a 260/280 quality ratio between 1.6 and 1.9. ReadyScript® cDNA synthesis kit (Sigma Aldrich, St Louis, MO) was used to prepare cDNA. Each reaction well contained 2 μ L of cDNA template, 100 nM of forward and reverse primers, 1x KiCqStart™ SYBR® green master mix, and nuclease free water up to 20 μ L, run in duplicate. mRNA concentrations were measured using an ABI StepOnePlus Real Time PCR system with a standard SYBR® green PCR cycling profile. Delta-delta C_T method was used to determine fold change.

Histopathology

Paraffin-embedded liver sections were stained with H&E and then examined by a board-certified veterinary pathologist. Tissues were incidence and severity scored using an established rodent NASH system(Kleiner et al., 2005) with endpoints including steatosis, necrosis, inflammation, hyperplasia, and biliary hyperplasia. Representative digital images were acquired.

Statistics

All results are represented as the mean \pm standard deviation (SD). Two-way ANOVA analyses with Bonferroni post-test were used to compare between groups. Student t-test was used to compare between two groups. Each group contained n=6 animals.

Results

Effects of Diet-Induced NASH and Oatp1a/1b Cluster Knockout on Sorafenib-Glucuronide Disposition

H&E stained liver sections were examined under a light microscope at 40x magnification to determine disease severity. NASH hallmarks were observed in mice fed an MCD diet for 6 weeks, including steatosis, inflammation, fibrosis, necrosis, and biliary hyperplasia (fig 4.1). This recapitulates the disease as seen in human patients and is consistent with previous findings (Canet et al., 2014; Kleiner et al., 2005). The effects of NASH and *Oatp1a/1b* cluster knockout were determined over the course of 8 hours. Plasma AUC levels of SFB-G increased by 108-fold in the $O^{-/-}$ -C group when compared to the WT-C. The WT-NASH group showed a 165-fold increase in SFB-G plasma concentrations when compared to its control. When compared to $O^{-/-}$ -C group, the $O^{-/-}$ -NASH group increased by 3.2-fold (fig 4.2). These data indicate that *Oatp* function is one determinant in the disposition of SFB-G, and the alterations to transporter function that occurs in NASH also impact SFB-G plasma concentrations.

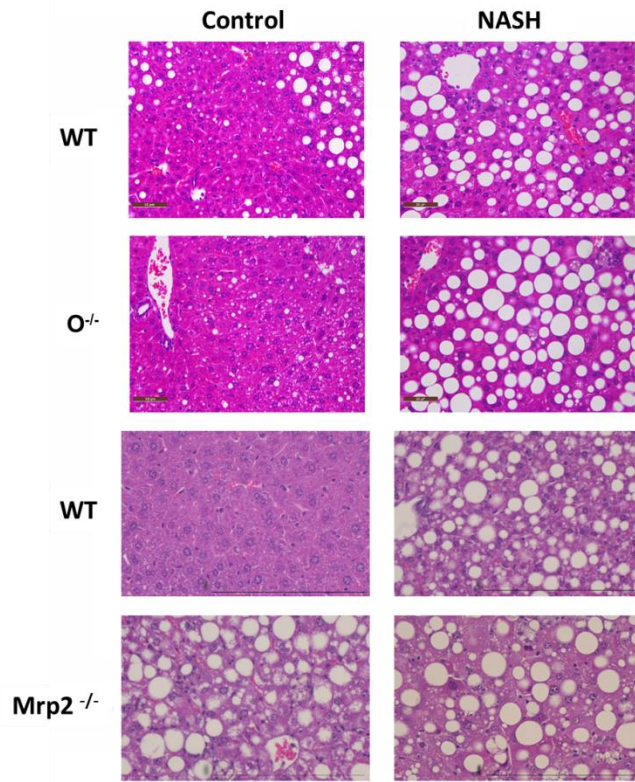


Fig 4.1. Liver histopathology of control and diet-induced NASH mice. H&E-stained liver sections of control rats and rats fed 8 weeks of MCD diet; WT, Oatp1a/1b cluster KOs, and Mrp2 KOs. Original magnification,

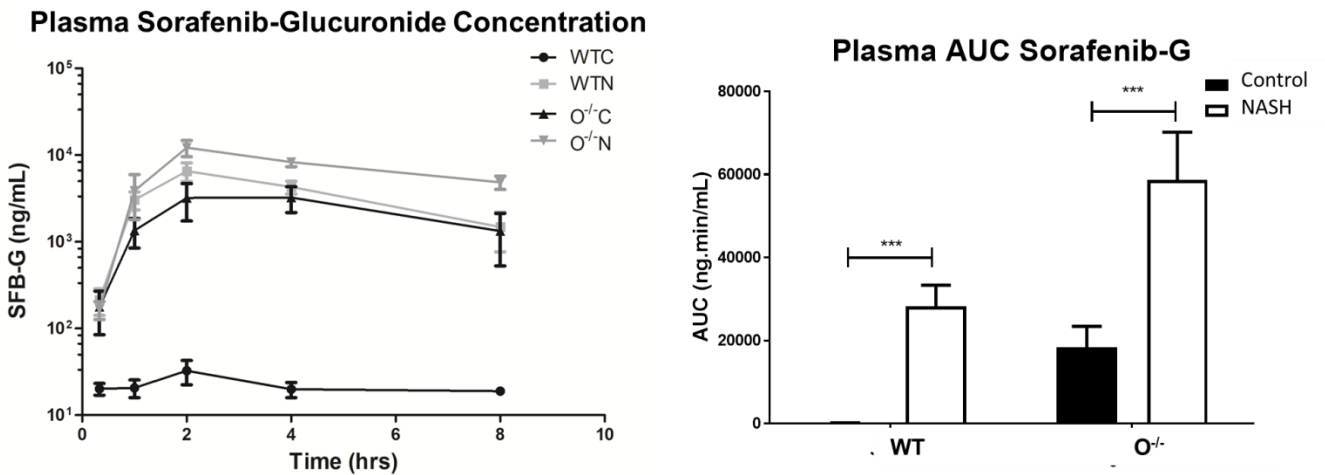


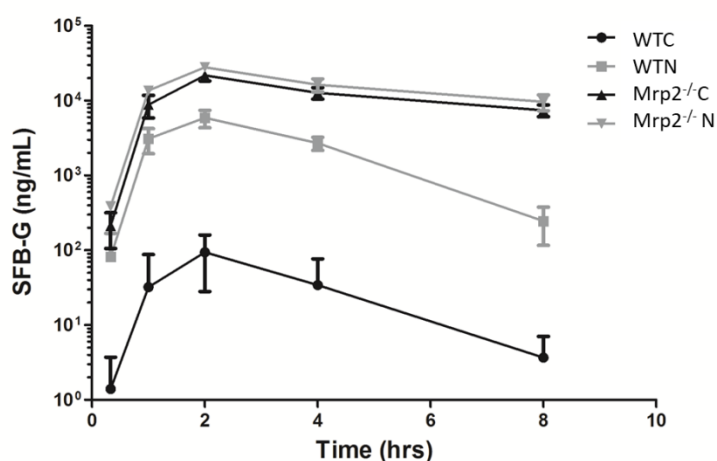
Fig 4.2. Effects of Oatp1a/1b cluster knockout and NASH on plasma sorafenib-glucuronide concentration. Plasma concentrations were taken over 8 hours after 10 mg/kg dose of sorafenib. Plasma AUC represents mean \pm SD, n=6.

* $P \leq .05$, ** $P \leq .01$, *** $P \leq .001$.

Effects of Diet-Induced NASH *Mrp2* Knockout on Sorafenib-Glucuronide Disposition

The effects of NASH and *Mrp2* knockout were determined over a period of 8 hours. The concentrations of SFB-G in the plasma of the *Mrp2*^{-/-}-C mice increased by 334.7-fold when compared to the WT-C mice. Concentrations of SFB-G in plasma increased by 67.5-fold in the WT-NASH group when compared to the WT-C group. The *Mrp2*^{-/-}-NASH group saw a 1.18-fold increase in SFB-G plasma concentrations when compared with the *Mrp2*^{-/-}-C group (fig 4.3). These data indicate that *Mrp2* function is the major determinant of SFB-G disposition, but not the sole mediator.

Plasma Sorafenib-Glucuronide Concentration



Plasma AUC Sorafenib-G

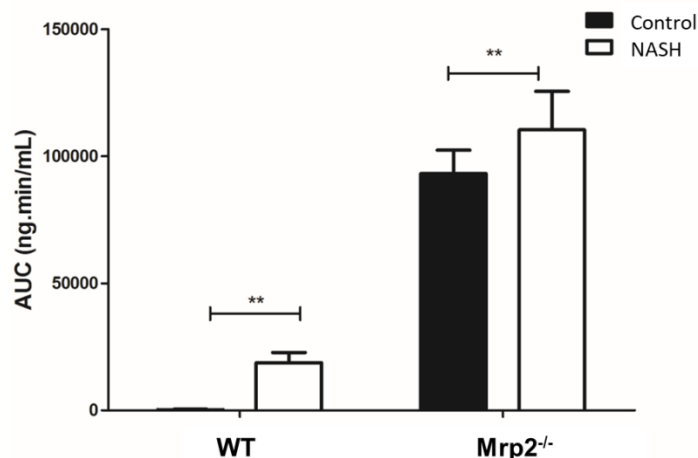


Fig 4.3. Effects of *Mrp2* knockout and NASH on plasma sorafenib-glucuronide concentration. Plasma concentrations were taken over 8 hours after 10 mg/kg dose of sorafenib. Plasma AUC represents mean \pm SD, n=6. * $P \leq .05$, ** $P \leq .01$, *** $P \leq .001$.

Effects of Diet-Induced NASH and *Oatp1a/1b* Cluster Knockout on Liver Concentrations of Sorafenib-Glucuronide

Hepatic concentrations of SFB-G were determined in order to assess the effect of diet-induced NASH and *Oatp1a/1b* cluster knockout on drug disposition. In the WT-NASH group, the

concentration of SFB-G decreased to 76% of its control, and in the $O^{-/-}$ -NASH group, the concentration decreased to 67% of its control. When comparing the $O^{-/-}$ -C group with the WT-C group to assess the impact of loss of *Oatp1a/1b* function alone, the SFB-G concentrations in the $O^{-/-}$ -C group decreased to 57% of the WT-C group. When comparing the $O^{-/-}$ -NASH group to the WT-C, the concentration of SFB-G in the liver decreased to 38% of control (fig 4.4). These data indicate that *Oatp* function contributes significantly to the uptake of SFB-G into hepatocytes, and loss of function results in decreased hepatic concentrations. The alterations to transporter function that occurs during NASH also impede *Oatp*-mediated uptake and retention in hepatocytes, resulting in lowered liver concentration.

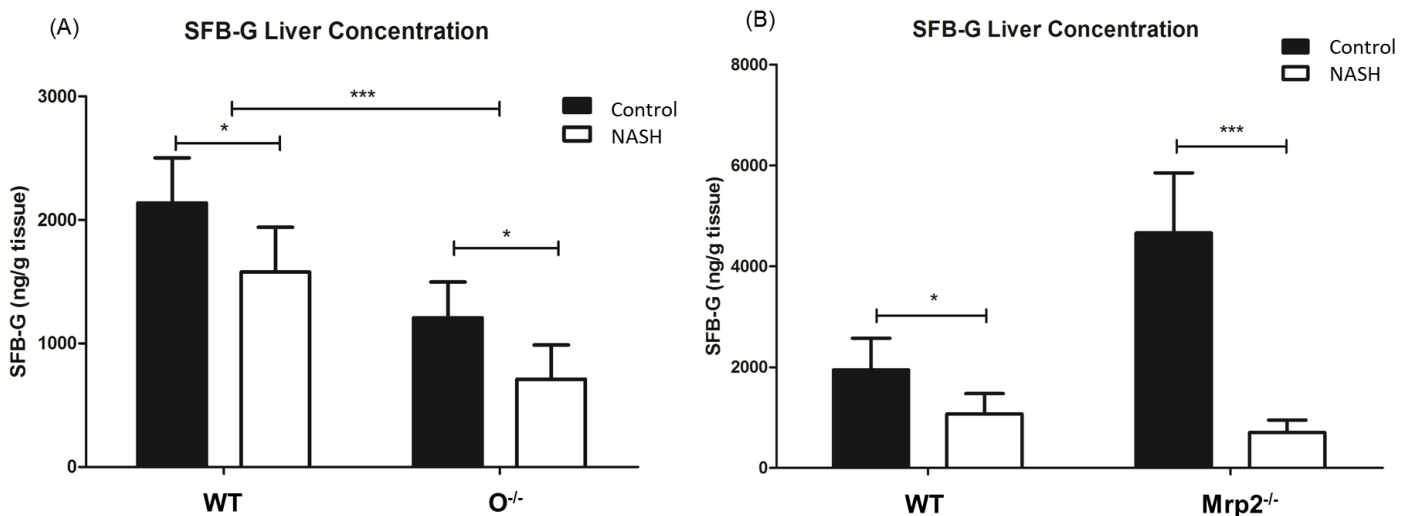


Fig 4.4. Effects of *Oatp1a/1b* cluster knockout and *Mrp2* knockout and NASH on liver tissue sorafenib-glucuronide concentration. SFB-G concentration in liver tissue in (A) *Oatp1a/1b* cluster knockout mice and (B) *Mrp2* knockout mice. Data represents mean mean \pm SD, n=6. * $P \leq .05$, ** $P \leq .01$, *** $P \leq .001$.

*Effects of Diet-Induced NASH and *Mrp2* Knockout on Liver Concentrations of Sorafenib-Glucuronide*

To assess the effect of diet-induced NASH and *Mrp2* knockout on drug disposition, the concentration of SFB-G in the liver tissue was determined. In the WT-NASH group, the

concentration of SFB-G decreased to 55% of its control, while the concentration of SFB-G in the *Mrp2*^{-/-}-NASH group decreased to 15% of its control. When assessing the impact of the genetic loss of *Mrp2* function alone, the SFB-G concentrations in the *Mrp2*^{-/-}-C group increased to 239% of the WT-C group. Between the *Mrp2*^{-/-}-NASH group and the WT-C, the concentration of SFB-G in the liver decreased to 36% of control (fig 4.4). These data indicate that *Mrp2* function contributes significantly to the efflux of SFB-G from hepatocytes, and loss of function will result in hepatic accumulation of the glucuronide. Loss of function of *Mrp2* combined with disruption of hepatocyte hopping due to diet-induced NASH, however, results in an even greater decrease in hepatic accumulation of SFB-G.

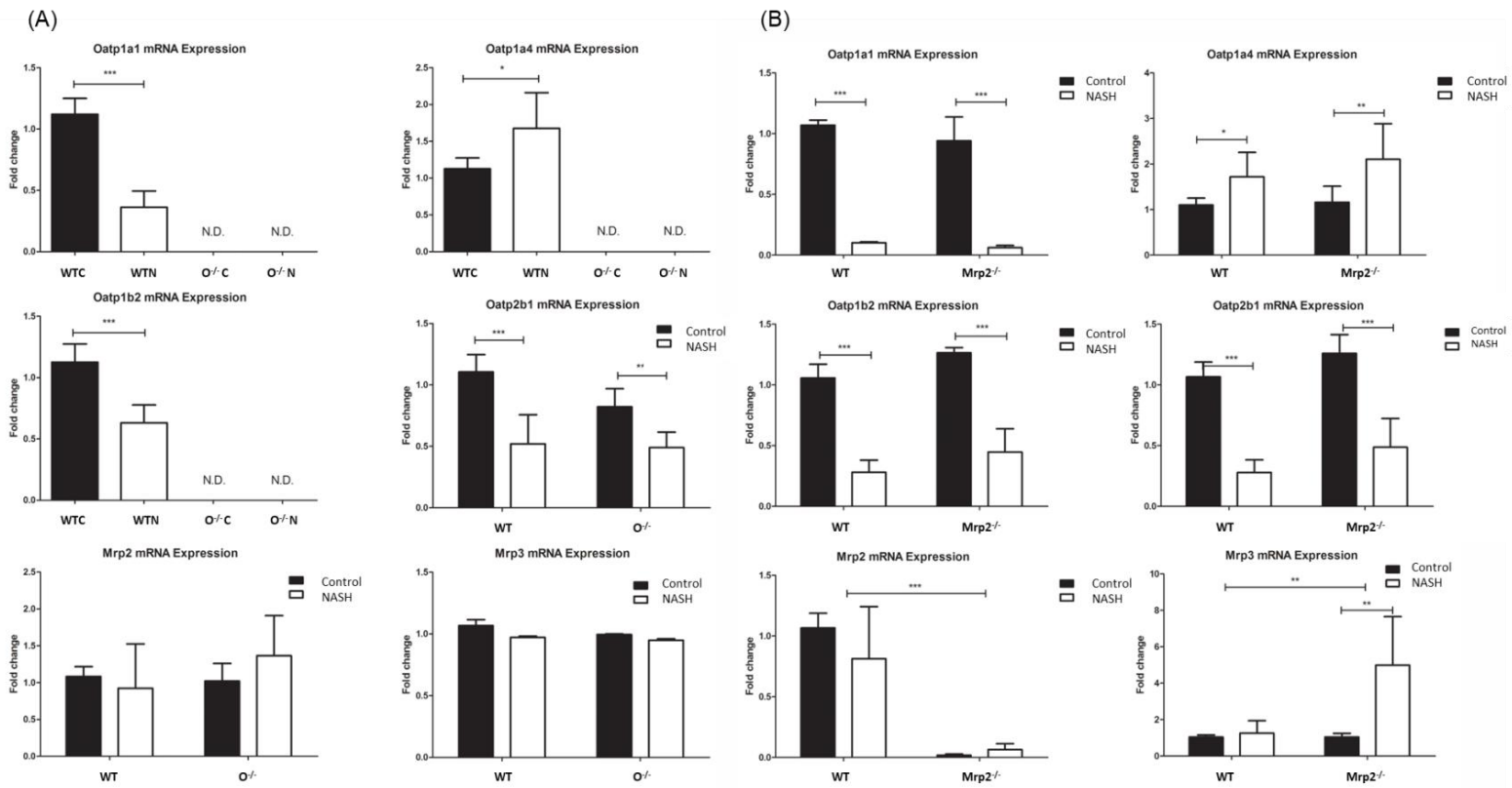


Fig 4.5. Altered mRNA expression of Oatp and Mrp transporters due to Oatp1a/1b cluster knockout and *Mrp2* knockout and diet-induced NASH.

mRNA expression of Oatp transporters and Mrp transporters in (A) *Oatp1a/1b* cluster knockout mice and (B) *Mrp2* knockout mice was determined through qRT-PCR and fold change was determined using the $\Delta\Delta C_T$ method. Data

represents mean mean \pm SD, n=6. * $P \leq .05$, ** $P \leq .01$, *** $P \leq .001$.

Effects of Diet-Induced NASH and Oatp1a/1b Cluster Knockout and Mrp2 Knockout on Xenobiotic Transporter Gene Expression

mRNA expression of Oatp uptake transporters and Mrp efflux transporters was assessed to determine the impact of NASH, *Oatp1a/1b* cluster knockout, and Mrp2 knockout on gene expression. The gene expression of *Oatp1a1* decreased to 36% of control in the WT-NASH group, and there was no mRNA detected in the $O^{-/-}$ -C or $O^{-/-}$ -NASH groups. In the $Mrp2^{-/-}$ -NASH group, the expression of *Oatp1a1* decreased to 10% of control. The gene expression of *Oatp1a4* increased to 167.6% of control in the WT-NASH group, to 181% of control in the $Mrp2^{-/-}$ -NASH group, and had no expression in either of the *Oatp1a/1b* knockout groups. The gene expression of *Oatp1b2* decreased to 63% of control in the WT-NASH group, to 44% of control in the $Mrp2^{-/-}$ -NASH group, and had no expression in either of the $O^{-/-}$ groups. The expression of *Oatp2b1* decreased to 52%, 58%, and 56% of control in the WT-NASH, $O^{-/-}$ -C, and $O^{-/-}$ -NASH groups, respectively. *Oatp2b1* expression also decreased to 40% of control in the $Mrp2^{-/-}$ -NASH group. There were no statistically significant alterations to the mRNA expression of *Mrp2* across any of the groups. *Mrp3* expression was only significantly altered in the $Mrp2^{-/-}$ -NASH group, where it increased to 479% of control. (fig 4.5).

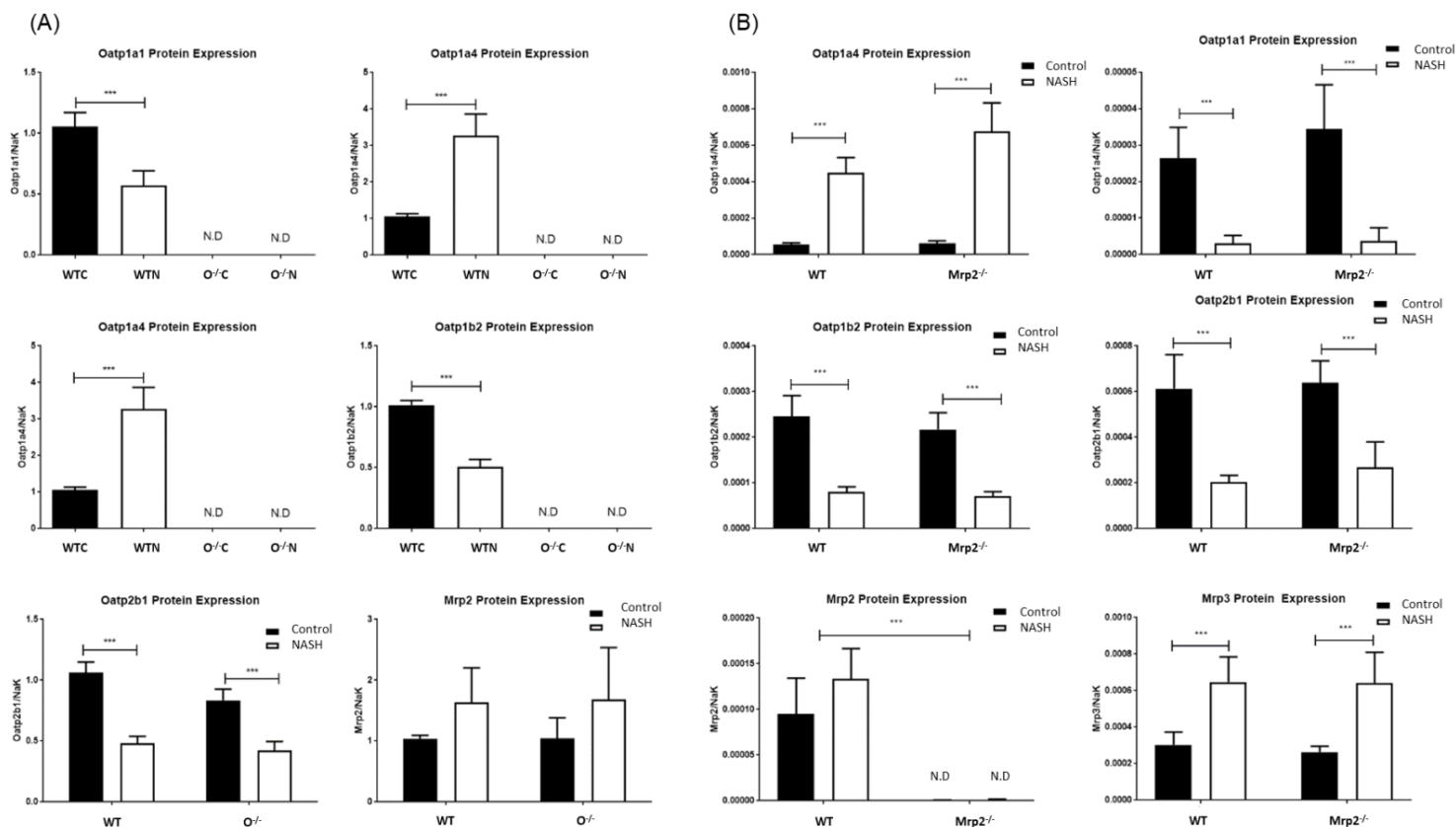


Fig 4.6. Altered protein expression of Oatp and Mrp transporters due to Oatp1a/1b cluster knockout and Mrp2 knockout and diet-induced NASH. Relative protein expression in (A) *Oatp1a/1b* cluster knockout mice and (B) *Mrp2* knockout mice was determined by proteomic analysis using LC-MS/MS and normalized to Na⁺/K⁺-ATPase expression with Mrp2 heavy labeled internal standard. Data represents mean ± SD, n=6. * P≤.05, ** P≤.01, *** P≤.001.

Effects of Diet-Induced NASH and Oatp1a/1b Cluster Knockout and Mrp2 Knockout on Xenobiotic Transporter Protein Expression

Relative protein concentrations of Oatp1a1, Oatp1a4, Oatp1b2, Oatp2b1, Mrp2, and Mrp3 were determined via LC-MS/MS and normalized to Na⁺/K⁺-ATPase (NaK). Oatp1a1 protein expression decreased to 57.2% of control in the WT-NASH group, to 10.8% of control in the Mrp2^{-/-}-NASH group, and was not detected in the *Oatp1a/1b* cluster knockout animals. Oatp1a4 protein expression increased to 326.6% of control in the WT-NASH group, to 806.3% of control in the Mrp2^{-/-}-NASH group, and was not detected in *Oatp1a/1b* cluster knockout animals. Oatp1b2 protein expression decreased to 50.5% of control in the WT-MCD group, to

32.9% of control in the *Mrp2*^{-/-}-NASH group, and was not detected in the *Oatp1a/1b* cluster knockout animals. *Oatp2b1* protein expression decreased to 48.1% of control in the WT-MCD group, to 42.1% of control in the *Mrp2*^{-/-}-NASH group, and to 42.0% of control in the *O*^{-/-}-NASH group. *Mrp3* protein expression increased to 425.4% of control in the WT-NASH group, to 244.6% of control in the *Mrp2*^{-/-}-NASH group, and to 386.3% of control in the *O*^{-/-}-NASH group. The protein expression of *Mrp2* did not significantly change between any group, and no *Mrp2* protein was detected in the *Mrp2* knockout groups. (fig 4.6).

Protein	Fragment	Q1 Mass	Q3 Mass
NaK	R.AAVPDAVGK.C	414.2	586.3
Oatp1a1	K.GVQHPLYGEK.N	564.3	706.3
Oatp1a4	K.YLEQQYGK.S	514.8	495.2
Oatp1b2	K.ALGGVIMK.S	400.7	486.2
Oatp2b1	R.VVQEALGK.S	422.3	517.3
Mrp2	R.INEYINVDNEAPWVTDK.K	1010.4	1174.5
Mrp3	K.ILSALAEK.I	451.3	588.3

Table 4.1. Peptide Fragments and MRM Transitions for LC-MS/MS Analysis.

Discussion

The disposition of SFB-G is mediated by sinusoidal efflux through *Mrp3*, biliary efflux via *Mrp2*, and sinusoidal uptake through *Oatp* transporters. During the progression of NASH, previous research in human patients has identified alterations to enzymes and transporters responsible for drug disposition (Lake et al., 2011). These alterations result in nearly identical changes to the functional disposition of several drugs in both human and rodent models of NASH. Importantly, the three mechanisms of hepatocyte hopping are concordantly regulated in both human NASH and MCD diet-induced NASH, and drugs that rely on any one of these three mechanisms show strikingly similar changes in disposition. In the case of APAP, after the administration of a nontoxic dose, the biliary concentrations of the 3 major metabolites (APAP-sulfate, APAP-glucuronide, APAP-glutathione) were significantly decreased in rats with diet-induced NASH.

Additionally, the Mrp3 substrate APAP-glucuronide was elevated in NASH rat plasma when compared to the other metabolites, and was also 80% higher in urine. (Lickteig et al., 2007) The increased levels of APAP-glucuronide in serum and urine that were found in the MCD rodent model also presented only in patients with NASH. This shift indicates that the increased expression of Mrp3 and mislocalization of Mrp2 in the MCD model of NASH is identical to that observed in human NASH patients (Canet et al., 2015). There was a similar agreement between the changes to morphine pharmacokinetics in the MCD rat model and human patients, showing an increase in systemic morphine-glucuronide exposure, and an increase in serum exposure of M3G due to decreased biliary efflux and increased sinusoidal efflux of the metabolite (A. L. Dzierlenga et al., 2015; Ferslew et al., 2015; Pierre et al., 2017). . While the extrapolation of animal data to predict toxicity in humans remains challenging, the MCD diet-induced model of NASH offers utility in that it closely resembles human NASH histology and recapitulates the molecular mechanisms of hepatic transporter alterations found in human patients (Canet et al., 2014; Li, Toth, & Cherrington, 2017).

In addition to the ABC efflux transporters, Oatp uptake transporters play a crucial role in the hepatocyte hopping process and are altered during the progression of NASH.. The MCD diet has been shown to recapitulate the alterations observed in human disease and alter the protein and mRNA expression of several Oatp proteins, including Oatp1a1, Oatp1a4, Oatp1b2, and Oatp2b1. In the rodent model, the mRNA expression of *Oatp1a1*, *Oatp1b2*, and *Oatp2b1* have been shown to decrease, whereas the expression of *Oatp1a4* increases. Similarly, the protein expression of Oatp1a1, Oatp1b2, and Oatp2b1 decrease, while expression of Oatp1a4 increases (Clarke et al., 2014). Disease-related transporter impairment is known to significantly decrease the hepatic uptake of ^{99m}Tc-mebrofenin, a known substrate of OATP1B1 and OATP1B3, in human patients (I. Ali et al., 2017). It has also been previously established that alterations to Oatp uptake transport can have a significant impact on the disposition of SFB and

SFB-G(Zimmerman et al., 2013), as well as other xenobiotics like SN-38(Iusuf et al., 2014). In the MCD rodent model, the interaction of NASH and *Oatp1b2* knockout was shown to significantly increase plasma and muscle concentrations of pravastatin, potentially leading to an increase in toxicity(Clarke et al., 2014). In addition to hepatic uptake transporters, efflux transporters are also known to have a significant impact on drug disposition. In the MCD rodent model of NASH, the disease causes an increase in the protein expression of Mrp3 and no change in the overall protein expression of Mrp2(Canet et al., 2014); however, the function of Mrp2 is significantly impaired due to mislocalization of the transporter from the bile canalicular membrane(A. L. Dzierlenga et al., 2016). This has been shown to impact the distribution of various xenobiotics such as pemetrexed, methotrexate, and ezetimibe(Anika L Dzierlenga et al., 2016; R. Hardwick et al., 2014; R. N. Hardwick et al., 2012). As SFB-G is known to be a substrate for *Oatp* uptake transporters and Mrp2, the functional status of these transporters will significantly impact the disposition of this compound. While Mrp3 is also known to be a contributor to the sinusoidal efflux of SFB-G, full genetic knockout of this protein has only a modest impact on pharmacokinetics(Vasilyeva et al., 2015), implicating the participation of an unknown transporter in this process.

There is evidence that the glycosylation status of transporter proteins is altered during NASH, and the presence or absence of these modifications also impact the function of the protein. N-linked glycosylation of transporter proteins serves several different purposes, including stability, function, and localization, and membrane-bound proteins require proper glycosylation for trafficking(Tannous et al., 2015; Urquhart et al., 2005). Several genes associated with N-linked glycosylation are downregulated in human NASH, indicating a possible perturbation; this is supported by an increase in unglycosylated OATP1B1, OATP1B3, OATP2B1, and NTCP in human NASH patients(Clarke et al., 2016). Impairment of N-linked glycosylation may be one mechanism by which NASH disrupts xenobiotic transporter function.

The disposition of SFB-G can also be affected by the activity of UDP-glucuronosyltransferases, though it is unlikely that UGT1A9 metabolism is a significant contributor to the variability in SFB-G disposition found in NASH. Uridine 5'-diphosphoglucuronosyltransferase (UGT) 1A9 is the major isoform responsible for the glucuronidation of SFB(Bins et al., 2017), and some polymorphisms of UGT1A9 have been associated with increased risk of toxicity in patients taking SFB(Boudou-Rouquette et al., 2012). In human NASH patients, UGT1A9 protein expression is downregulated(R. N. Hardwick et al., 2013), and a similar decrease was observed in the mRNA expression of this enzyme in steatotic mice(Merrell & Cherrington, 2011). This makes it unlikely that the alterations to the disposition of SFB-G would be due to the effects of NASH on the expression of the enzyme.

Systemic inflammation and other disease processes could provide the mechanistic basis for the larger category of interindividual variability that cannot be explained by genetics. Disease state, however, can also be a factor that impacts the expression and function of hepatic xenobiotic transporters. Xenobiotic transporters from both the Oatp and Abcc families are known to be significantly altered during the progression of NASH, leading to significant changes in drug disposition. Previous studies have investigated the synergistic effects of gene-by-environment interactions of NASH and hepatic transporter polymorphisms, and found that the interaction between NASH and deleterious polymorphisms can result in significant increases in plasma exposure and potential toxicity of xenobiotics(Clarke et al., 2014; Toth et al., 2018). This is the first study to attempt to isolate the mechanisms involved in hepatocyte hopping and quantitate their impact on pharmacokinetics in NASH. The effects can be readily seen in the significant increase in SFB-G plasma concentrations when comparing the WT-NASH group to its control, as well as in the 3.2-fold increase in plasma concentrations when comparing the O^{-/-}-NASH group to the O^{-/-}-C group. Disruption of Oatp uptake in the knockout group prevents the reuptake of SFB-G into downstream hepatocytes, prolonging plasma exposure. The additional

alterations to Mrp2 and Mrp3 function due to the effects of diet-induced NASH further exacerbate the disruption to hepatocyte hopping, as the loss of Mrp2 function prevents biliary excretion and increased Mrp3 protein expression at the plasma membrane increases the shuttling of SFB-G back into circulation. This can be most readily seen in the Mrp2 knockout groups, where the genetic disruption of Mrp2 alone causes a significant increase in plasma SFB-G concentrations, and the addition of the MCD diet further increases the plasma retention of the compound. These data, taken in conjunction with the tissue data that show an increase in hepatic SFB-G concentrations in *Mrp2* knockout animals but a significant decrease in the knockout MCD group, indicates that the disruption of biliary efflux via Mrp2 is not the sole mediator of plasma retention of SFB-G, and that alterations to sinusoidal uptake and efflux during MCD diet induced NASH contributes to the changes in pharmacokinetics. These data therefore confirm that the hepatocellular shuttling of SFB-G is significantly impaired during NASH due to disruption of the three cooperative transport mechanisms of 1) Mrp3 sinusoidal efflux, 2) impaired Mrp2 biliary efflux due to mislocalization, as well as 3) Oatp sinusoidal uptake, and quantifies the contribution of these mechanisms towards the overall changes to pharmacokinetics. This elucidates the mechanistic basis behind pharmacokinetic interindividual variability seen in patients undergoing treatment with sorafenib or other glucuronidated compounds. The disruption of the hepatocyte hopping process during NASH forms the underlying mechanism of pharmacokinetic alteration that has been seen in the progression of this disease and demonstrates the importance of the three major processes of hepatocyte hopping to drug disposition in human patients.

Acknowledgements

The authors would like to acknowledge Dr. Sharyn Baker for her generous gift of sorafenib-glucuronide standard, and Dr. Xinxin Ding and Dr. Leif Abrell for their assistance in LC-MS/MS method development and validation.

CHAPTER FIVE: ALTERATION OF IRON REGULATORY PROTEINS IN NONALCOHOLIC STEATOHEPATITIS

Introduction

Nonalcoholic steatohepatitis (NASH) is the more advanced form of nonalcoholic fatty liver disease (NAFLD). While NAFLD refers to simple steatosis, NASH presents with greater severity, with pathological symptoms including steatosis, fibrosis, inflammation, and significant hepatic oxidative stress. Fatty liver disease is widely considered the hepatic manifestation of metabolic syndrome, and NAFLD is also rapidly becoming one of the most common chronic liver diseases, manifesting in an estimated 30-40% of adults (Clarke et al., 2013). Approximately 90% of these patients also exhibit at least one clinical symptom. The frequency of NASH in the population is estimated to be within the range of 5-17%; as NASH can only be definitively diagnosed through biopsy, however, true incidence rates are difficult to determine (R. Ali & Cusi, 2009; McCullough, 2006). The progression from NAFLD to NASH is marked by the dysregulation of over 9,000 genes, many of which are key for absorption, disposition, metabolism, and excretion pathways (Lake et al., 2011). This can have serious ramifications for the disposition and toxicity of both exogenous and endogenous compounds. Since NASH also frequently manifests with comorbidities like hyperlipidemia and diabetes, it is likely that patients with NASH will also be on long-term, multi-drug medication regimens, and thus at risk for adverse drug reactions.

It has also been noted in the literature that a significant number of patients with chronic liver diseases like NASH tend to present with abnormal serum iron and hepatic iron stores; in NAFLD and NASH, roughly one-third and over 60% of them have increased hepatic iron concentrations, respectively (Bacon, Farahvash, Janney, & Neuschwander-Tetri, 1994; Nelson et al., 2011). These patients also tend to have increased fibrosis and histology scores, indicating that iron overload may contribute to the severity and pathogenesis of NASH (Bonkovsky, Banner, Lambrecht, & Rubin, 1996; Fargion et al., 2001; George et al., 1998). This is supported by studies

that have shown that iron removal via phlebotomy or chelation attenuates the progression of the disease (Yoshio Sumida et al., 2006; Valenti et al., 2007). Though iron is necessary for normal function, excess iron in hepatocytes can cause cellular damage through reactive oxygen species (ROS) production, which may play a role in disease progression.

Under normal conditions, iron levels are strictly maintained to prevent the deleterious effects of overload or deficiency. One of the major methods of controlling iron levels is through iron transport proteins. Ferroportin, a transporter protein found in hepatocytes and enterocytes, functions to move iron from the inside of a cell to the bloodstream. As the only known mammalian iron exporter, ferroportin plays a key role in the retention of iron, and dysregulation of the transporter can be the root cause of iron accumulation (D. Chen et al., 2007; Ward & Kaplan, 2012). The hormone hepcidin is the main regulator of ferroportin function, and therefore is one of the principal regulators of iron metabolism as a whole. In addition to ferroportin, transferrin receptor-1 transports iron into hepatocytes through endocytosis of transferrin, a glycoprotein that contains high-affinity Fe(III) binding sites and mediates iron concentrations in blood. TfR1 is controlled post-transcriptionally by intracellular iron levels through the interaction of iron response proteins (IRP1/2) and the iron response element (IRE) on mRNA. Regulation of IRP1 comes through post-translational alterations in structure in response to the presence or absence of iron. As the progression of NASH is known to result in the dysregulation of over 9,000 genes, it was hypothesized that NASH would disrupt the normal expression of genes involved in iron regulation and thus result in the hepatic iron accumulation seen in the disease.

Materials and Methods

Reagents

UPLC-grade water and acetonitrile, potassium ferrocyanide, hydrochloric acid, Nuclear Fast Red, ReadyScript cDNA synthesis kit, KiCqStart SYBR Green quantitative polymerase chain reaction (PCR) with low ROX master mix, and PCR primers for Bcrp and b-actin were obtained from Sigma-Aldrich. RNA Bee isolation reagent was obtained from Amsbio (Cambridge, MA).

Rat and Human Liver Tissue

Liver tissue from male Sprague-Dawley rats at 16 weeks of age that had been treated with either MCD diet to induce NASH or control diet was formalin-fixed and paraffin-embedded (FFPE). A portion of liver tissue was also flash-frozen in liquid nitrogen and stored at -80°C. Sections of liver tissue were H&E stained and evaluated by a board-certified veterinary pathologist for disease severity according to an established rodent NASH scoring system (Kleiner et al., 2005). Endpoints for NASH scoring included steatosis, necrosis, fibrosis, inflammation, and hyperplasia. Rank-order statistical methods and one-way analysis of variance were used to determine differences between groups. Incidence and severity scores were published previously (Toth et al., 2018).

Frozen and FFPE adult human liver tissue was obtained through the Liver Tissue Cell Distribution System that is coordinated through the University of Minnesota, Virginia Commonwealth University, and the University of Pittsburgh. The samples were scored by a medical pathologist within the Liver Tissue Cell Distribution System, and all scoring was performed according to an established NASH scoring system (Kleiner et al., 2005). Results were confirmed through histological examination at the University of Arizona. Metadata, including age and gender, has been previously published (Fisher, Lickteig, Augustine, Ranger-Moore, et al., 2009). Diagnoses consisted of: normal, steatotic, NASH with fatty liver, and NASH without fatty liver (NASH not fatty/cirrhosis). Samples were diagnosed as steatotic if there was >10% fatty infiltration of hepatocytes, as NASH (fatty) with >5% fatty infiltration of

hepatocytes with significant fibrosis and inflammation, as NASH (not fatty) when fatty infiltration was <5% with significant inflammation and fibrotic branches.

Quantitative Reverse-Transcription PCR

RNA isolation from liver tissue was performed using the RNA Bee isolation reagent. Approximately 300 mg of liver tissue was added to 4 mL of RNA Bee, homogenized, then treated according to the manufacturer's protocol. The RNA pellet was reconstituted in 250 μ L DEPC (diethyl decarbonate) water per 100 mg tissue, then stored at -80°C. RNA concentrations were determined via NanoDrop 2000 UV-visible spectrophotometer (Thermo Fisher Scientific, Waltham, MA). Final RNA preparations had a 260/280 quality ratio between 1.6 and 1.9. cDNA preparations were made from the isolated RNA using the ReadyScript cDNA synthesis kit (Sigma-Aldrich, St. Louis, MO). Reaction wells contained 1x KiCqStart SYBR Green master mix, 100 nM forward/reverse primers, 2 μ L cDNA template, and nuclease-free water. All reactions were run in duplicate. Reactions were run on a StepOnePlus Real Time PCR system (ABI, Waltham, MA) with standard SYBR green cycling profile. Fold change was determined via $\delta\text{-}\delta$ C_T method.

Perl's Prussian Blue Iron Staining

Iron staining was performed on liver sections according to the Perl's method. Solutions of 5% hydrochloric acid (HCl) and 5% potassium ferrocyanide were combined 1:1 to make the working solution. Slides were deparaffinized in xylene and hydrated in distilled (DI) water, then placed in the working solution for 30 minutes at room temperature. After 30 minutes, the slides were rinsed with DI water and then placed into nuclear fast red solution for 3 minutes. Slides were then rinsed three times in DI water and dehydrated in ethanol and xylene. The stained slides were then mounted with resin for microscopic analysis.

Protein Preparation

Membrane and cytosolic preparations were made from frozen liver tissue. Approximately 100 mg of tissue was homogenized in 1 mL of cold ST buffer (sucrose Tris buffer; 10 mM Tris base and 250 mM sucrose) with protease inhibitor (Roche, Indianapolis, IN). Homogenates were centrifuged at 10,000xg for 20 minutes to remove nuclei and then the supernatant was decanted into a second set of ultracentrifuge tubes. The supernatant was spun at 100,000xg for 60 minutes to pellet the membrane fraction. The supernatant, which contains the cytosolic fraction, was transferred into a separate set of microcentrifuge tubes and stored at -80°C. Membrane pellets were rinsed with buffer, then resuspended in 100 µl buffer and stored at -80°C. Protein concentrations were determined via bicinchoninic acid assay (Thermo Fisher Scientific).

Targeted Proteomic Quantification of Iron Regulatory Proteins

Denaturing buffer was prepared, consisting of 3.7% sodium deoxycholate in 100mM of ammonium bicarbonate. Membrane or cytosolic preparations were diluted to 300 µg in 100 µL of denaturing buffer. Samples were reduced by adding DTT to a final concentration of 6 mM and incubated for 5 minutes at 95°C. The samples were then alkylated by adding iodoacetamide to 15 mM and incubating for 30 minutes at room temperature. Protein digestion was then performed using sequencing-grade trypsin at an enzyme:substrate ratio of 1:100. Proteins were digested in a water bath at 37°C overnight. The next day, the reaction was quenched using 0.4% formic acid. Samples were centrifuged at 16,000 xg for 30 minutes and the supernatant was collected, then desalted on a Waters Sep Pak C18 solid phase extraction cartridge (Milford, MA) as per the manufacturer's instructions. The eluted peptides were dried down using a centrivap. Samples were then reconstituted in mobile phase and run on a Sciex Qtrap 6500 with triple quad LC-MS/MS system (Framingham, MA) using a Waters Acquity UPLC BEH C19 column (1.7µm, 2.1 x 50 mm). Mobile phase consisted of 0.1% formic acid in water (A) and 0.1 % formic acid in 80% acetonitrile (B). Runs were 30 minutes long at 0.2 mL/min with a 10 µL injection volume. The UPLC gradient ran at 5.5% B from 0-2 minutes, then

increased to 33.3% B from 2-22 minutes, held at 33% B until 24 minutes, then increased to 100% B from 24-26 minutes. The gradient then returned to 5.5% B from 26-28 minutes and maintained for 2 minutes before the start of the next run. Raw data were analyzed using Analyst 1.6.2 (SCIEX, Ontario, Canada). Protein fragments and MRM transitions can be found in table 1. Statistical analyses were performed in GraphPad Prism 7.

Statistics

Human liver mRNA and protein data were presented as box and whisker plots comparing median values. Data were analyzed using a nonparametric trend analysis with a significance level of $p \leq 0.05$, which allows for the determination of changes with disease progression.

Rodent mRNA and protein data were presented as column graphs and analyzed using student's t-test and presented as mean \pm SD.

Results

Effect of Disease Progression on Human mRNA Expression

The mRNA expression of iron regulatory genes in human liver tissue was determined via Affymetrix Plex 2.0 assay in normal, steatosis, NASH (fatty), and NASH (not fatty) groups (fig 5.1). The genes investigated included hepcidin (*HAMP*), ferroportin (*SLC40A1*), divalent metal transporter 1 (*SLC11A2*), transferrin receptor-1 (*TFRC*), transferrin (*TF*), ferritin heavy and light chain (*FTH*, *FTL*), and iron response binding protein (*ACO1*). The only significant trends seen in the data were for *HAMP*, *SLC11A2*, and *ACO1*, the expression of which decreased throughout the progression of the disease. *TFRC*, *TF*, and *FTH* appeared to have an increasing trend from normal to NASH (fatty), but the trend was not statistically significant.

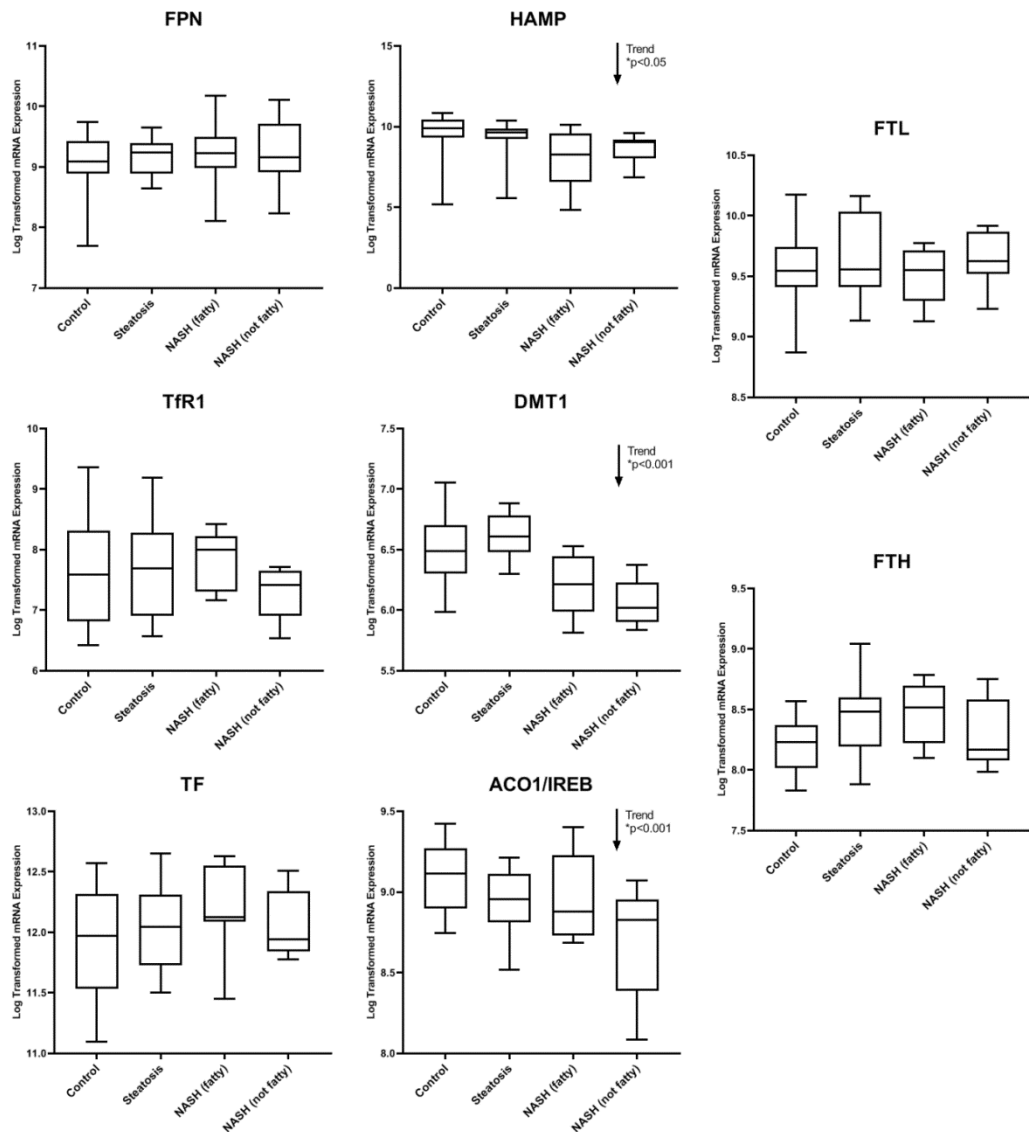


Fig. 5.1. Altered mRNA expression during the progression of NASH in human liver tissue. Transcriptomic analysis of human liver samples was done by Affymetrix chip and previously published. Expression change was determined using nonparametric trend analysis. Data represents mean \pm SD, n=10.

Effect of Disease Progression on Human Protein Expression

Protein expression of iron regulatory proteins was determined by targeted proteomic analysis in normal, steatosis, NASH (fatty), and NASH (not fatty) groups (fig 5.2). The proteins investigated included hepcidin (HEPC), ferroportin (FPN), divalent metal transporter 1 (DMT1),

transferrin receptor-1 (TFRC), transferrin (TRFE), ferritin heavy chain (FtH), and ferritin light chain (FtL), and the proteins were normalized to either the sodium-potassium pump (Na⁺/K⁺-ATPase) in the case of membrane proteins, or to cyclophilin A for cytosolic proteins. Mass/charge ratios and retention times can be found in table 1. Of these proteins, TRFE, TFR1, FtH, and FtL increased in expression with disease progression, while HEPC, DMT1, and FPN showed a decreasing trend.

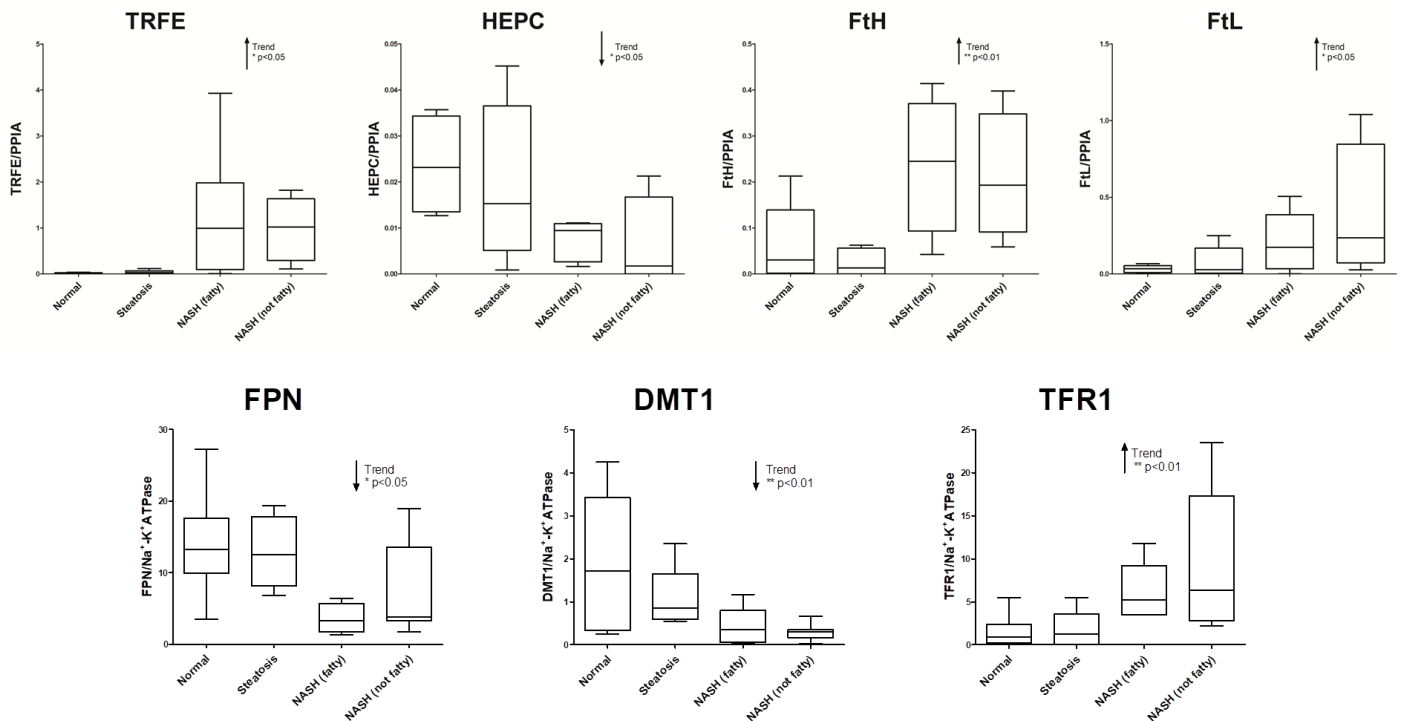


Fig 5.2. Altered protein expression during the progression of NASH in human liver tissue. Relative protein expression in human liver tissue was determined via proteomic analysis using LC-MS/MS and normalized to Na⁺/K⁺-ATPase or Cyclophilin A (PPIA) expression. Data represents mean ± SD, n=10.

Effect of Disease Progression on Human Hepatic Iron Levels

Perl's Prussian blue iron stain was used to assess the amount of ferric iron deposits within human hepatocytes in normal, steatotic, NASH (fatty), and NASH (not fatty) patient groups (fig 5.3). The percent of stained tissue was determined by assessing the area of stained tissue

divided by total tissue area (fig 5.4). Trend analysis determined an increase in iron deposits as the disease progressed.

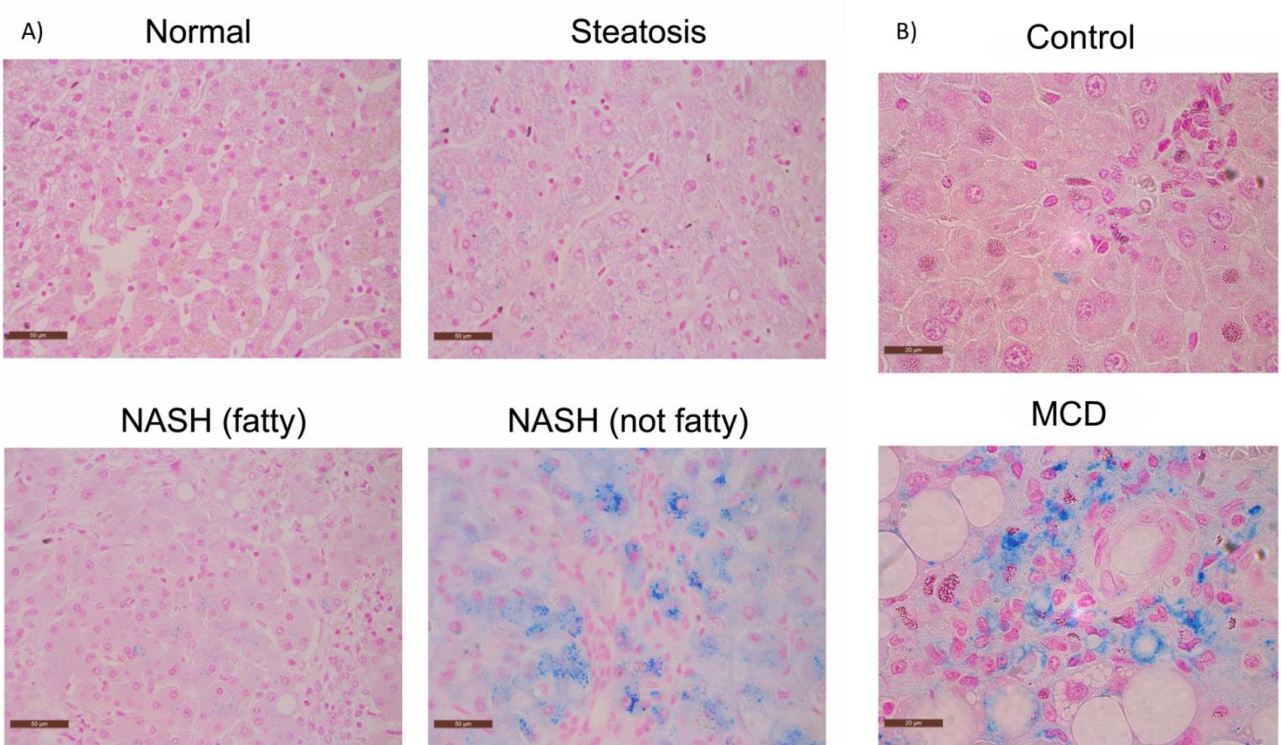


Fig 5.3. Altered protein expression during the progression of NASH in human liver tissue. Relative protein expression in human liver tissue was determined via proteomic analysis using LC-MS/MS and normalized to Na⁺/K⁺-ATPase or Cyclophilin A (PPIA) expression. Data represents mean \pm SD, n=10.

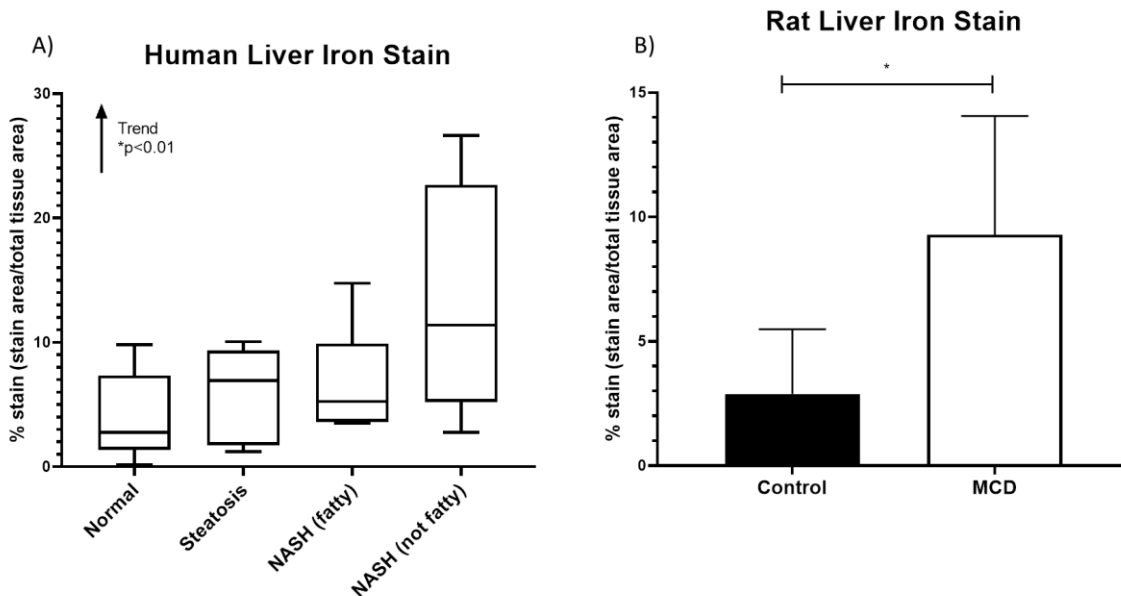


Fig. 5.4. Percent area of Perl's Prussian blue iron staining in liver tissue. Percentage of stained area on histology slides was determined by stained area/total area in A) human and B) rat liver tissue sections. Change in percent area was determined using nonparametric trend analysis for human samples and student t-test for rat samples. Data represents mean \pm SD, n=10 for human, n=5 for rat. * $P \leq .05$.

Effect of NASH on Rat mRNA Expression

The mRNA expression of iron regulatory genes in rat liver tissue was determined via qRT-PCR in normal and MCD diet-induced NASH animals (fig 5.5). The genes investigated included (*Hamp*), ferroportin (*Slc40a1*), divalent metal transporter 1 (*Slc11a2*), transferrin receptor-1 (*Tfrc*), transferrin (*Tf*), and iron response binding protein (*Aco1*). Between the control and MCD groups, the mRNA expression changes were as follows: the expression of *Hamp* increased by 2-fold, of *Slc40a1* increased by 1.6-fold, of *Slc11a2* increased by 1.5-fold, of *Tfrc* decreased by 0.24-fold, of *Tf* increased by 2.4-fold, and of *Aco1* increased by 2.5-fold.

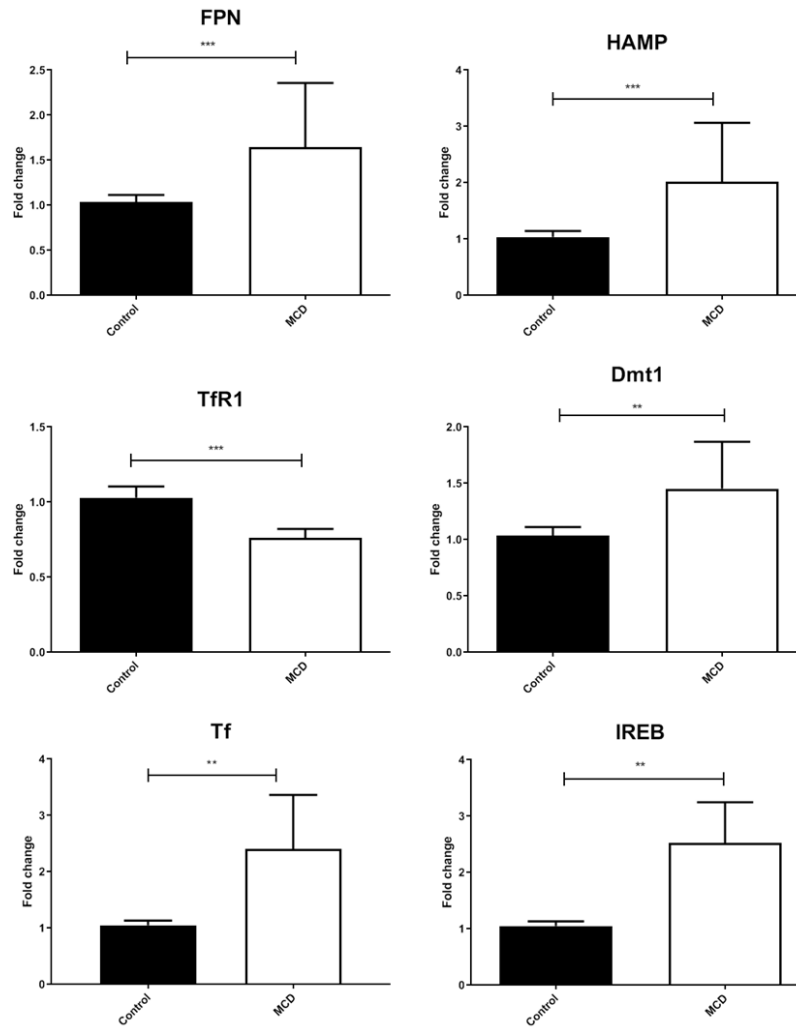


Fig. 5.5. Altered mRNA expression in rodent diet-induced NASH. mRNA expression was determined through qRT-PCR and fold change was determined using the $\Delta\Delta C_T$ method. Data represents mean \pm SD, n=5. * $P \leq .05$, ** $P \leq .01$, *** $P \leq .001$.

Effect of NASH on Rat Protein Expression

Protein expression of iron regulatory proteins was determined by targeted proteomic analysis in normal, steatosis, NASH (fatty), and NASH (not fatty) groups (fig 5.6). The proteins investigated included hepcidin (Hepc), ferroportin (Fpn), divalent metal transporter 1 (Dmt1), transferrin receptor-1 (Tfrc), transferrin (Trfe), ferritin heavy chain (Fth), and ferritin light chain (Ftl), and the proteins were normalized to either the sodium-potassium pump (Na^+/K^+ -ATPase)

in the case of membrane proteins, or to cyclophilin A for cytosolic proteins. Mass/charge ratios and retention times can be found in table 1. Of the proteins investigated, Fth and FtL expression in the MCD group decreased to 59% and 53% of control, respectively, and Fpn increased to 500% of control. No significant changes were observed in Hepc or Trfe expression.

Effect of NASH on Rat Hepatic Iron Levels

Perl's Prussian blue iron stain was used to assess the amount of ferric iron deposits within rat hepatocytes in control and MCD diet-induced NASH animals (fig 5.3). Percent of stained tissue was determined by dividing the area of the stained tissue by the total tissue area. Iron deposits in the MCD diet-induced NASH rats increased by 3.2-fold when compared to controls.

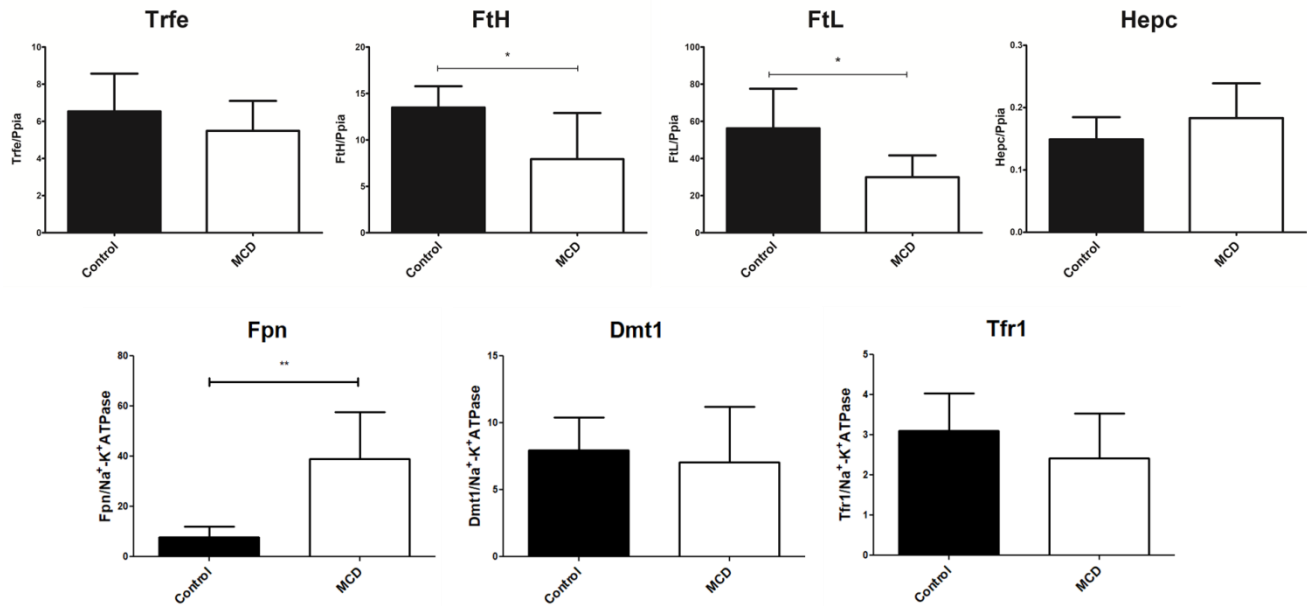


Fig. 5.6. Altered protein expression in rodent diet-induced NASH. Relative protein expression was determined by proteomic analysis using LC-MS/MS and normalized to Na⁺/K⁺-ATPase expression. Data represents mean ± SD, n=5. * P≤.05, ** P≤.01.

<u>Peptide</u>	<u>Sequence</u>	<u>Q1 Mass</u>	<u>Q3 Mass</u>
Hepcidin	K.TDDSALLMLK.R	553.7	688.4
FPN (h)	K.SVPIISVSLLFAGVIAAR.I	907.0	1030.6
Fpn (r)	K.SVPIISVSLLFAGVIAAR.I	907.0	917.5
FTH (h)	R.DDWESGLNAMR.C	647.2	661.3
Fth (r)	K.MGAPESGMAEYLFDK.H	823.3	1016.4
FTL (h)	R.ASYTYLSLGFDFR.D	843.9	901.4
Ftl (r)	K.TLEAMEAALALEK.N	695.3	715.4
DMT1 (h)	K.LLWVLLLATIVGLLLQR.L	967.6	1012.6
Dmt1 (r)	K.LLWVLLLATIVGLLLQR.L	967.6	1196.7
TRFE (h)	K.SASDLTWDNLK.G	625.3	675.3
Trfe (r)	K.ASDSSINWNNLK.G	674.8	901.4
TFR1	K.AFTYINLDK.V	542.7	765.4
PPIA	K.EGMNIVEAMER.F	639.7	961.4
Na+/K+ATPase	R.AAVPDAVGK.C	414.2	586.3

Table 5.1. Peptide Fragments and MRM Transitions for LC-MS/MS Analysis.

Discussion

It is not uncommon for patients with chronic liver diseases, including NASH, to present with atypical serum iron and hepatic iron overload. Approximately 60% of NASH patients present with abnormally high hepatic iron stores, and these patients also tend to present with increased fibrosis histology scores (Bacon et al., 1994; Bonkovsky et al., 1996; Fargion et al., 2001; George et al., 1998; Nelson et al., 2011). This iron overload may be a contributing factor to the progression of NAFLD to NASH, especially as iron removal via phlebotomy has been shown to reduce the NAS scores of biopsy-verified NASH patients (Yoshio Sumida et al., 2006; Valenti et al., 2007). The attenuation of the disease that occurs post-phlebotomy treatments may be due

to the reduction of labile iron pools within hepatocytes; free iron can participate in Fenton reactions within the cell, producing hydroxyl radicals that can cause cellular damage. Certain liver enzymes also require iron-containing heme cofactors to function, and therefore produce reactive oxygen species during their normal function.

Hepatic iron stores are tightly regulated in order to prevent the deleterious consequences associated with iron overload. As there are limited ways to remove iron from the body after it has been absorbed, much of the mechanisms that regulate it are either associated with transporting iron or sequestering it in storage proteins. One of the major transporters involved in the movement of iron is ferroportin, a transmembrane protein found in a variety of cells, including hepatocytes and enterocytes. This protein is the only known mammalian iron exporter, and therefore plays a key role in managing the intracellular concentrations of iron, and dysregulation of this protein can have significant impacts on iron stores (D. Chen et al., 2007; Ward & Kaplan, 2012). Ferroportin is negatively regulated by hepcidin, a hormone produced by the liver that binds to the active site of ferroportin and causes its internalization (Bogdan et al., 2016; Nemeth & Ganz, 2006).

Transferrin receptor-1, on the other hand, is the major mediator of iron uptake by hepatocytes through the binding of transferrin, an iron carrier glycoprotein. The process by which transferrin receptor-1 internalizes iron-laden transferrin has been extensively studied. When diferric TF binds to TfR1, the glycoprotein and the receptor are internalized in a clathrin-coated pit via endocytosis. The resulting endosome undergoes a drop in pH, which causes a structural change in TF. The histidine³⁴⁹ residue of TF and the tryptophan⁶⁴¹ and phenylalanine⁷⁶⁰ residues of TfR1 interact and trigger the transformation, which then results in the release of iron from TF. The TF-TfR1 complex is then recycled back to the surface of the cell, where TF is released back into circulation and TfR1 returns to its membrane localization (Daniels, Delgado, Rodriguez, Helguera, & Penichet, 2006). Alterations to this

mechanism either through TF or TfR1 could result in significant dysregulation of iron uptake and intracellular iron concentrations. This is particularly relevant for TfR1, as its expression is primarily mediated through post-transcriptional modifications rather than transcriptional regulators. TfR1 is mediated by the binding of iron response proteins to the iron response element (IRE) on its mRNA, as is the only known protein to contain multiple of these IRE hairpins. Binding of IRPs to these hairpins stabilizes the mRNA and allows for its translation into protein (PANTOPOULOS, 2004). IRPs themselves are regulated directly by iron, as they undergo conformational changes when in the presence of high or low iron concentrations; however, IRPs can be activated by ROS, which could result in inappropriate binding to IREs in conditions of high oxidative stress, such as chronic liver diseases (Mueller et al., 2001; Pantopoulos & Hentze, 1998).

It has been known for some time that chronic liver diseases impact hepatic iron levels, and the purpose of this study is to describe the alterations to hepatic iron regulator proteins that occur during the progression of NASH in human patients and the rodent MCD model. Perl's Prussian blue iron staining revealed that there is a trend of increasing hepatic iron deposition during the progression of the disease, which is recapitulated in the rodent MCD model of NASH. Transcriptomic analysis of human samples also determined that several genes responsible for mediating iron regulation are altered during NASH, including *ACO1*, *HAMP*, and *DMT1*. These changes, however, were not reflected in the MCD model, which instead presented with upregulation of *Fpn*, *Hamp*, *Dmt1*, *Tf*, and *Aco1* and downregulation of *TfR1*. The protein expression of these iron proteins was also incongruent between the human disease and animal model; in human patients, TfR1, TRFE, FTH, and FTL were upregulated, and HEPC, FPN, and DMT1 were downregulated. In the MCD rat model, only Fth and Ftl were downregulated, while Fpn was upregulated. These differences between human and MCD diet-induced NASH likely arise from the disparate pathogenesis between the human disease and the MCD model. While

the development of NASH in humans is a complex process that takes many years to manifest and involves comorbidities and other complicating factors, the MCD diet utilizes methionine and choline deficiency to impair the hepatic production and secretion of very-low-density lipoprotein (VLDL), alter mitochondrial bioenergetics and fatty acid β -oxidation, and disrupt hepatic methyl balance(Li, Toth, et al., 2017). Though the end result of the MCD diet is a liver that histologically mirrors human NASH and presents with similar alterations to hepatic xenobiotic transporter proteins, its pathogenesis mechanisms are otherwise dissimilar and do not result in the same alterations to iron regulatory proteins as human NASH. Other rodent models that more closely mimic the human pathogenesis of NASH may provide better insights into the mechanisms of iron regulation during the disease than the MCD model.

While it is unlikely that dysregulation of any one individual iron regulatory protein is solely responsible for the increase in hepatic iron seen in NASH human tissue, alterations to several of them are likely contributory factors. Increases in TfR1 protein expression in NASH, possibly due to ROS activation of ACO1 or post-translational modifications that prolong the half-life of the protein, along with increased TRFE expression could result in increased iron import into hepatocytes, while decreased ferroportin expression may contribute to the hepatic accumulation of iron through reduced efflux. Decreased serum hepcidin also results in increased intestinal absorption by increasing FPN expression in the duodenum, as has been seen in chronic hepatitis C patients(Sato et al., 2018). While the upregulation of ferritin subunits would indicate increased iron storage potential in the hepatocyte, the high oxidative stress that occurs during NASH(R. N. Hardwick et al., 2010; Y Sumida, Niki, Naito, & Yoshikawa, 2013) inhibits ferritin's ability to sequester iron. The heavy subunits of ferritin have ferroxidase activity to convert iron from the ferrous to the more stable ferric form for storage. When antioxidants are depleted, as in conditions of high oxidative stress, ferroxidase activity becomes downregulated, preventing the removal of ferrous iron from iron pools in the cell. Additionally, a rapid release of

iron from ferritin occurs during these conditions due to increasing reducing potential and anaerobiosis.(Manuel Fernandez-Real et al., 2002) Overall, then, the iron storage capacity of ferritin would likely be reduced in NASH despite upregulation of protein expression due to high oxidative stress. Though this research gives some insight into the potential alterations to iron regulation that may drive the hepatic iron accumulation seen in human NASH patients, further investigation is necessary to pinpoint the responsible mechanisms.

Acknowledgments

The authors would like to thank Dr. Xinxin Ding for his assistance with the LC-MS/MS targeted proteomic method development.

CHAPTER SIX: CURRENT PERSPECTIVES AND FUTURE DIRECTIONS

Summary of Studies

Alterations to hepatic uptake and efflux transporters are responsible for variable drug response in human patients, as many compounds rely on active transport for their disposition and elimination. The extensive remodeling of ADME processes that occurs during the progression of NASH also dysregulates the expression of hepatic uptake and efflux transporters, resulting in pharmacokinetic alterations. While simple genetic polymorphisms or NASH alone can be sufficient to cause changes to disposition, the interaction between genes and disease state can result in pharmacokinetic alterations that are greater than the sum of their parts. The purpose of this doctoral work was to determine the impact of synergistic gene-by-environment interactions between NASH and polymorphisms of hepatic uptake and efflux transporters on drug disposition and to determine the underlying mechanism of altered pharmacokinetics in NASH.

Chapters 2 and 3 investigated the impact of genetic polymorphisms of *Bcrp* and *Oatp1b2* and NASH on drug disposition using the MCD rodent model. The results in this model indicate that the combination of a full genetic knockout with NASH is sufficient to cause significant pharmacokinetic alterations, potentially increasing the risk of toxicity. In the *Bcrp* study, the combination of *Bcrp*^{-/-} and NASH resulted in a dramatic decline in biliary excretion of both parent compound and metabolite, demonstrating the both a compensatory mechanism by which the liver can upregulate *Bcrp* expression in order to offset the decrease in function of the mislocalized *Mrp2* transporter as well as the synergistic gene-by-environment interaction. In the *Oatp1b2* gene dose study, the *Oatp1b2*^{-/+} mice showed no significant alterations to plasma AUC or tissue concentrations; the full genetic knockout was necessary to observe altered pharmacokinetics. This is likely due to the upregulation of *Oatp1a4* during NASH, which can participate enough in the transport of pravastatin to avoid significant pharmacokinetic

consequences so long as there is some amount of function Oatp1b2. The loss of compensatory transport through genetic polymorphisms during NASH disrupts normal disposition and elimination, resulting in increases in plasma retention and potentially increased risk of toxicity for patients.

In chapter 4, the underlying mechanism by which alterations to hepatic uptake and efflux transporters impact pharmacokinetics was described through the use of the MCD diet in combination with *Oatp1a/1b* cluster knockouts and *Mrp2* knockouts. The disposition of SFB-G is mediated through Oatps, Mrp3, and Mrp2, though the sinusoidal uptake and efflux transporters are the major players in the hepatocyte hopping pathway, as disruption of Oatps would prevent downstream reuptake and upregulation of Mrp3 would increase efflux into plasma. The reduction in hepatic uptake due to either the *Oatp1a/1b* cluster knockout or the MCD diet resulted in plasma retention of SFB-G, as did the *Mrp2* knockout; the addition of the MCD diet with the *Mrp2* knockout, however, also showed a significant increase in the plasma concentrations of SFB-G, representing the impact of the decreased Oatp expression and increased Mrp3 expression that occurs during NASH on plasma concentrations. These data, when taken with the liver tissue concentration data that showed an increase in hepatic SFB-G concentration in the *Mrp2* knockout but decreased concentration in the *Mrp2* knockouts with NASH, indicate that sinusoidal uptake and efflux transporters are mediators of hepatocyte hopping, not Mrp2, and that pharmacokinetic interindividual variability seen in NASH patients is due to disruption of the hepatocyte hopping mechanism. As the Oatp and Mrp transporters have broad substrate specificities, and many pharmaceutical compounds undergo glucuronidation, it is likely that a wide range of therapeutics would be affected by the disruption of hepatocyte hopping during this disease.

The purpose of chapter 5 was to investigate the impact of NASH on hepatic iron regulatory mechanisms, including transporters, iron storage proteins, and other mediators. It was

determined that the progression of NASH resulted in the hepatic accumulation of iron in both human NASH and the MCD rodent model, and that the disease also caused alterations to mRNA and protein expression of iron transport and storage proteins. While NASH impacted expression in both the human disease and the MCD diet rats, the specific alterations to iron regulatory proteins was disparate between those two groups, and the MCD diet did not adequately reflect the changes that were found in the human disease. This was likely due to the inherent differences in the pathogenesis of NASH in humans and the MCD diet. Though the hepatic iron accumulation could not be fully explained by the mRNA and protein alterations observed in the human disease, some insight could be gained on the contributory factors that may impact the increased iron concentrations observed in human NASH liver tissue.

Future Directions

Renal ADME Alterations During NASH

There has been significant research in recent years on the impact of crosstalk between the liver and kidney and the relationship between liver function and kidney dysfunction. Hepatorenal syndrome is one notable example, where acute renal injury occurs secondary to cirrhosis due to circulatory changes that cause vasoconstriction in the kidney. There is also some evidence that NAFLD and NASH may result in kidney injury through the release of inflammatory cytokines, ROS, and other deleterious mediators.

Findings from the Cherrington lab also have indicated that there may be alterations to renal kidney transporter expression as a compensatory mechanism for the decreased hepatobiliary excretion seen during NASH. The disposition of metformin, which is primarily eliminated through renal excretion, has been shown to be altered in the diabetic *ob/ob* mouse model of NASH, and a previous study with adefovir indicated that there was a decreased filtrate rate but increased secretion rate of the compound in the NASH model (Clarke et al., 2015; Laho

et al., 2016). This indicates that NASH significantly impacts transport mechanisms in the kidney and could thus contribute to the inter-individual variability of drug response in human patients.

This study endeavors to identify the impact of NASH on renal function in human patients, as these changes may significantly impact the fate of drug therapies. There is little information on the effect of NASH on renal filtration and secretion, despite the potential influence on the risk of toxicity in certain patient populations. It is therefore hypothesized that NASH alters the expression and function of renal xenobiotic transporter proteins, changing the pharmacokinetics of drug therapies in NASH patients and increasing the risk of adverse drug reactions. The following aims intend to test the hypothesis:

Aim 1. Determine the changes in expression and localization of renal transporter enzymes in human NASH patients

A collection of kidney tissue from biopsy-verified NASH and normal patients is available to the Cherrington lab. The mRNA and protein expression of transporters of interest, including but not limited to OAT1, OAT3, OCT1, OCT2, MATE1, MATE2-K, BCRP, MRP4, and various OATPs, will be determined through transcriptomic and proteomic analyses.

Aim 2: Determine the functional changes in individual secretion pathways and resulting potential for toxicity in a rodent model of NASH

Using the data gained from Aim 1, an appropriate animal model of NASH will be selected from a pool of potential models based on which best recapitulates the mRNA and protein changes observed in the human disease. A battery of transport studies will then be conducted to assess secretion pathways. An appropriate probe compound will be used in the animal model to determine the impact of NASH on toxic potential.

Aim 3: Determine the impact of NASH on GFR and secretion in human patients

Bariatric surgery volunteers will be recruited with the help of surgeon collaborators for a clinical study. Patients will be categorized into NASH or not NASH groups, then a subtherapeutic dose of a probe cocktail of adefovir and metformin, along with a dose of iohexol to determine GFR, will be administered, with urine and plasma being collected for a period of 10 hours after dosing. Anticipated results include decreased GFR in the NASH patients, with altered pharmacokinetics of adefovir and metformin following the changes in transporter expression as determined in Aim 1.

Iron Regulation in NASH

The progression of NASH, as with other chronic liver diseases, results in the increased deposition of iron in hepatocytes. The increased labile iron pools have the potential to participate in Fenton reactions, thereby producing reactive oxygen species and compounding oxidative stress in the cells, potentially exacerbating the disease. It has been previously found that the progression of NASH causes alterations to the mRNA and protein expression of iron transport and storage mediators in the liver, which likely contribute to the aberrant iron levels found in human NASH hepatocytes. These changes do not entirely explain the accumulation observed in hepatocytes, however, nor does the commonly used MCD rodent model of NASH recapitulate the human alterations. Therefore, further research is necessary to probe the mechanisms behind the dysregulated iron storage in NASH and to determine an animal model that would be more appropriate for studying iron regulation in NASH than the MCD model.

Many factors beyond the transcriptional can influence the expression of a particular protein; in the case of iron transport and storage proteins, the IREB/ACO1 iron response binding factor plays a major role in up- or down-regulating proteins involved in iron storage, and post-translational modifications like glycosylation are important for the appropriate localization of transporter proteins like ferroportin or DMT1. While it has been previously determined that the glycosylation of some transporter proteins is decreased in NASH and this may impact their

proper function and localization(Clarke, Novak, Lake, Hardwick, & Cherrington, 2017), there is a dearth of information on the glycosylation status of FPN, DMT1, and TfR1 during the disease. The glycosylation status is particularly important for the function of DMT1 and TfR1, as TfR1 has a critical glycosylation and the affinity of DMT1 for iron is altered based on glycosylation(Dunham et al., 2018; Zhao & Enns, 2013). Other post-translational modifications, like phosphorylation and ubiquitination(Czuba, Hillgren, & Swaan, 2018; Ward & Kaplan, 2012). Additionally, there is some evidence that increased oxidative stress can alter the ferroxidase activity of ferritin, preventing iron storage within the protein complex. These non-transcriptional mechanisms thus may contribute to the hepatic iron accumulation seen in NASH.

While the MCD diet may have utility for investigating pharmacokinetic alterations in NASH due to transporter alterations, it does not successfully recapitulate the disease in any other facet(Li, Toth, et al., 2017). Other diet-induced NASH models may have greater success at modeling the changes that occur during this disease to other pathways, including iron regulation. Long-term high fat/high fructose diets are known to induce NASH in rodent models, and these animals also exhibit similar perturbations to lipid metabolism and insulin sensitivity that is found in human NASH patients(Dowman et al., 2014). As these diets more faithfully reproduce the pathogenesis of NAFLD and NASH in the rodent model, there is a greater likelihood that it may also alter the pathways involved in iron regulation in a similar pattern to human patients.

This study aims to identify the mechanisms behind the hepatic iron accumulation found in human NASH and to determine an effective rodent model that recapitulates the changes seen in the human disease. It is hypothesized that NASH causes alterations to IREB/ACO1 binding activity, post-translational modifications to transporter proteins such as glycosylation, phosphorylation, and ubiquitination, and ferroxidase activity of ferritin, and that the changes to

iron regulation observed in human NASH will be recapitulated in a long-term high fat/high fructose rodent diet model.

Aim 1. Determine the changes to the functional activity of IREB/ACO1 binding and ferroxidase in human NASH

Liver tissue from biopsy-verified NASH patients is available to the Cherrington lab. Aconitase activity kits are commercially available and will determine the activity of IREB/ACO1 in these samples. Ferroxidase activity of ferritin will be determined through the transferrin reaction (Bakker & Boyer, 1986).

Aim 2. Determine the changes to post-translational modifications of iron regulatory proteins in human NASH

Using the available human samples, the mRNA and protein expression of glycosylation mediators, kinases, and ubiquitin ligases will be determined through PCR and targeted proteomic LC-MS/MS analysis. Targeted proteomic LC-MS/MS analysis will also be used to determine the ratio of modified protein to unmodified protein during the progression of the disease.

Aim 3. Characterize the alterations to iron regulation in a high fat/high fructose NASH rodent diet

With the data gained from the human NASH patients in Aim 1 and Aim 2, and from data gained in previous studies, diet-induced rodent NASH models can be assessed to determine which best recapitulates the changes seen in human disease.

BIBLIOGRAPHY

- Aharoni-simon, M., Hann-obercyger, M., Pen, S., Madar, Z., & Tirosh, O. (2011). Fatty liver is associated with impaired activity of PPAR γ -coactivator 1 α (PGC1 α) and mitochondrial biogenesis in mice, *91*(August 2010), 1018–1028. <https://doi.org/10.1038/labinvest.2011.55>
- Aleksunes, L. M., Scheffer, G. L., Jakowski, A. B., Pruijboom-Brees, I. M., & Manautou, J. E. (2005). Coordinated expression of multidrug resistance-associated proteins (Mrps) in mouse liver during toxicant-induced injury. *Toxicological Sciences*, *89*(2), 370–379.
- Aleksunes, L. M., Slitt, A. M., Cherrington, N. J., Thibodeau, M. S., Klaassen, C. D., & Manautou, J. E. (2004). Differential expression of mouse hepatic transporter genes in response to acetaminophen and carbon tetrachloride. *Toxicological Sciences*, *83*(1), 44–52.
- Ali, I., Slizgi, J. R., Kaullen, J. D., Ivanovic, M., Niemi, M., Stewart, P. W., ... Brouwer, K. L. R. (2017). Transporter-Mediated Alterations in Patients With NASH Increase Systemic and Hepatic Exposure to an OATP and MRP2 Substrate. *CLINICAL PHARMACOLOGY & THERAPEUTICS*, *00*(00), 1–8. <https://doi.org/10.1002/cpt.997>
- Ali, R., & Cusi, K. (2009). New diagnostic and treatment approaches in non-alcoholic fatty liver disease (NAFLD). *Annals of Medicine*, *41*(4), 265–278. <https://doi.org/10.1080/07853890802552437>
- Bacon, B. R., Farahvash, M. J., Janney, C. G., & Neuschwander-Tetri, B. (1994). Nonalcoholic steatohepatitis: an expanded clinical entity. *Gastroenterology*, *107*(4), 1103–1109.
- Bakker, G. R., & Boyer, R. F. (1986). Iron incorporation into apoferritin. The role of apoferritin as a ferroxidase. *Journal of Biological Chemistry*, *261*(28), 13182–13185.
- Bates, D. W., Spell, N., Cullen, D. J., Burdick, E., Laird, N., Petersen, L. A., ... Leape, L. L. (1997). The costs of adverse drug events in hospitalized patients. *Jama*, *277*(4), 307–311.
- Batts, K. P. (2007). Iron overload syndromes and the liver. *Modern Pathology*, *20*, S31. Retrieved from <https://doi.org/10.1038/modpathol.3800715>
- Bekri, S., Gual, P., Anty, R., Luciani, N., Dahman, M., Ramesh, B., ... Le Marchand-Brustel, Y. (2006). Increased Adipose Tissue Expression of Hepcidin in Severe Obesity Is Independent From Diabetes and NASH. *Gastroenterology*, *131*(3), 788–796. <https://doi.org/10.1053/j.gastro.2006.07.007>
- Berlanga, A., Guiu-jurado, E., Porras, J. A., & Auguet, T. (2014). Molecular pathways in non-alcoholic fatty liver disease. *Clinical and Experimental Gastroenterology*, *4*(7), 221–239.
- Bins, S., van Doorn, L., Phelps, M. A., Gibson, A. A., Hu, S., Li, L., ... Baker, S. D. (2017). Influence of OATP1B1 Function on the Disposition of Sorafenib- β -D-Glucuronide. *Clinical and Translational Science*, *10*(4), 271–279. <https://doi.org/10.1111/cts.12458>
- Bogdan, A. R., Miyazawa, M., Hashimoto, K., & Tsuji, Y. (2016). Regulators of Iron Homeostasis: New Players in Metabolism, Cell Death, and Disease. *Trends in Biochemical Sciences*. <https://doi.org/10.1016/j.tibs.2015.11.012>
- Bonkovsky, H., Banner, B., Lambrecht, R., & Rubin, R. (1996). Iron in liver diseases other than hemochromatosis. *Seminars in Liver Disease*, *16*(1), 65–82.

- Boudou-Rouquette, P., Narjoz, C., Golmard, J. L., Thomas-Schoemann, A., Mir, O., Taieb, F., ... Blanchet, B. (2012). Early Sorafenib-induced toxicity is associated with drug exposure and UGT1A9 genetic polymorphism in patients with solid tumors: A preliminary study. *PLoS ONE*, 7(8), 1–9. <https://doi.org/10.1515/cclm-2016-0207>
- Bourgeois, F. T., Shannon, M. W., Valim, C., & Mandl, K. (2010). Adverse drug events in the outpatient setting: an 11-year national analysis. *Pharmacoepidemiology and Drug Safety*, 19, 901–910. <https://doi.org/10.1002/pds.1984>
- Brown, S.-A., & Pereira, N. (2018). Pharmacogenomic impact of CYP2C19 variation on clopidogrel therapy in precision cardiovascular medicine. *Journal of Personalized Medicine*, 8(1), 8.
- Bruckert, E., Hayem, G., Dejager, S., Yau, C., & Bégaud, B. (2005). Mild to moderate muscular symptoms with high-dosage statin therapy in hyperlipidemic patients - The PRIMO study. *Cardiovascular Drugs and Therapy*, 19(6), 403–414. <https://doi.org/10.1007/s10557-005-5686-z>
- Brunham, L. R., Lansberg, P. J., Zhang, L., Miao, F., Carter, C., Hovingh, G. K., ... Hayden, M. R. (2012). Differential effect of the rs4149056 variant in SLCO1B1 on myopathy associated with simvastatin and atorvastatin. *Pharmacogenomics Journal*, 12(3), 233–237. <https://doi.org/10.1038/tpj.2010.92>
- Buzzetti, E., Pinzani, M., & Tsochatzis, E. A. (2016). The multiple-hit pathogenesis of non-alcoholic fatty liver disease (NAFLD). *Metabolism*, 65(8), 1038–1048. <https://doi.org/10.1016/j.metabol.2015.12.012>
- Canet, M. J., Hardwick, R. N., Lake, A. D., Dzierlenga, A. L., Clarke, J. D., & Cherrington, N. J. (2014). Modeling Human Nonalcoholic Steatohepatitis-Associated Changes in Drug Transporter Expression Using Experimental Rodent Models. *Drug Metabolism and Disposition*, 42(4), 586–595.
- Canet, M. J., Merrell, M. D., Hardwick, R. N., Bataille, A. M., Campion, S. N., Ferreira, D. W., ... Erickson, R. P. (2015). Altered regulation of hepatic efflux transporters disrupts acetaminophen disposition in pediatric nonalcoholic steatohepatitis. *Drug Metabolism and Disposition*, 43(6), 829–835.
- Cappola, T. P., & Margulies, K. B. (2011). Functional genomics applied to cardiovascular medicine. *Circulation*, 124(1), 87–94.
- Carr, D. F., O'Meara, H., Jorgensen, A. L., Campbell, J., Hobbs, M., McCann, G., ... Pirmohamed, M. (2013). SLCO1B1 genetic variant associated with statin-induced myopathy: A proof-of-concept study using the clinical practice research datalink. *Clinical Pharmacology and Therapeutics*, 94(6), 695–701. <https://doi.org/10.1038/clpt.2013.161>
- Chen, D., Wilkinson, C. R. M., Watt, S., Penkett, C. J., Toone, W. M., Jones, N., & Bähler, J. (2007). The Molecular Mechanism of Hepcidin-mediated Ferroportin Down-Regulation. *Molecular Biology of the Cell*, 19(1), 308–317. <https://doi.org/10.1091/mbc.E07>
- Chen, Y., Xiao, J., Zhang, X., & Bian, X. (2016). MicroRNAs as key mediators of hepatic detoxification. *Toxicology*, 368, 80–90.
- Cheng, Y., Freeden, C., Zhang, Y., Abraham, P., Shen, H., Wescott, D., ... Lai, Y. (2016). Biliary excretion of pravastatin and taurocholate in rats with bile salt export pump (Bsep) impairment. *Biopharmaceutics & Drug Disposition*, 37(5), 276–286.

- Chu, X., Kato, Y., Niinuma, K., Sudo, K., Hakusui, H., & Sugiyama, Y. (1997). Multispecific Organic Anion Transporter Is Responsible for the Biliary Excretion of the Camptothecin Derivative Irinotecan and its Metabolites in Rats 1. *The Journal of Pharmacology and Experimental Therapeutics*, *281*(1), 304–314.
- Clarke, J. D., Dzierlenga, A. L., Nelson, N. R., Li, H., Werts, S., Goedken, M. J., & Cherrington, N. J. (2015). Mechanism of altered metformin distribution in nonalcoholic steatohepatitis. *Diabetes*, *64*(9), 3305–3313. <https://doi.org/10.2337/db14-1947>
- Clarke, J. D., Hardwick, R. N., Lake, A. D., Lickteig, A. J., Goedken, M. J., Klaassen, C. D., & Cherrington, N. J. (2014). Synergistic interaction between genetics and disease on pravastatin disposition. *Journal of Hepatology*, *61*(1), 139–147. <https://doi.org/10.1016/j.jhep.2014.02.021>
- Clarke, J. D., Novak, P., Lake, A. D., Hardwick, R. N., & Cherrington, N. J. (2016). Impaired N-linked glycosylation of uptake and efflux transporters in human non-alcoholic fatty liver disease. *Metabolic Liver Disease*, *37*(7), 1074–1081. <https://doi.org/10.1111/liv.13362>
- Clarke, J. D., Novak, P., Lake, A. D., Hardwick, R. N., & Cherrington, N. J. (2017). Impaired N-linked glycosylation of uptake and efflux transporters in human non-alcoholic fatty liver disease. *Liver International*, *37*(7), 1074–1081. <https://doi.org/10.1111/liv.13362>
- Clarke, J. D., Novak, P., Lake, A. D., Shipkova, P., Aranibar, N., Robertson, D., ... Cherrington, N. J. (2013). Characterization of Hepatocellular Carcinoma Related Genes and Metabolites in Human Nonalcoholic Fatty Liver Disease. *Digestive Diseases and Sciences*. <https://doi.org/10.1007/s10620-013-2873-9>
- Classen, D. C., Pestotnik, S. L., Evans, R. S., Lloyd, J. F., & Burke, J. P. (1997). Adverse drug events in hospitalized patients: excess length of stay, extra costs, and attributable mortality. *Jama*, *277*(4), 301–306.
- Colivicchi, F., Bassi, A., Santini, M., & Caltagirone, C. (2007). Discontinuation of statin therapy and clinical outcome after ischemic stroke. *Stroke*, *38*(10), 2652–2657. <https://doi.org/10.1161/STROKEAHA.107.487017>
- Cortez-Pinto, H., Chatham, J., Chacko, V. P., Arnold, C., Rashid, A., & Diehl, A. M. (1999). Alterations in Liver ATP Homeostasis in Human Nonalcoholic Steatohepatitis A Pilot Study. *JAMA*, *282*(17), 1659–1664. <https://doi.org/10.1001/jama.282.17.1659>
- Crespo, M., Lappe, S., Feldstein, A. E., & Alkhouri, N. (2016). Similarities and differences between pediatric and adult nonalcoholic fatty liver disease. *Metabolism*, *65*(8), 1161–1171.
- Csanaky, I. L., Lu, H., Zhang, Y., Ogura, K., Choudhuri, S., & Klaassen, C. D. (2011). Organic anion-transporting polypeptide 1b2 (Oatp1b2) is important for the hepatic uptake of unconjugated bile acids: Studies in Oatp1b2-null mice. *Hepatology*, *53*(1), 272–281.
- Czuba, L. C., Hillgren, K. M., & Swaan, P. W. (2018). Post-translational modifications of transporters. *Pharmacology & Therapeutics*, *192*, 88–99.
- D'Esposito, F., Tattam, B. N., Ramzan, I., & Murray, M. (2008). A liquid chromatography/electrospray ionization mass spectrometry (LC-MS/MS) assay for the determination of irinotecan (CPT-11) and its two major metabolites in human liver microsomal incubations and human plasma samples. *Journal of Chromatography B: Analytical Technologies in the Biomedical and Life Sciences*, *875*(2), 522–530.

<https://doi.org/10.1016/j.jchromb.2008.10.011>

- Daniels, T. R., Delgado, T., Rodriguez, J. A., Helguera, G., & Penichet, M. L. (2006). The transferrin receptor part I: Biology and targeting with cytotoxic antibodies for the treatment of cancer. *Clinical Immunology*, 121(2), 144–158.
- Dowman, J. K., Hopkins, L. J., Reynolds, G. M., Nikolaou, N., Armstrong, M. J., Shaw, J. C., ... Hübscher, S. G. (2014). Development of hepatocellular carcinoma in a murine model of nonalcoholic steatohepatitis induced by use of a high-fat/fructose diet and sedentary lifestyle. *The American Journal of Pathology*, 184(5), 1550–1561.
- Dunham, J. L., Shawki, A., Ruwe, T. A., Vieth, K. R., Canonne-Hergaux, F., & Mackenzie, B. (2018). Role of N-glycosylation in the activity of divalent metal-ion transporter-1. *The FASEB Journal*, 32(1_supplement), 871–876.
- Dzierlenga, A. L., Clarke, J. D., & Cherrington, N. J. (2016). Nonalcoholic steatohepatitis modulates membrane protein retrieval and insertion processes. *Drug Metabolism and Disposition*, 44(11), 1799–1807. <https://doi.org/10.1124/dmd.116.071415>
- Dzierlenga, A. L., Clarke, J. D., Hargraves, T. L., Ainslie, G. R., Vanderah, T. W., Paine, M. F., & Cherrington, N. J. (2015). Mechanistic Basis of Altered Morphine Disposition in Nonalcoholic Steatohepatitis. *Journal of Pharmacology and Experimental Therapeutics*, 352(3), 462–470. <https://doi.org/10.1124/jpet.114.220764>
- Dzierlenga, Anika L, Clarke, J. D., Hargraves, T. L., Ainslie, G. R., Vanderah, T. W., Paine, M. F., & Cherrington, N. J. (2014). Mechanistic Basis of Altered Morphine Disposition in Nonalcoholic Steatohepatitis. *Journal of Pharmacology and Experimental Therapeutics*, 352(3), 462–470. <https://doi.org/10.1124/jpet.114.220764>
- Dzierlenga, Anika L, Clarke, J. D., Klein, D. M., Anumol, T., Snyder, S. A., Li, H. Y., & Cherrington, N. (2016). Biliary Elimination of Pemetrexed is Dependent on Mrp2 in Rats: Potential Mechanism of Variable Response in Nonalcoholic Steatohepatitis. *Journal of Pharmacology and Experimental Therapeutics* . <https://doi.org/10.1124/jpet.116.234310>
- Edginton, A. N., Zimmerman, E. I., Vasilyeva, A., Baker, S. D., & Panetta, J. C. (2016). Sorafenib metabolism , transport , and enterohepatic recycling : physiologically based modeling and simulation in mice. *Cancer Chemotherapy and Pharmacology*, 77(5), 1039–1052. <https://doi.org/10.1007/s00280-016-3018-6>
- Edwards, I. R., & Aronson, J. K. (2000). Adverse drug reactions: definitions, diagnosis, and management. *The Lancet*, 356(9237), 1255–1259.
- Etienne-Grimaldi, M. C., Boyer, J. C., Thomas, F., Quaranta, S., Picard, N., Lorient, M. A., ... Le Guellec, C. (2015). UGT1A1 genotype and irinotecan therapy: General review and implementation in routine practice. *Fundamental and Clinical Pharmacology*, 29(3), 219–237. <https://doi.org/10.1111/fcp.12117>
- Falcone, A., Ricci, S., Brunetti, I., Pfanner, E., Allegrine, G., Barbara, C., ... Masi, G. (2007). Phase III trial of infusional fluorouracil, leucovorin, oxaliplatin, and irinotecan (FOLFOXIRI) compared with infusional fluorouracil, leucovorin, and irinotecan (FOLFIRI) as first-line treatment for metastatic colorectal cancer: The gruppo oncologico nor. *Journal of Clinical Oncology*, 25(13), 1670–1676. <https://doi.org/10.1200/JCO.2006.09.0928>
- Fargion, S., Mattioli, M., Fracanzani, A. L., Sampietro, M., Tavazzi, D., Fociani, P., ... Fiorelli, G. (2001). Hyperferritinemia, iron overload, and multiple metabolic alterations identify patients

- at risk for nonalcoholic steatohepatitis. *American Journal of Gastroenterology*.
[https://doi.org/10.1016/S0002-9270\(01\)02615-6](https://doi.org/10.1016/S0002-9270(01)02615-6)
- Farrell, G. C., Cooksley, W. G. E., & Powell, L. W. (1979). Drug metabolism in liver disease: activity of hepatic microsomal metabolizing enzymes. *Clinical Pharmacology & Therapeutics*, *26*(4), 483–492.
- Ferslew, B. C., Johnston, C. K., Tsakalozou, E., Bridges, A. S., Paine, M. F., Jia, W., ... Brouwer, K. L. R. (2015). Altered morphine glucuronide and bile acid disposition in patients with nonalcoholic steatohepatitis. *Clinical Pharmacology and Therapeutics*, *97*(4), 419–427. <https://doi.org/10.1002/cpt.66>
- Fisel, P., Schaeffeler, E., & Schwab, M. (2016). DNA methylation of ADME genes. *Clinical Pharmacology & Therapeutics*, *99*(5), 512–527.
- Fisher, C. D., Lickteig, A. J., Augustine, L. M., Oude Elferink, R. P. J., Besselsen, D. G., Erickson, R. P., & Cherrington, N. J. (2009). Experimental non-alcoholic fatty liver disease results in decreased hepatic uptake transporter expression and function in rats. *European Journal of Pharmacology*, *613*(1), 119–127. <https://doi.org/10.1016/j.ejphar.2009.04.002>
- Fisher, C. D., Lickteig, A. J., Augustine, L. M., Ranger-Moore, J., Jackson, J. P., Ferguson, S. S., & Cherrington, N. J. (2009). Hepatic cytochrome P450 enzyme alterations in humans with progressive stages of nonalcoholic fatty liver disease. *Drug Metabolism and Disposition*, *37*(10), 2087–2094.
- Fleischman, M. W., Budoff, M., Zeb, I., Li, D., & Foster, T. (2014). NAFLD prevalence differs among hispanic subgroups: The multi-ethnic study of atherosclerosis. *World Journal of Gastroenterology*, *20*(17), 4987–4993. <https://doi.org/10.3748/wjg.v20.i17.4987>
- Franke, R. M., Gardner, E. R., & Sparreboom, A. (2010). Pharmacogenetics of drug transporters. *Current Pharmaceutical Design*, *16*(2), 220–230.
- Frelinger, A. L., Bhatt, D. L., Lee, R. D., Mulford, D. J., Wu, J., Nudurupati, S., ... Barnard, M. R. (2013). Clopidogrel pharmacokinetics and pharmacodynamics vary widely despite exclusion or control of polymorphisms (CYP2C19, ABCB1, PON1), noncompliance, diet, smoking, co-medications (including proton pump inhibitors), and pre-existent variability in platelet f. *Journal of the American College of Cardiology*, *61*(8), 872–879.
- Fujita, D., Saito, Y., Nakanishi, T., & Tamai, I. (2015). Organic Anion Transporting Polypeptide (OATP)2B1 Contributes to Gastrointestinal Toxicity of Anticancer Drug SN-38, Active Metabolite of CPT-11. *Drug Metabolism and Disposition*, *46*(7).
<https://doi.org/10.1124/dmd.115.066712>
- Fukudo, M., Ikemi, Y., Togashi, Y., Masago, K., Kim, Y. H., Mio, T., ... Inui, K. (2013). Population pharmacokinetics/pharmacodynamics of erlotinib and pharmacogenomic analysis of plasma and cerebrospinal fluid drug concentrations in Japanese patients with non-small cell lung cancer. *Clinical Pharmacokinetics*, *52*(7), 593–609.
- George, D. K., Goldwurm, S., Macdonald, G. A., Cowley, L. L., Walker, N. I., Ward, P. J., ... Powell, L. W. (1998). Increased hepatic iron concentration in nonalcoholic steatohepatitis is associated with increased fibrosis. *Gastroenterology*, *114*(2), 311–318.
[https://doi.org/10.1016/S0016-5085\(98\)70482-2](https://doi.org/10.1016/S0016-5085(98)70482-2)
- Giacomini, K. M., Huang, S.-M., Tweedie, D. J., Benet, L. Z., Brouwer, K. L. R., Chu, X., ... Hillgren, K. M. (2010). Membrane transporters in drug development. *Nature Reviews Drug*

Discovery, 9(3), 215.

- Goswami, T., & Andrews, N. C. (2006). Hereditary hemochromatosis protein, HFE, interaction with transferrin receptor 2 suggests a molecular mechanism for mammalian iron sensing. *Journal of Biological Chemistry*, 281(39), 28494–28498. <https://doi.org/10.1074/jbc.C600197200>
- Habano, W., Kawamura, K., Iizuka, N., Terashima, J., Sugai, T., & Ozawa, S. (2015). Analysis of DNA methylation landscape reveals the roles of DNA methylation in the regulation of drug metabolizing enzymes. *Clinical Epigenetics*, 7(1), 105.
- Haile, D. J., Rouault, T. a, Tang, C. K., Chin, J., Harford, J. B., & Klausner, R. D. (1992). Reciprocal control of RNA-binding and aconitase activity in the regulation of the iron-responsive element binding protein: role of the iron-sulfur cluster. *P Natl Acad Sci USA*, 89(16), 7536–7540. <https://doi.org/10.1073/pnas.89.16.7536>
- Hakkarainen, K. M., Hedna, K., Petzold, M., & Hägg, S. (2012). Percentage of patients with preventable adverse drug reactions and preventability of adverse drug reactions—a meta-analysis. *PloS One*, 7(3), e33236.
- Hardwick, R., Clarke, J. D., Lake, A. D., Canet, M., Anumol, T., Street, S., ... Cherrington, N. J. (2014). Increased Susceptibility to Methotrexate-Induced Toxicity in Nonalcoholic Steatohepatitis. *Toxicological Sciences*, (520).
- Hardwick, R. N., Ferreira, D. W., More, V. R., Lake, A. D., Lu, Z., Manautou, J. E., ... Cherrington, N. J. (2013). Altered UDP-glucuronosyltransferase and sulfotransferase expression and function during progressive stages of human nonalcoholic fatty liver diseases. *Drug Metabolism and Disposition*, 41(3), 554–561. <https://doi.org/10.1124/dmd.112.048439>
- Hardwick, R. N., Fisher, C. D., Canet, M. J., Lake, A. D., & Cherrington, N. J. (2010). Diversity in antioxidant response enzymes in progressive stages of human nonalcoholic fatty liver disease. *Drug Metabolism and Disposition*, 38(12), 2293–2301.
- Hardwick, R. N., Fisher, C. D., Canet, M. J., Scheffer, G. L., & Cherrington, N. J. (2011). Variations in ATP-Binding Cassette Transporter Regulation during the Progression of Human Nonalcoholic Fatty Liver Disease □ ABSTRACT : *Drug Metab Dispos.*, 39(12), 2395–2402. <https://doi.org/10.1124/dmd.111.041012>.
- Hardwick, R. N., Fisher, C. D., Street, S. M., Canet, M. J., & Cherrington, N. J. (2012). Molecular mechanism of altered ezetimibe disposition in nonalcoholic steatohepatitis. *Drug Metabolism and Disposition*, 40(3), 450–460. <https://doi.org/10.1124/dmd.111.041095>
- Hasegawa, Y., Ando, Y., Ando, M., Hashimoto, N., Imaizumi, K., & Shimokata, K. (2006). Pharmacogenetic approach for cancer treatment-tailored medicine in practice. *Annals of the New York Academy of Sciences*, 1086, 223–232. <https://doi.org/10.1196/annals.1377.020>
- Hirano, M., Maeda, K., Hayashi, H., Kusuhara, H., & Sugiyama, Y. (2005). Bile Salt Export Pump (BSEP/ABCB11) Can Transport a Nonbile Acid Substrate, Pravastatin. *Journal of Pharmacology and Experimental Therapeutics*, 314(2), 876–882. <https://doi.org/10.1124/jpet.105.084830>
- Hirose, K., Kozu, C., Yamashita, K., Maruo, E., Kitamura, M., Hasegawa, J., ... Maeda, Y. (2012). Correlation between plasma concentration ratios of SN-38 glucuronide and sn-38

- and neutropenia induction in patients with colorectal cancer and wild-type UGT1A1 gene. *Oncology Letters*, 3(3), 694–698. <https://doi.org/10.3892/ol.2011.533>
- Houghton, P. J., Germain, G. S., Harwood, F. C., Schuetz, J. D., Stewart, C. F., Buchdunger, E., & Traxler, P. (2004). Imatinib Mesylate Is a Potent Inhibitor of the ABCG2 (BCRP) Transporter and Reverses Resistance to Topotecan and SN-38 in Vitro. *Cancer Research*, 64(7), 2333–2337. <https://doi.org/10.1158/0008-5472.CAN-03-3344>
- Howard, J. K., & Flier, J. S. (2006). Attenuation of leptin and insulin signaling by SOCS proteins. *Trends in Endocrinology & Metabolism*, 17(9), 365–371.
- Hsiang, B., Zhu, Y., Wang, Z., Wu, Y., Sasseville, V., Yang, W.-P., & Kirchgessner, T. G. (1999). A novel human hepatic organic anion transporting polypeptide (OATP2) Identification of a liver-specific human organic anion transporting polypeptide and identification of rat and human hydroxymethylglutaryl-CoA reductase inhibitor transporters. *Journal of Biological Chemistry*, 274(52), 37161–37168.
- Ibrahim, S. H., Kohli, R., & Gores, G. J. (2011). Mechanisms of Lipotoxicity in NAFLD and Clinical Implications. *J Pediatr Gastroenterol Nutr*, 53(2), 131–140. <https://doi.org/10.1097/MPG.0b013e31822578db.Mechanisms>
- Imai, Y., Nakane, M., Kage, K., Tsukahara, S., Ishikawa, E., Tsuruo, T., ... Sugimoto, Y. (2002). C421A polymorphism in the human breast cancer resistance protein gene is associated with low expression of Q141K protein and low-level drug resistance. *Molecular Cancer Therapeutics*, 1(8), 611–616. Retrieved from <http://www.ncbi.nlm.nih.gov/pubmed/12479221>
- Iusuf, D., Ludwig, M., Elbatsh, A., van Esch, A., van de Steeg, E., Wagenaar, E., ... Schinkel, A. H. (2014). OATP1A/1B Transporters Affect Irinotecan and SN-38 Pharmacokinetics and Carboxylesterase Expression in Knockout and Humanized Transgenic Mice. *Molecular Cancer Therapeutics*, 13(2), 492–503. <https://doi.org/10.1158/1535-7163.MCT-13-0541>
- Iusuf, D., Steeg, E. Van De, & Schinkel, A. H. (2012). Hepatocyte Hopping of OATP1B Substrates Contributes to Efficient Hepatic Detoxification, 92(5), 559–562. <https://doi.org/10.1038/clpt.2012.143>
- Iwai, K., Klausner, R. D., & Rouault, T. A. (1995). Requirements for iron-regulated degradation of the RNA binding protein, iron regulatory protein 2. *The EMBO Journal*, 14(21), 5350–5357.
- Iyer, L., Das, S., Janisch, L., Wen, M., Ramírez, J., Karrison, T., ... Ratain, M. J. (2002). UGT1A1*28 polymorphism as a determinant of irinotecan disposition and toxicity. *Pharmacogenomics Journal*, 2(1), 43–47. <https://doi.org/10.1038/sj.tpj.6500072>
- Jain, K. K. (1991). Systemic lupus erythematosus (SLE)-like syndromes associated with carbamazepine therapy. *Drug Safety*, 6(5), 350–360.
- Jigorel, E., Le Vee, M., Boursier-Neyret, C., Parmentier, Y., & Fardel, O. (2006). Differential regulation of sinusoidal and canalicular hepatic drug transporter expression by xenobiotics activating drug-sensing receptors in primary human hepatocytes. *Drug Metabolism and Disposition*, 34(10), 1756–1763.
- Johansson, I., & Ingelman-Sundberg, M. (2008). CNVs of human genes and their implication in pharmacogenetics. *Cytogenetic and Genome Research*, 123(1–4), 195–204.
- Joy, T. R., & Hegele, R. A. (2009). Narrative Review: Statin-Related Myopathy. *Annals of*

Internal Medicine, 150(12), 858–868.

- Kacevska, M., Ivanov, M., Wyss, A., Kasela, S., Milani, L., Rane, A., & Ingelman-Sundberg, M. (2012). DNA methylation dynamics in the hepatic CYP3A4 gene promoter. *Biochimie*, 94(11), 2338–2344.
- Kalliokoski, A., & Niemi, M. (2009). Impact of OATP transporters on pharmacokinetics. *British Journal of Pharmacology*, 158, 693–705. <https://doi.org/10.1111/j.1476-5381.2009.00430.x>
- Kato, Y., Suzuki, H., & Sugiyama, Y. (2002). Toxicological implications of hepatobiliary transporters. *Toxicology*, 181–182, 287–290. [https://doi.org/10.1016/S0300-483X\(02\)00458-4](https://doi.org/10.1016/S0300-483X(02)00458-4)
- Kawabata, S., Oka, M., Shiozawa, K., Tsukamoto, K., Nakatomi, K., Soda, H., ... Kohno, S. (2001). Breast cancer resistance protein directly confers SN-38 resistance of lung cancer cells. *Biochemical and Biophysical Research Communications*, 280(5), 1216–1223. <https://doi.org/10.1006/bbrc.2001.4267>
- Khan, S., Ahmad, A., Guo, W., Wang, Y. F., Abu-Qare, A., & Ahmad, I. (2005). A simple and sensitive LC/MS/MS assay for 7-ethyl-10-hydroxycamptothecin (SN-38) in mouse plasma and tissues: Application to pharmacokinetic study of liposome entrapped SN-38 (LE-SN38). *Journal of Pharmaceutical and Biomedical Analysis*, 37(1), 135–142. <https://doi.org/10.1016/j.jpba.2004.09.053>
- Kim, I., Han, N., Burckart, G. J., & Oh, J. M. (2014). Epigenetic changes in gene expression for drug-metabolizing enzymes and transporters. *Pharmacotherapy: The Journal of Human Pharmacology and Drug Therapy*, 34(2), 140–150.
- Kivistö, K. T., Grisk, O., Hofmann, U., Meissner, K., Möritz, K. U., Ritter, C., ... Kroemer, H. K. (2005). Disposition of oral and intravenous pravastatin in MRP2-Deficient TR-rats. *Drug Metabolism and Disposition*, 33(11), 1593–1596. <https://doi.org/10.1124/dmd.105.006262>
- Kleiner, D. E., Brunt, E. M., Van Natta, M., Behling, C., Contos, M. J., Cummings, O. W., ... Sanyal, A. J. (2005). Design and validation of a histological scoring system for nonalcoholic fatty liver disease. *Hepatology*, 41(6), 1313–1321. <https://doi.org/10.1002/hep.20701>
- Kobayashi, D., Ieiri, I., Hirota, T., Takane, H., Maegawa, S., Kigawa, J., ... Sugiyama, Y. (2005). Functional assessment of ABCG2 (BCRP) gene polymorphisms to protein expression in human placenta. *Drug Metabolism and Disposition: The Biological Fate of Chemicals*, 33(1), 94–101. <https://doi.org/10.1124/dmd.104.001628.speculated>
- Köck, K., & Brouwer, K. L. R. (2012). A Perspective on Efflux Transport Proteins in the Liver. *CLINICAL PHARMACOLOGY & THERAPEUTICS*, 92(5), 599–612. <https://doi.org/10.1038/clpt.2012.79>
- Koek, G. H., Liedorp, P. R., & Bast, A. (2011). The role of oxidative stress in non-alcoholic steatohepatitis. *Clinica Chimica Acta*, 412(15–16), 1297–1305. <https://doi.org/10.1016/j.cca.2011.04.013>
- Kohgo, Y., Ohtake, T., Ikuta, K., Suzuki, Y., Hosoki, Y., Saito, H., & Kato, J. (2005). Iron Accumulation in Alcoholic Liver Diseases. *Alcoholism: Clinical and Experimental Research*, 29(s2), 189S-193S. <https://doi.org/10.1097/01.alc.0000189274.00479.62>
- König, J. (2011). Uptake Transporters of the Human OATP Family. In M. F. Fromm & R. B. Kim (Eds.), *Drug Transporters* (pp. 1–28). Berlin, Heidelberg: Springer Berlin Heidelberg.

https://doi.org/10.1007/978-3-642-14541-4_1

- Kroetz, D. L. (2006). Role for drug transporters beyond tumor resistance: Hepatic functional imaging and genotyping of multidrug resistance transporters for the prediction of irinotecan toxicity. *Journal of Clinical Oncology*, *24*(26), 4225–4227. <https://doi.org/10.1200/JCO.2006.07.2355>
- Laho, T., Clarke, J. D., Dzierlenga, A. L., Li, H., Klein, D. M., Goedken, M., ... Cherrington, N. J. (2016). Effect of nonalcoholic steatohepatitis on renal filtration and secretion of adefovir. *Biochemical Pharmacology*, *115*, 144–151.
- Lake, A. D., Novak, P., Fisher, C. D., Jackson, J. P., Hardwick, R. N., Billheimer, D. D., ... Cherrington, N. J. (2011). Analysis of global and absorption, distribution, metabolism, and elimination gene expression in the progressive stages of human nonalcoholic fatty liver disease. *Drug Metabolism and Disposition*. <https://doi.org/10.1124/dmd.111.040592>
- Lake, A. D., Novak, P., Hardwick, R. N., Flores-Keown, B., Zhao, F., Klimecki, W. T., & Cherrington, N. J. (2013). The Adaptive Endoplasmic Reticulum Stress Response to Lipotoxicity in Progressive Human Nonalcoholic Fatty Liver Disease. *Toxicological Sciences*, *137*(1), 26–35. <https://doi.org/10.1093/toxsci/kft230>
- Lal, S., Wong, Z. W., Sandanaraj, E., Xiang, X., Ang, P. C. S., Lee, E. J. D., & Chowbay, B. (2008). Influence of ABCB1 and ABCG2 polymorphisms on doxorubicin disposition in Asian breast cancer patients. *Cancer Science*, *99*(4), 816–823. <https://doi.org/10.1111/j.1349-7006.2008.00744.x>
- Lazo, M., Hernaez, R., Eberhardt, M. S., Bonekamp, S., Kamel, I., Guallar, E., ... Clark, J. M. (2013). Prevalence of nonalcoholic fatty liver disease in the United States: The third national health and nutrition examination survey, 1988-1994. *American Journal of Epidemiology*, *178*(1), 38–45. <https://doi.org/10.1093/aje/kws448>
- LECLERCQ, I. A. (2004). Antioxidant defence mechanisms: new players in the pathogenesis of non-alcoholic steatohepatitis? *Clinical Science*, *106*(3), 235 LP – 237. <https://doi.org/10.1042/CS20030368>
- Lee, H. H., & Ho, R. H. (2017). Interindividual and interethnic variability in drug disposition: polymorphisms in organic anion transporting polypeptide 1B1 (OATP1B1; SLCO1B1). *British Journal of Clinical Pharmacology*, *83*(6), 1176–1184. <https://doi.org/10.1111/bcp.13207>
- Li, H., Canet, M. J., Clarke, J. D., Billheimer, D., Xanthakos, S. A., Lavine, J. E., ... Cherrington, N. J. (2017). Pediatric cytochrome P450 activity alterations in nonalcoholic steatohepatitis. *Drug Metabolism and Disposition*, *45*(12), 1317–1325.
- Li, H., Toth, E., & Cherrington, N. J. (2017). Asking the right questions with animal models: methionine-and choline-deficient model in predicting adverse drug reactions in human NASH. *Toxicological Sciences*, *161*(1), 23–33.
- Lickteig, A. J., Fisher, C. D., Augustine, L. M., Aleksunes, L. M., Besselsen, D. G., Slitt, A. L., ... Cherrington, N. J. (2007). Efflux transporter expression and acetaminophen metabolite excretion are altered in rodent models of nonalcoholic fatty liver disease. *Drug Metabolism and Disposition*, *35*(10), 1970–1978. <https://doi.org/10.1124/dmd.107.015107>
- Liu, X., Cheng, D., Kuang, Q., Liu, G., & Xu, W. (2014). Association of UGT1A1*28 polymorphisms with irinotecan-induced toxicities in colorectal cancer: A meta-analysis in

- Caucasians. *Pharmacogenomics Journal*, 14(2), 120–129.
<https://doi.org/10.1038/tpj.2013.10>
- Liutkeviciene, R., Vilkeviciute, A., Slavinskaite, A., Petrauskaite, A., Tatarunas, V., & Kriauciuniene, L. (2018). Evaluation of serum SLCO1B1 levels and genetic variants of SLCO1B1 rs4149056 and rs2306283 in patients with early and exudative age-related macular degeneration. *Gene*, 676, 139–145.
- Loomba, R., & Sanyal, A. J. (2013). The global NAFLD epidemic. *Nature Reviews Gastroenterology and Hepatology*, 10(11), 686+.
- Lu, H., Choudhuri, S., Ogura, K., Csanaky, I. L., Lei, X., Cheng, X., ... Klaassen, C. D. (2008). Characterization of organic anion transporting polypeptide 1b2-null mice: essential role in hepatic uptake/toxicity of phalloidin and microcystin-LR. *Toxicological Sciences*, 103(1), 35–45.
- Ludwig, J., Viggiano, T., McGill, D., & Oh, B. (1980). Nonalcoholic Steatohepatitis: Mayo Clinic experiences with a hitherto unnamed disease. *Mayo Clinic Proceedings*, 55(7), 434–438.
- Maeda, K. (2015). Organic anion transporting polypeptide (OATP) 1B1 and OATP1B3 as important regulators of the pharmacokinetics of substrate drugs. *Biological and Pharmaceutical Bulletin*, 38(2), 155–168.
- Mallal, S., Phillips, E., Carosi, G., Molina, J.-M., Workman, C., Tomažič, J., ... Cid, J. F. (2008). HLA-B* 5701 screening for hypersensitivity to abacavir. *New England Journal of Medicine*, 358(6), 568–579.
- Manuel Fernandez-Real, J., Lopez-Bermejo, A., & Ricart, W. (2002). Cross-Talk Between Iron Metabolism and Diabetes. *Perspectives in Diabetes*, 51, 2348–2354.
- Marra, F., Gastaldelli, A., Svegliati Baroni, G., Tell, G., & Tiribelli, C. (2008). Molecular basis and mechanisms of progression of non-alcoholic steatohepatitis. *Trends in Molecular Medicine*, 14(2), 72–81. <https://doi.org/10.1016/j.molmed.2007.12.003>
- McCullough, A. J. (2006). Pathophysiology of nonalcoholic steatohepatitis. *Journal of Clinical Gastroenterology*, 40 Suppl 1(March), S17-29. <https://doi.org/DOI:10.1097/01.mcg.0000168645.86658.22>
- Mehta, K., Van Thiel, D. H., Shah, N., & Mobarhan, S. (2002). Nonalcoholic fatty liver disease: pathogenesis and the role of antioxidants. *Nutrition Reviews*, 60(9), 289–293.
- Merrell, M. D., & Cherrington, N. J. (2011). Drug metabolism alterations in nonalcoholic fatty liver disease. *Drug Metabolism Reviews*, 43(3), 317–334.
<https://doi.org/10.3109/03602532.2011.577781>
- Mizuno, T., Fukudo, M., Terada, T., Kamba, T., & Nakamura, E. (2012). Impact of Genetic Variation in Breast Cancer Resistance Protein. *Drug Metabolism and Pharmacokinetics*, 27(6), 631–639. <https://doi.org/10.2133/dmpk.DMPK-12-RG-026>
- Morigny, P., Houssier, M., Mouisel, E., & Langin, D. (2016). Adipocyte lipolysis and insulin resistance. *Biochimie*, 125, 259–266. <https://doi.org/10.1016/j.biochi.2015.10.024>
- Mortensen, M. B., & Falk, E. (2018). Primary prevention with statins in the elderly. *Journal of the American College of Cardiology*, 71(1), 85–94.
- Mueller, S., Pantopoulos, K., Hübner, C. a, Stremmel, W., & Hentze, M. W. (2001). IRP1

- activation by extracellular oxidative stress in the perfused rat liver. *The Journal of Biological Chemistry*, 276(25), 23192–23196. <https://doi.org/10.1074/jbc.M100654200>
- Nelson, J. E., Wilson, L., Brunt, E. M., Yeh, M. M., Kleiner, D. E., Unalp-Arida, A., & Kowdley, K. V. (2011). Relationship between the pattern of hepatic iron deposition and histological severity in nonalcoholic fatty liver disease. *Hepatology*, 53(2), 448–457. <https://doi.org/10.1002/hep.24038>
- Nemeth, E., & Ganz, T. (2006). Regulation of iron metabolism by hepcidin. *Annual Review of Nutrition*, 26, 323–342. <https://doi.org/10.1146/annurev.nutr.26.061505.111303>
- Nemeth, E., Tuttle, M. S., Powelson, J., Vaughn, M. B., Donovan, A., Ward, D. M., ... Kaplan, J. (2004). Hepcidin regulates cellular iron efflux by binding to ferroportin and inducing its internalization. *Science (New York, N.Y.)*, 306(5704), 2090–2093. <https://doi.org/10.1126/science.1104742>
- Newman, C. B., & Tobert, J. A. (2018). Statin-Related Myopathy and Rhabdomyolysis. *Endocrine and Metabolic Medical Emergencies: A Clinician's Guide*, 760–774.
- Niemi, M., Schaeffeler, E., Lang, T., Fromm, M. F., Neuvonen, M., Kyrklund, C., ... Kivistö, K. T. (2004). High plasma pravastatin concentrations are associated with single nucleotide polymorphisms and haplotypes of organic anion transporting polypeptide-C (OATP-C, SLCO1B1). *Pharmacogenetics*, 14(7), 429–440. <https://doi.org/10.1097/01.fpc.0000114750.08559.32>
- Nishizato, Y., Ieiri, I., Suzuki, H., Kimura, M., Kawabata, K., Hirota, T., ... Sugiyama, Y. (2003). Polymorphisms of OATP-C (SLC21A6) and OAT3 (SLC22A8) genes: Consequences for pravastatin pharmacokinetics. *Clinical Pharmacology and Therapeutics*, 73(6), 554–565. [https://doi.org/10.1016/S0009-9236\(03\)00060-2](https://doi.org/10.1016/S0009-9236(03)00060-2)
- Noguchi, K., Katayama, K., Mitsuhashi, J., & Sugimoto, Y. (2009). Functions of the breast cancer resistance protein (BCRP/ABCG2) in chemotherapy. *Advanced Drug Delivery Reviews*, 61(1), 26–33. <https://doi.org/10.1016/j.addr.2008.07.003>
- Ogawa, K., Suzuki, H., Hirohashi, T., Ishikawa, T., Meier, P. J., Hirose, K., ... Sugiyama, Y. (2000). Characterization of inducible nature of MRP3 in rat liver. *American Journal of Physiology-Gastrointestinal and Liver Physiology*, 278(3), G438–G446.
- Pacifici, G. M., Viani, A., Franchi, M., Santerini, S., Temellini, A., Giuliani, L., & Carrai, M. (1990). Conjugation pathways in liver disease. *British Journal of Clinical Pharmacology*, 30(3), 427–435.
- Paglialunga, S., & Dehn, C. A. (2016). Clinical assessment of hepatic de novo lipogenesis in non-alcoholic fatty liver disease. *Lipids in Health and Disease*, 1–10. <https://doi.org/10.1186/s12944-016-0321-5>
- Pan, Y.-Z., Gao, W., & Yu, A.-M. (2009). MicroRNAs regulate CYP3A4 expression via direct and indirect targeting. *Drug Metabolism and Disposition*, 37(10), 2112–2117.
- PANTOPOULOS, K. (2004). Iron Metabolism and the IRE/IRP Regulatory System: An Update. *Annals of the New York Academy of Sciences*, 1012(1), 1–13. <https://doi.org/10.1196/annals.1306.001>
- Pantopoulos, K., & Hentze, M. W. (1998). Activation of iron regulatory protein-1 by oxidative stress in vitro. *Proceedings of the National Academy of Sciences of the United States of*

- America*, 95(18), 10559–10563. <https://doi.org/10.1073/pnas.95.18.10559>
- Patel, M., Taskar, K. S., & Zamek-Gliszczyński, M. J. (2016). Importance of hepatic transporters in clinical disposition of drugs and their metabolites. *The Journal of Clinical Pharmacology*, 56, S23–S39.
- Pawlak, M., Lefebvre, P., & Staels, B. (2015). Molecular mechanism of PPAR α action and its impact on lipid metabolism, inflammation and fibrosis in non-alcoholic fatty liver disease. *Journal of Hepatology*. <https://doi.org/10.1016/j.jhep.2014.10.039>
- Pierre, V., Johnston, C. K., Ferslew, B. C., Brouwer, K. L. R., & Gonzalez, D. (2017). Population pharmacokinetics of morphine in patients with nonalcoholic steatohepatitis (NASH) and healthy adults. *CPT: Pharmacometrics & Systems Pharmacology*, 6(5), 331–339.
- Pigeon, C., Ilyin, G., Courselaud, B., Leroyer, P., Turlin, B., Brissot, P., & Loréal, O. (2001). A New Mouse Liver-specific Gene, Encoding a Protein Homologous to Human Antimicrobial Peptide Hecidin, Is Overexpressed during Iron Overload. *Journal of Biological Chemistry*, 276(11), 7811–7819. <https://doi.org/10.1074/jbc.M008923200>
- Pirmohamed, M. (2010). Pharmacogenetics of idiosyncratic adverse drug reactions. In *Adverse Drug Reactions* (pp. 477–491). Springer.
- Price, L., & Kowdley, K. V. (2009). The role of iron in the pathophysiology and treatment. *Canadian Journal of Gastroenterology*, 23(12).
- Rasmussen, J. N., Chong, A., & Alter, D. A. (2007). Relationship Between Adherence to Evidence-Based Pharmacotherapy and Long-term Mortality After Acute Myocardial Infarction. *JAMA*, 297(2), 177. <https://doi.org/10.1001/jama.297.2.177>
- Rawlins, M. D. (1981). Clinical pharmacology. Adverse reactions to drugs. *British Medical Journal (Clinical Research Ed.)*, 282(6268), 974–976. <https://doi.org/10.1136/bmj.282.6268.974>
- Reisman, S. A., Csanaky, I. L., Aleksunes, L. M., & Klaassen, C. D. (2009). Altered Disposition of Acetaminophen in Nrf2-null and Keap1-knockdown Mice. *Toxicological Sciences*, 109(1), 31–40. <https://doi.org/10.1093/toxsci/kfp047>
- Rimola, J., Pons, F., Hernandez-guerra, M., Darnell, A., Delgado, M., Castroagudin, J., ... Bruix, J. (2018). Complete Response Under Sorafenib in Patients With Hepatocellular Carcinoma : Relationship With, 67(2), 612–622. <https://doi.org/10.1002/hep.29515>
- Rolo, A. P., Teodoro, J. S., & Palmeira, C. M. (2012). Role of oxidative stress in the pathogenesis of nonalcoholic steatohepatitis. *Free Radical Biology and Medicine*, 52(1), 59–69.
- Sadée, W., & Dai, Z. (2005). Pharmacogenetics/genomics and personalized medicine. *Human Molecular Genetics*, 14(SUPPL. 2), 207–214. <https://doi.org/10.1093/hmg/ddi261>
- Sadee, W., Wang, D., Papp, A. C., Pinsonneault, J. K., Smith, R. M., Moyer, R. A., & Johnson, A. D. (2011). Pharmacogenomics of the RNA world: structural RNA polymorphisms in drug therapy. *Clinical Pharmacology & Therapeutics*, 89(3), 355–365.
- Saponaro, C., Gaggini, M., & Gastaldelli, A. (2015). Nonalcoholic Fatty Liver Disease and Type 2 Diabetes : Common Pathophysiologic Mechanisms, 1–13. <https://doi.org/10.1007/s11892-015-0607-4>

- Sato, M., Miyanishi, K., Tanaka, S., Sakurada, A., Sakamoto, H., Kawano, Y., ... Kato, J. (2018). Increased Duodenal Iron Absorption through Upregulation of Ferroportin 1 due to the Decrement in Serum Hepcidin in Patients with Chronic Hepatitis C. *Canadian Journal of Gastroenterology and Hepatology*, 2018.
- Sayiner, M., Koenig, A., Henry, L., & Younossi, Z. M. (2016a). Epidemiology of Nonalcoholic Fatty Liver Disease and Nonalcoholic Steatohepatitis in the United States and the Rest of the World. *Clinics in Liver Disease*, 20(2), 205–214. <https://doi.org/10.1016/j.cld.2015.10.001>
- Sayiner, M., Koenig, A., Henry, L., & Younossi, Z. M. (2016b). Epidemiology of Nonalcoholic Fatty Liver Disease and Nonalcoholic Steatohepatitis in the United States and the Rest of the World. *Clinics in Liver Disease*, 20(2), 205–214. <https://doi.org/10.1016/j.cld.2015.10.001>
- Schinkel, A. H., & Jonker, J. W. (2012). Mammalian drug efflux transporters of the ATP binding cassette (ABC) family: an overview. *Advanced Drug Delivery Reviews*, 64, 138–153.
- Schneider, A. L. C., Lazo, M., Selvin, E., & Clark, J. M. (2014). Racial differences in nonalcoholic fatty liver disease in the U.S. population. *Obesity*, 22(1), 292–299. <https://doi.org/10.1002/oby.20426>
- Schwabe, R. F., Seki, E., & Brenner, D. A. (2006). Toll-like receptor signaling in the liver. *Gastroenterology*, 130(6), 1886–1900.
- SEARCH Collaborative Group. (2008). SLCO1B1 variants and statin-induced myopathy--a genomewide study. *New England Journal of Medicine*, 359(8), 789–799. <https://doi.org/10.1056/NEJMp1002530>
- Seki, E., De Minicis, S., Österreicher, C. H., Kluwe, J., Osawa, Y., Brenner, D. A., & Schwabe, R. F. (2007). TLR4 enhances TGF- β signaling and hepatic fibrosis. *Nature Medicine*, 13(11), 1324.
- Senates, E., Yusuf, Y., Colak, Y., Ozturk, O., Altunoz, M. E., Kurt, R., ... Ovunc, A. O. K. (2011). Serum Levels of Hepcidin in Patients with Biopsy-Proven Nonalcoholic Fatty Liver Disease. *Metabolic Syndrome and Related Disorders*, 9(4), 287–290.
- Shitara, Y., & Sugiyama, Y. (2006). Pharmacokinetic and pharmacodynamic alterations of 3-hydroxy-3-methylglutaryl coenzyme A (HMG-CoA) reductase inhibitors: drug–drug interactions and interindividual differences in transporter and metabolic enzyme functions. *Pharmacology & Therapeutics*, 112(1), 71–105.
- Siegel, R., Desantis, C., & Jemal, A. (2014). Colorectal Cancer Statistics, 2014. *CA: Cancer Journal for Clinicians*, 64(1), 104–117. <https://doi.org/10.3322/caac.21220>.
- Silva-Gomes, S., Santos, A. G., Caldas, C., Silva, C. M., Neves, J. V., Lopes, J., ... Duarte, T. L. (2014). Transcription factor NRF2 protects mice against dietary iron-induced liver injury by preventing hepatocytic cell death. *Journal of Hepatology*, 60(2), 354–361. <https://doi.org/10.1016/j.jhep.2013.09.004>
- Simões, I. C. M., Fontes, A., Pinton, P., Zischka, H., & Wieckowski, M. R. (2018). International Journal of Biochemistry and Cell Biology Mitochondria in non-alcoholic fatty liver disease. *International Journal of Biochemistry and Cell Biology*, 95(October 2017), 93–99. <https://doi.org/10.1016/j.biocel.2017.12.019>
- Simon, N., Marsot, A., Villard, E., Choquet, S., Khe, H. X., Zahr, N., ... Hulot, J. S. (2013).

- Impact of ABCC2 polymorphisms on high-dose methotrexate pharmacokinetics in patients with lymphoid malignancy. *The Pharmacogenomics Journal*, 13(6), 507.
- Soresi, M., Noto, D., Cefalù, A. B., Martini, S., Vigna, G. B., Fonda, M., ... Notarbartolo, A. (2013). Nonalcoholic fatty liver and metabolic syndrome in Italy: Results from a multicentric study of the Italian Arteriosclerosis society. *Acta Diabetologica*, 50(2), 241–249. <https://doi.org/10.1007/s00592-012-0406-1>
- Sparidans, R. W., Iusuf, D., Schinkel, A. H., Schellens, J. H. M., & Beijnen, J. H. (2010). Liquid chromatography-tandem mass spectrometric assay for pravastatin and two isomeric metabolites in mouse plasma and tissue homogenates. *Journal of Chromatography B*, 878(28), 2751–2759.
- Sparidans, R. W., Vlaming, M. L. H., Lagas, J. S., Schinkel, A. H., Schellens, J. H. M., & Beijnen, J. H. (2009). Liquid chromatography-tandem mass spectrometric assay for sorafenib and sorafenib-glucuronide in mouse plasma and liver homogenate and identification of the glucuronide metabolite. *Journal of Chromatography B: Analytical Technologies in the Biomedical and Life Sciences*, 877(3), 269–276. <https://doi.org/10.1016/j.jchromb.2008.12.026>
- Sparreboom, A., Gelderblom, H., Marsh, S., Ahluwalia, R., Obach, R., Principe, P., ... McLeod, H. L. (2004). Diflomotecan pharmacokinetics in relation to ABCG2 421C>A genotype. *Clinical Pharmacology and Therapeutics*, 76(1), 38–44. <https://doi.org/10.1016/j.clpt.2004.03.003>
- Stausberg, J. (2014). International prevalence of adverse drug events in hospitals: an analysis of routine data from England, Germany, and the USA. *BMC Health Services Research*, 14(1), 125. <https://doi.org/10.1186/1472-6963-14-125>
- Stewart, A. (2013). SLCO1B1 Polymorphisms and Statin - Induced Myopathy. *PLOS Currents Evidence on Genomic Tests*, 5(1). <https://doi.org/10.1371/currents.eogt.d21e7f0c58463571bb0d9d3a19b82203>.Author
- Stroes, E. S., Thompson, P. D., Corsini, A., Vladutiu, G. D., Raal, F. J., Ray, K. K., ... Wiklund, O. (2015). Statin-associated muscle symptoms: impact on statin therapy—European Atherosclerosis Society Consensus Panel Statement on Assessment, Aetiology and Management. *European Heart Journal*, 36(17), 1012–1022. <https://doi.org/10.1093/eurheartj/ehv043>
- Sumida, Y., Niki, E., Naito, Y., & Yoshikawa, T. (2013). Involvement of free radicals and oxidative stress in NAFLD/NASH. *Free Radical Research*, 47(11), 869–880.
- Sumida, Yoshio, Kanemasa, K., Fukumoto, K., Yoshida, N., Sakai, K., Nakashima, T., & Okanoue, T. (2006). Effect of iron reduction by phlebotomy in Japanese patients with nonalcoholic steatohepatitis: A pilot study. *Hepatology Research*, 36(4), 315–321. <https://doi.org/10.1016/j.hepres.2006.08.003>
- Syn, W., Naisbitt, D. J., Holt, A. P., Pirmohamed, M., & Mutimer, D. J. (2005). Carbamazepine-induced acute liver failure as part of the DRESS syndrome. *International Journal of Clinical Practice*, 59(8), 988–991.
- Takeda, H., Nishikawa, H., Osaki, Y., Tsuchiya, K., Joko, K., & Ogawa, C. (2014). Clinical features associated with radiological response to sorafenib in unresectable hepatocellular carcinoma : a large multicenter study in. *Liver International*, 1581–1589. <https://doi.org/10.1111/liv.12591>

- Takehara, I., Yoshikado, T., Ishigame, K., Mori, D., Furihata, K., Watanabe, N., ... Kusahara, H. (2018). Comparative Study of the Dose-Dependence of OATP1B Inhibition by Rifampicin Using Probe Drugs and Endogenous Substrates in Healthy Volunteers. *Pharmaceutical Research*, 35(7), 138. <https://doi.org/10.1007/s11095-018-2416-3>
- Tanaka, Y., Ikeda, T., Yamamoto, K., Ogawa, H., & Kamisako, T. (2012). Dysregulated expression of fatty acid oxidation enzymes and iron-regulatory genes in livers of Nrf2-null mice. *Journal of Gastroenterology and Hepatology*, 27(11), 1711–1717. <https://doi.org/10.1111/j.1440-1746.2012.07180.x>
- Tannous, A., Brambilla, G., Hebert, D. N., & Molinari, M. (2015). N-linked sugar-regulated protein folding and quality control in the ER. *Seminars in Cell and Developmental Biology*, 41, 79–89. <https://doi.org/10.1016/j.semcdb.2014.12.001>
- ten Kate, J., Wolthuis, A., Westerhuis, B., & van Deursen, C. (1997). The iron content of serum ferritin: physiological importance and diagnostic value. *European Journal of Clinical Chemistry and Clinical Biochemistry: Journal of the Forum of European Clinical Chemistry Societies*, 35(1), 53–56.
- Terada, T., & Hira, D. (2015). Intestinal and hepatic drug transporters: pharmacokinetic, pathophysiological, and pharmacogenetic roles. *Journal of Gastroenterology*, 50(5), 508–519.
- Thakkar, N., Slizgi, J. R., & Brouwer, K. L. R. (2017). Effect of liver disease on hepatic transporter expression and function. *Journal of Pharmaceutical Sciences*, 106(9), 2282–2294.
- Tolson, A. H., & Wang, H. (2010). Regulation of drug-metabolizing enzymes by xenobiotic receptors: PXR and CAR. *Advanced Drug Delivery Reviews*, 62(13), 1238–1249.
- Toth, E. L., Li, H., Dzierlenga, A. L., Clarke, J. D., Vildhede, A., Goedken, M., & Cherrington, N. J. (2018). Gene-by-Environment Interaction of Bcrp 2 / 2 and Methionine- and Choline-Deficient Diet – Induced Nonalcoholic Steatohepatitis Alters SN-38 Disposition. *Drug Metabolism and Disposition*, 46(11), 1478–1486.
- Tuy, H. D., Shiomi, H., Mukaisho, K. I., Naka, S., Shimizu, T., Sonoda, H., ... Tani, T. (2016). ABCG2 expression in colorectal adenocarcinomas may predict resistance to irinotecan. *Oncology Letters*, 12(4), 2752–2760. <https://doi.org/10.3892/ol.2016.4937>
- Ucar, F., Sezer, S., Erdogan, S., Akyol, S., Armutcu, F., & Akyol, O. (2013). The relationship between oxidative stress and nonalcoholic fatty liver disease: Its effects on the development of nonalcoholic steatohepatitis. *Redox Report*, 18(4), 127–133. <https://doi.org/10.1179/1351000213Y.0000000050>
- Utrecht, J. (2007). Idiosyncratic drug reactions: current understanding. *Annu. Rev. Pharmacol. Toxicol.*, 47, 513–539.
- Urquhart, P., Pang, S., & Hooper, N. M. (2005). N-glycans as apical targeting signals in polarized epithelial cells. *Biochemical Society Symposium*, 72, 39–45. <https://doi.org/10.1042/bss0720039>
- Valenti, L., Fracanzani, A. L., Dongiovanni, P., Bugianesi, E., Marchesini, G., Manzini, P., ... Fargion, S. (2007). Iron Depletion by Phlebotomy Improves Insulin Resistance in Patients With Nonalcoholic Fatty Liver Disease and Hyperferritinemia: Evidence from a Case-Control Study. *American Journal of Gastroenterology* / *Am J Gastroenterol*, 102, 1251–1258.

<https://doi.org/10.1111/j.1572-0241.2007.01192.x>

- Vasilyeva, A., Durmus, S., Li, L., Wagenaar, E., Hu, S., Gibson, A. A., ... Schinkel, A. H. (2015). Hepatocellular shuttling and recirculation of sorafenib-glucuronide is dependent on Abcc2, Abcc3, and Oatp1a/1b. *Cancer Research*, *75*(13), 2729–2736. <https://doi.org/10.1158/0008-5472.CAN-15-0280>
- Vos, K., Sciuto, C. Lo, Piedade, R., Ashton, M., Björkman, A., Ngasala, B., ... Gil, J. P. (2017). MRP2/ABCC2 C1515Y polymorphism modulates exposure to lumefantrine during artemether-lumefantrine antimalarial therapy. *Pharmacogenomics*, *18*(10), 981–985.
- Wang, X., Rao, Z., Qin, H., Zhang, G., Ma, Y., Jin, Y., & Han, M. (2016). Effect of hesperidin on the pharmacokinetics of CPT-11 and its active metabolite SN-38 by regulating hepatic Mrp2 in rats, *432*(July), 421–432. <https://doi.org/10.1002/bdd>
- Wanless, I., & Lentz, J. (1990). Fatty liver hepatitis (steatohepatitis) and obesity: an autopsy study with analysis of risk factors. *Hepatology*, *12*(5), 1106–1110.
- Ward, D. M., & Kaplan, J. (2012). Ferroportin-mediated iron transport: Expression and regulation. *Biochimica et Biophysica Acta (BBA) - Molecular Cell Research*, *1823*(9), 1426–1433. <https://doi.org/10.1016/j.bbamcr.2012.03.004>
- Wieckowska, A., Papouchado, B. G., Li, Z., Lopez, R., Zein, N. N., & Feldstein, A. E. (2008). Increased hepatic and circulating interleukin-6 levels in human nonalcoholic steatohepatitis. *The American Journal of Gastroenterology*, *103*(6), 1372.
- Williamson, R. M., Price, J. F., Glancy, S., Perry, E., Nee, L. D., Hayes, P. C., ... Strachan, M. W. J. (2011). Prevalence of and risk factors for hepatic steatosis and nonalcoholic fatty liver disease in people with type 2 diabetes: The Edinburgh type 2 diabetes study. *Diabetes Care*, *34*(5), 1139–1144. <https://doi.org/10.2337/dc10-2229>
- Y., D. (2007). Pathology of hepatic iron overload. *World Journal of Gastroenterology*, *13*(35), 4755–4760. Retrieved from <http://ovidsp.ovid.com/ovidweb.cgi?T=JS&PAGE=reference&D=emed8&NEWS=N&AN=2007465557>
- Yang, W. S., & Stockwell, B. R. (2016). Ferroptosis: Death by Lipid Peroxidation. *Trends in Cell Biology*, *26*(3), 165–176. <https://doi.org/10.1016/j.tcb.2015.10.014>
- Ye, L., Yang, X., Guo, E., Chen, W., Lu, L., Wang, Y., ... Liu, Z. (2014). Sorafenib Metabolism Is Significantly Altered in the Liver Tumor Tissue of Hepatocellular Carcinoma Patient. *PLoS ONE*, *9*(5), 1–8. <https://doi.org/10.1371/journal.pone.0096664>
- Yee, S. W., Brackman, D. J., Ennis, E. A., Sugiyama, Y., Kamdem, L. K., Blanchard, R., ... Giacomini, K. M. (2018). Influence of Transporter Polymorphisms on Drug Disposition and Response : A Perspective From the International Transporter Consortium. *CLINICAL PHARMACOLOGY & THERAPEUTICS*, *00*(00), 1–15. <https://doi.org/10.1002/cpt.1098>
- Yokoi, T., & Nakajima, M. (2013). microRNAs as mediators of drug toxicity. *Annual Review of Pharmacology and Toxicology*, *53*, 377–400.
- Younossi, Z., Anstee, Q. M., Marietti, M., Hardy, T., Henry, L., Eslam, M., ... Bugianesi, E. (2018). Global burden of NAFLD and NASH: Trends, predictions, risk factors and prevention. *Nature Reviews Gastroenterology and Hepatology*, *15*(1), 11–20. <https://doi.org/10.1038/nrgastro.2017.109>

- Younossi, Z. M., Koenig, A. B., Abdelatif, D., Fazel, Y., Henry, L., & Wymer, M. (2016). Global epidemiology of nonalcoholic fatty liver disease—Meta-analytic assessment of prevalence, incidence, and outcomes. *Hepatology*, *64*(1), 73–84. <https://doi.org/10.1002/hep.28431>
- Yu, A.-M., Tian, Y., Tu, M.-J., Ho, P. Y., & Jilek, J. L. (2016). MicroRNA pharmacoepigenetics: posttranscriptional regulation mechanisms behind variable drug disposition and strategy to develop more effective therapy. *Drug Metabolism and Disposition*, *44*(3), 308–319.
- Zanger, U. M., & Schwab, M. (2013). Cytochrome P450 enzymes in drug metabolism: regulation of gene expression, enzyme activities, and impact of genetic variation. *Pharmacology & Therapeutics*, *138*(1), 103–141.
- Zhang, W., Yu, B. N., He, Y. J., Fan, L., Li, Q., Liu, Z. Q., ... Zhou, H. H. (2006). Role of BCRP 421C>A polymorphism on rosuvastatin pharmacokinetics in healthy Chinese males. *Clinica Chimica Acta*, *373*(1–2), 99–103. <https://doi.org/10.1016/j.cca.2006.05.010>
- Zhao, N., & Enns, C. A. (2013). N-linked glycosylation is required for transferrin-induced stabilization of transferrin receptor 2, but not for transferrin binding or trafficking to the cell surface. *Biochemistry*, *52*(19), 3310–3319.
- Zimmerman, E. I., Hu, S., Roberts, J. L., Gibson, A. A., Orwick, S. J., Li, L., ... Baker, S. D. (2013). Contribution of OATP1B1 and OATP1B3 to the disposition of sorafenib and sorafenib-glucuronide. *Clinical Cancer Research*, *19*(6), 1458–1466. <https://doi.org/10.1158/1078-0432.CCR-12-3306>
- Zimmermann, A., Zimmermann, T., Schattenberg, J., Pöttgen, S., Lotz, J., Rossmann, H., ... Weber, M. M. (2011). Alterations in lipid, carbohydrate and iron metabolism in patients with non-alcoholic steatohepatitis (NASH) and metabolic syndrome. *European Journal of Internal Medicine*, *22*(3), 305–310. <https://doi.org/10.1016/j.ejim.2011.01.011>